



Design and Fabrication of a Novel Cell-Derived Matrix Scaffold for Dermal Wound Healing

A Major Qualifying Project Report
Submitted to the Faculty
of
WORCESTER POLYTECHNIC INSTITUTE
In partial fulfillment of the requirements for the
Degree of Bachelor of Science
by

Jennifer Cooper

Sarah Mattessich

Fioleda Prifti

26 April 2012

Approved:

Professor Marsha Rolle, Advisor

Professor George Pins, Advisor

1. extracellular matrix
2. scaffold
3. antimicrobial peptide
4. wound healing

Table of Contents

Table of Contents.....	2
Authorship Page	6
Acknowledgments.....	7
Abstract.....	8
Table of Figures	9
Table of Tables	11
1 Introduction	12
2 Literature Review	14
2.1 Scaffolds for Tissue Engineering.....	14
2.1.1 Improved Wound Healing.....	14
2.1.2 Considerations and Characteristics.....	15
2.1.3 Common Scaffold Materials	16
2.2 Skin	18
2.2.1 Structure and Composition.....	19
2.2.2 Mechanical Properties	21
2.3 The Extracellular Matrix	23
2.4 Dermal Injury	25
2.4.1 Natural Course of Wound Healing.....	25
2.4.2 Chronic Wounds	28
2.4.3 Wound Infection.....	29
2.5 Current Treatments.....	32
2.5.1 Debridement	32
2.5.2 Antimicrobial Treatments	32
2.5.3 Skin Grafting	35
2.6 ECM Scaffolds for Dermal Regeneration	39
2.6.1 Decellularized Tissue-Derived ECM.....	40
2.6.2 Decellularization Process.....	40
2.6.3 Advantages of cultured cell-derived extracellular matrix scaffolds.....	43
2.6.4 Strategies for enhancing extracellular matrix scaffolds.....	44
3 Project Definition and Strategy	49
3.1 Initial Client Statement	49

3.2	Initial Approach	49
3.3	Attributes List	50
3.3.1	Pruned Objectives	51
3.3.2	Ranking the Objectives	54
3.3.3	Finalizing the Priority of Objectives	58
3.4	Constraints	59
3.5	Revised Client Statement.....	60
3.6	Project Approach	60
4	Alternative Designs	62
4.1	Generation of Alternative Designs.....	62
4.1.1	Initial Functions List	62
4.1.2	Initial Specifications/Requirements	63
4.1.3	Development of Conceptual Designs	64
4.1.4	Preliminary Functions and Means	67
4.2	Evaluation of Alternative Designs.....	71
4.2.1	Generation of final functions and means.....	71
4.2.2	Description of Alternative Designs	73
4.2.3	Decision Matrix	74
4.2.4	Results of Decision Matrix.....	78
4.3	Final Conceptual Design.....	80
4.3.1	Design Fabrication.....	81
4.4	Conclusion.....	84
5	Design Verification	85
5.1	Developing Recombinant Cathelicidin.....	85
5.1.1	Gene Design.....	85
5.1.2	Cathelicidin Isolation.....	88
5.1.3	Ligation into pGEM Vector	90
5.1.4	<i>E.Coli</i> Transformation, Screening, and pGEM Isolation	90
5.1.5	Restriction Digest and Fragment Purification	92
5.1.6	Sequence Analysis	93
5.1.7	p3xFLAG Ligation, Transformation, and Verification	94
5.1.8	H1299 Transfection.....	96
5.1.9	Western Blot	97

5.2	Cell-Derived Sheet Culture	99
5.2.1	Experiment 1: Fibroblast Sheets on UpCell™ Plate	100
5.2.2	Experiment 1A: Fibroblast Sheets on UpCell Plate	103
5.2.3	Experiment 2: Anchors on RASMC Sheets	104
5.2.4	Experiment 3: Lower Density Fibroblast CDSs on UpCell™ Plates	108
5.2.5	Experiment 4: Final Validation of Fabricating CDSs	112
5.3	Decellularization	116
5.3.1	Experiment 5: SDS Decellularization	116
5.3.2	Experiment 6: Freeze-Thaw Decellularization	122
5.3.3	Experiment 7: Hypotonic and Hypertonic Solutions Decellularization	127
5.4	Mechanical Testing of Tissues	130
5.4.1	Uniaxial Tensile Testing of Decellularized Foreskins	130
5.4.2	Uniaxial Tensile Testing of CDSs	131
6	Discussion	136
6.1	Analysis and Limitations of Experiments	137
6.1.1	Fabrication of Cell-derived Sheets	138
6.1.2	ECM Isolation	139
6.1.3	Antimicrobial Peptide	140
6.2	Impact Analysis	140
6.2.1	Economics	141
6.2.2	Environmental Impact	141
6.2.3	Societal Influence	141
6.2.4	Political Ramifications	142
6.2.5	Ethical Concerns	142
6.2.6	Health and Safety Issues	143
6.2.7	Manufacturability	143
6.2.8	Sustainability	143
7	Final Design and Validation	144
7.1	Part 1: Fabricating Fibroblast Sheets	144
7.2	Part 2: Isolating the ECM via Decellurization	145
7.3	Part 3: Incorporating Antimicrobial Protein into the ECM	145
8	Conclusions and Recommendations	146
8.1	Future Work	146

8.2	Recommendations	147
8.2.1	Fibroblast Sheet Fabrication	147
8.2.2	Histological Analysis	148
8.2.3	Mechanical Testing	148
8.2.4	Mechanical Strength of the Cell Sheets	149
	References	150
	Appendices	154
	Appendix A: B-Term Gantt Chart.....	154
	Appendix B: Metrics	155
	Appendix C: Decision Matrices.....	159
	Appendix D: Conceptual Designs	164
	Appendix E: C-Term Gantt Chart	167
	Appendix F: Materials List	168
	Appendix G: Tissue Processing Protocol	169
	Appendix H: Staining Protocols for Paraffin Sections	170
	Hematoxylin and Eosin Staining	170
	Picrosirius Red Staining	170
	Hoechst Staining	2
	Appendix I: Decellularization Protocols	3
	Original SDS Decellularization (Elder et al., 2009).....	3
	Modified SDS Decellularization	3
	Original Freeze-Thaw Decellularization (Ngangan & McDevitt, 2009).....	3
	Modified Freeze-Thaw Decellularization	3
	Original Hypotonic and Hypertonic Solutions Decellularization (Meyer et al., 2006)	4
	Modified Hypotonic and Hypertonic Solutions Decellularization.....	4

Authorship Page

This project is the product of the collaborative effort of three students. Sections were primarily written by one student as listed below. All sections were reviewed and edited by all members.

Section		Name	Section		Name
1	Introduction	All	4.3	Final Design	SPM
2	Literature Review	All	4.4	Conclusion	All
2.1	Scaffolds for Tissue Engineering	JLC	5	Design Verification	All
2.2	Skin	JLC	5.1	Genetic Engineering	FP
2.3	The Extracellular Matrix	JLC	5.2	Cell and Tissue Culture	SPM
2.4	Dermal Injury	FP	5.3	Decellularization	JLC
2.5	Current Treatments	FP	6	Discussion	All
2.6	ECM Scaffolds for Dermal Regeneration	SPM	6.1	Analysis of Experiments	All
3	Project Definition and Strategy	All	6.2	Limitations of the Design/Product	All
3.1	Initial Client Statement	FP	6.3	Impact Analysis	All
3.2	Initial Approach	SPM	7	Final Design and Validation	All
3.3	Attributes List	SPM	7.1	Part 1: Fabricating fibroblast sheets	SPM
3.4	Constraints	JLC	7.2	Part 2: Isolating the ECM via Decellurization	JLC
3.5	Revised Client Statement	FP	7.2	Part 3: Modifying the Fibroblasts with Genetic Engineering	FP
3.6	Project Approach	JLC	7.4	Final Approach	All
4	Alternative Designs	All	8	Conclusions and Recommendations	All
4.1	Generation of Alternative Designs	SPM	8.1	Future Work	All
4.2	Evaluation of Alternative Designs	All	8.2	Recommendations	All

Acknowledgments

We would like to thank our BME advisors, Professor George Pins and Professor Marsha Rolle, as well as Professor Destin Heilman for his the guidance in completing the biochemistry component of the project. We would also like to acknowledge Professor Terri Camesano and Professor Tanja Dominko for their expertise, as well as Professor Sakthikumar Ambady and Lisa Wall for directing the MQP program. Finally, we'd like to thank the following graduate students for supporting us throughout this project: Dr. Tracy Hookway, Amanda Zoe Reidingner, Amanda Clement, Jen Sansom, Denis Kole, Jason Hu, Karen Levi, Evans John Burford, Sagar Antala, and Ryan Richards.

Abstract

Approximately 35 million cases of significant skin loss require clinical intervention annually. Tissue engineering has shown promise in the development of therapies to regenerate full-thickness skin wounds. Here we present the design of a novel cell-derived extracellular matrix scaffold with antimicrobial properties for dermal wound healing. We optimized decellularization methods, cultured dermal fibroblast sheets, cloned a cathelicidin construct, and expressed cathelicidin in a model cell type as steps toward achieving an antimicrobial dermal scaffold with tailored mechanical strength and bioactivity.

Table of Figures

Figure 1: Three-Dimensional View of Skin	19
Figure 2: Three phases of natural wound healing.....	25
Figure 3: Spectrum of Bacterial Contamination-to-Infection	29
Figure 4: The Objectives Tree for the Design of a Novel ECM Ccaffold	53
Figure 5: The Objectives Tree for the Design of in vitro Assays to Analyze the Properties of the Novel ECM Scaffold.....	54
Figure 6: Project Approach	61
Figure 7: Brainstorming Session (a).....	64
Figure 8: Brainstorming Session (b).....	65
Figure 9: Final Functions/Means Tree.....	74
Figure 10: Schematic of Final Design.....	80
Figure 11: Amino acid sequence of human cathelicidin, hCAP-18.....	85
Figure 12: Proposed Gene Design of Recombinant Collagen-binding Cathelicidin Insert.....	86
Figure 13: Design of Forward and Reverse PCR Primers	88
Figure 14 : Purified PCR Fragments of Recombinant Cathelicidin.....	89
Figure 15: pGEM Transformations in JM109 <i>E. Coli</i>	91
Figure 16: Restriction Analysis of pGEM Containing Recombinant Cathelicidin inserts.....	93
Figure 17: Alignment of Theoretical and Isolated Fib-CBD	94
Figure 18: Alignment of Theoretical and Sequenced Col-CBD	94
Figure 19: Map of p3xFLAG-Myc-CMV-26 vector.....	95
Figure 20: <i>E. coli</i> Transformation of p3xFLAG Final Constructs	96
Figure 21: Restriction Digest of p3xFLAG with Ligated Recombinant Cathelicidin Inserts.....	96
Figure 22: H1299 Transfection.....	98
Figure 23: Fibroblast CDSs after 24 Hours on UpCell Plate	102
Figure 24: Histology of fibroblast CDSs after 24 hours on UpCell plate.....	103
Figure 25: Fibroblast CDS after 12 Days on UpCell Plate	104
Figure 26: Histology of Fibroblast CDSs after 17 Days on UpCell Plate.....	104
Figure 27: Anchor System.....	105
Figure 28: RASMC CDSs with Anchors after 24 Hours on TCPS.....	107
Figure 29: Setup for Anchor Experiment	107
Figure 30: RASMC CDSs at 50,000 and 100,000 cells/cm ² with and without anchors.....	108
Figure 31: Freshly harvested fibroblast sheets (100,000 cells/cm ²)	110
Figure 32: Fibroblast sheets with ascorbic acid.....	111
Figure 33: Picrosirius Red/Fast Green Stains of CDSs	112
Figure 34: Freshly Harvested Fibroblast Sheet for Mechanical Testing.....	114
Figure 35: Cellular Alignment of Fibroblast Sheets.....	114
Figure 36: Picrosirius Red/Fast Green Stain of Fibroblast Sheets.....	115
Figure 37: Picrosirius Red/Fast Green Stain of Fibroblast Sheets.....	116
Figure 38: SDS Decellularization Approach	117
Figure 39: H&E Staining of SDS Decellularized Foreskin.....	118
Figure 40: Hoechst Staining of SDS Decellularized Foreskins.....	118
Figure 41: Histology of SDS with DNase Decellularized Foreskins Green.....	119

Figure 42: Hoechst Stains of Decellularized CDSs.....	120
Figure 43: Hoechst and H&E Stains of SDS-decellularized Foreskins.....	122
Figure 44: Freeze-Thaw Decellularization Approach.....	123
Figure 45: Histology of Freeze-Thaw with DNase Decellularized Foreskins.....	124
Figure 46: "Boat" for Freeze-Thaw. Red arrow indicates CDS.	125
Figure 47: Hoechst Stains of Freeze-thawed CDSs	125
Figure 48: Hoechst and H&E Stains of Freeze-thawed Foreskins	127
Figure 49: Histology Staining of Hypotonic and Hypertonic Solutions.....	129
Figure 50: Hoechst Stains of Hypotonic/Hypertonic-Solutions Decellularized CDSs	130
Figure 51: Mechanical Testing Setup Accessories.	131
Figure 52: Decellularized Foreskin in Grips during Mechanical Testing.....	131
Figure 53: Tensile Testing of Cell-Derived Fibroblast Sheets	132
Figure 54: CDS Loaded on Instron.....	133
Figure 55: Stress vs. Strain for Cell Sheets with and without Ascorbic Acid	134
Figure 56: Maximum Stress of Fibroblast Sheets with and without Ascorbic Acid	135
Figure 57: Final Design Approach.....	144

Table of Tables

Table 1: Microorganisms Causing Invasive Wound Infections.....	31
Table 2: Types of Topical Antiseptic Treatments.....	34
Table 3: Dermal Substitutes.....	38
Table 4: Various Decellularization Methods).....	41
Table 5: Range of Microbiocidal Activity of LL-37.....	47
Table 6: Overall Scaffold Characteristics PCC Results.....	55
Table 7: Ease of Production PCC Results.....	55
Table 8: Structurally and Mechanically Similar to Native Dermal Tissue PCC Results.....	56
Table 9: Clinical Ease of Use PCC Results.....	56
Table 10: Ease of Laboratory Processing PCC Results.....	57
Table 11: Bioactive PCC Results.....	57
Table 12: In Vitro Assays Characteristics PCC Results.....	57
Table 13: Summary of Overall Prioritized Objectives.....	59
Table 14: Decision Matrix Results for “Withstands Mechanical Forces Similar to Native Dermis”	78
Table 15: Decision Matrix Results for “Actively Inhibits Microbial Infection”.....	79
Table 16: Decision Matrix Results for “Actively Inhibits Microbial Infection”.....	79
Table 17: Cell Type Decision Chart.....	82
Table 18: Experimental Setup of Fibroblast Sheets.....	101
Table 19: Experimental Setup using Anchors on RASMCs.....	106
Table 20: Experimental Setup of Fibroblasts on UpCell™ Plate 1.....	109
Table 21: Experimental Setup of Fibroblasts on UpCell™ Plate 2.....	110
Table 22: Experimental Setup for Final Fibroblast Sheets.....	113
Table 23: Cell Sheet Thickness.....	115
Table 24: Measurements and Observations of Mechanical Testing.....	132
Table 25: Measurements and Results for Tensile Testing of Fibroblast Sheets.....	134

1 Introduction

Skin is the body's main protective barrier against environmental insults. As the largest organ in the body, skin maintains thermoregulation, blood vessel dilation, and the secretion of sweat. Significant skin wounds, caused by burns, physical trauma, surgery, and underlying pathologies, affect more than 35 million people annually in the United States (Clark, Ghosh, & Tonnesen, 2007). Of these, 20% develop into chronic, difficult-to-heal wounds, overall costing the U.S. more than \$25 billion annually (Sen et al., 2009). Due to the extensive loss of tissue and damage to subcutaneous layers, such as fat, muscle, and bone, full-thickness wounds lead to impaired tissue regeneration and loss of barrier function (Hess, 2005).

Scaffolds have been explored as a therapeutic method for regenerating, rather than repairing, skin at the wound site. In repair, a large amount of granulation tissue is synthesized to fill in the wound void, leading to scarring and impaired tissue functionality. Instead, scaffolds provide a three-dimensional support through which cells can migrate, adhere, and regenerate a functional new tissue (O'Brien, 2011). Current scaffolds, however, are plagued by inadequate biocompatibility and biodegradability, mechanical and structural mismatch with the native tissue, and susceptibility to infection (James, 2009).

Extracellular matrix (ECM) is an appealing scaffold material that provides several advantages over other natural and synthetic polymers currently used for skin therapies including structural support in the wound bed with mechanical properties closely matching those of native tissue. The ECM in skin is produced mainly by fibroblasts which reside in the dermal layer. The matrix is a biological substance composed of fibers and an interfibrillary matrix of glycosaminoglycans (GAGs) and proteoglycans, adhesive glycoproteins, solutes, and water. The ECM structurally supports the keratinocytes of the epidermal layer and provides a matrix to which keratinocytes can adhere and differentiate (Badylak, 2007). Furthermore, ECM scaffolds provide growth factors and cytokines that mediate cellular migration, proliferation, and

differentiation, thereby stimulating the natural wound healing response (Liu, Xia, & Czernuszka, 2007; Macri & Clark, 2009).

In this study, we designed a novel cell-derived ECM scaffold. Our goal was to address the limitations of current scaffolds by creating a product that (1) provides the structural and mechanical properties of native dermis and (2) actively prevents wound infection. Our approach follows a stepwise design process towards achieving a scaffold with antimicrobial activity and tailored mechanical properties. To accomplish goal (1), human dermal fibroblasts were cultured into tissue sheets in media supplemented with ascorbic acid in order to increase collagen expression. To accomplish goal (2), this process will be iterated and fibroblasts will be genetically modified to produce an antimicrobial protein that adheres to the ECM. In the end, the modified ECM scaffold will be isolated from the cell-derived tissue through decellularization.

To produce a scaffold entirely from ECM, we cultured dermal fibroblasts into cell sheets and subjected them to different decellularization techniques in order to optimize the removal of cellular debris. A gene construct was developed to produce human cathelicidin (LL-37), an antimicrobial protein (AMP) that is naturally synthesized in the epidermis (Heilborn et al., 2003). The AMP was also designed to include the collagen-binding domain (CBD) of either collagenase or fibronectin to allow fibroblasts to express, secrete, and tether the protein within the ECM.

The following chapters describe the clinical significance of fabricating a novel cell-derived matrix for dermal wound healing, our project approach, and the validation testing of our design. The results describe how we were able to fabricate fibroblast sheets in the presence of ascorbic acid, assess mechanical strength of the fibroblast sheets, optimize decellularization protocols, and verify cathelicidin expression in a model cell type. Lastly, we provide an analysis of our final design and recommendations for future work.

2 Literature Review

Literature research was conducted to become familiar with the project and understand current technology, protocols, and results. The following sections give a general overview of the of the project, including details about skin as an organ, the importance of scaffolds for wound healing, and rationale for using cell-derived matrices.

2.1 Scaffolds for Tissue Engineering

The number of organs and tissue needed to maintain control over treatment for current diseases and trauma greatly exceeds the number available for transplantation (Saltzman, 2004). Shortcomings in donor sources have led to progress in the field of tissue engineering (TE), which is aimed at regenerating new, healthy tissue. TE has the potential to be an alternative to drug therapy, gene therapy, and whole-organ transplantation; a method to control the normal processes of tissue repair and healing; and a means to replace missing cells from functional tissue or organ (Saltzman, 2004). TE is a tri-faceted approach to regenerating native tissue. It requires a scaffold, which acts as a template to guide newly forming tissue, growth factors to provide chemical signals, and cells, to reconstruct tissue (O'Brien, 2011).

2.1.1 Improved Wound Healing

In tissue engineering, scaffolds are ultimately a three-dimensional support structure for new tissue growth. Scaffolds provide a support system for migrating cells to adhere and grow to, while providing a template for the forming tissue (O'Brien, 2011). These structures, however, are paramount for normal wound healing. As discussed later, there are three classic states of wound healing: inflammation, new tissue formation, and remodeling (Gurtner, Werner, Barrandon, & Longaker, 2008). The importance of scaffolds lies within the new tissue formation phase. In normal healing, fibroblasts and vascular endothelial cells begin synthesize new stroma, also referred to as granulation tissue, around four days post-injury (Singer & Clark,

1999). The granulation tissue eventually replaces the fibrin clot that was initially produced to shield the wound and act as a provisional matrix (Martin, 1997). Collagen, mostly type III initially, and proteoglycans are synthesized at the wound site by the fibroblasts, while the endothelial cells begin recreating the vasculature system in the wounded area (Morgan, Sheridan, Tompkins, Yarmush, & Burke, 2004).

Scaffolds are a key factor in establishing regeneration versus repair during wound healing. In repair, large amounts of granulation tissue are synthesized to fill in the wound void, leading to scarring (Morgan et al., 2004). If a scaffold is placed in the void instead, the cells are able to recognize the temporary structure filling in the defect and control the rate of granulation tissue deposition. Scaffolds provide the opportunity for regeneration of the tissue, instead of simply plugging the hole, resulting in scar tissue.

2.1.2 Considerations and Characteristics

There are several design considerations when selecting a scaffold—biocompatibility, biodegradability, mechanical properties, scaffold architecture, bioactivity, and manufacturing technology (Ma, 2004). These factors will determine the most appropriate material for the application and how it should be fabricated. In regard to biocompatibility, if the material is toxic to the cells and native tissue, then the material should not be used for biomedical applications. Non-biocompatibility can elicit a chronic inflammatory response or severe immune response, ultimately resulting in rejection of the scaffold and physiological complications in the patient. In addition, if cells will not adhere to the surface or migrate through the scaffold, the material is not suitable for the application (Ma, 2004; O'Brien, 2011). This is extremely important when tissue engineering skin. The native cells must be able to integrate into the scaffold and begin degrading the fibers and synthesizing new matrix in order to restore the lost functions that skin regulate (MacNeil, 2008). Scaffolds for tissue engineering applications can be permanent implants, but they are typically temporary guides to enhance tissue regeneration. For this

reason, the material must also be biodegradable so that it gradually reduces its influence as cells begin synthesizing their own matrix at the wound site (Yoon & Fisher, 2009). It is crucial that the material does not release toxic, highly acidic, or highly basic by-products as it degrades, which is commonly observed in synthetic materials (Liu et al., 2007). Another criteria, mechanical properties and integrity. Strength, stiffness, and shear resistance are key properties and should be consistent between the scaffold and native tissue. Insufficient properties may hinder cellular ingrowth, vascularization, uniform healing, and may result in damage of the scaffold upon handling (O'Brien, 2011). The scaffold should also demonstrate a porous structure to permit cellular permeability, diffusivity of molecular substrates and nutrients, and vascularization throughout the material (Place, George, & Williams, 2009). Developing a scaffold for tissue engineering applications however, can be a complex challenge as positively affecting one category may be detrimental to the other. For example, improving porosity to enhance biological processes can compromise the mechanical integrity of the scaffold (Place et al., 2009; Yoon & Fisher, 2009). A final consideration for selecting a scaffold is manufacturing capacity and technology. For a TE scaffold to be commercially available as a possible therapy, the scaffold should be cost effective and it should be possible to scale-up the production from one-at-a-time in a research laboratory or small batch production (O'Brien, 2011).

2.1.3 Common Scaffold Materials

There are two main groups of biomaterials in TE applications: synthetic materials, including ceramics, and natural or biological materials. Ceramic polymers are typically not used in soft tissue applications (O'Brien, 2011) and are thus not discussed in the context of this paper.

2.1.3.1 Synthetic Materials and Limitations

Synthetic materials for tissue engineering applications typically include, poly(L-lactide) (PLA), polyglycolic acid (PGA), and poly-DL-lactic-co-glycolic acid (PLGA) (Liu et al., 2007;

O'Brien, 2011). Synthetic materials are advantageous because their composition and subsequent properties, including porosity, strength, stiffness, and degradation rate, can be tailored according to need and function (Yoon & Fisher, 2009). Moreover, these materials offer the advantage of easy processing, permitting for a reproducible manufacturing process. This ultimately results in the control and predictability of properties from batch-top-batch (Liu et al., 2007).

However, synthetic materials are limited by bioactivity and biocompatibility. The majority of synthetic polymers for TE degrade by bulk degradation (Liu et al., 2007). For the polymers that are hydrolyzed in the body, such as PGA and PLA, acidic by-products are released into the surrounding tissue, which lowers the pH of the area, possibly creating an inflammatory response and potentially killing the cells and tissue (Lavik & Langer, 2004). Unlike natural materials, synthetic materials lack biological recognition. Without any biological signaling from the scaffold, cell ingrowth, proliferation, and differentiation may be negatively impacted. Cells rely on anchoring sites for attachment and cell-material interactions for guidance. Without these components, the material may present itself as a foreign object, creating a severe inflammatory response or even apoptosis (Liu et al., 2007).

2.1.3.2 Natural Materials and Limitations

Based on the limitations of synthetic scaffolds, research started to focus on using natural materials for biological applications. Natural materials are bioactive and provide the essential biological cues, biofunctional molecules, and signaling required for cell adhesion, growth, and function (Yoon & Fisher, 2009). Because these materials are natural, they are less likely to induce an inflammatory response, and the material can be enzymatically degraded as in normal processes without the release of toxic by-products (O'Brien, 2011). Natural polymers for tissue engineering can be broken down into two categories, polysaccharides, which are chains of sugar units, or polypeptides, which are chains of amino acid units. Examples of polysaccharide

materials include agarose, alginate, hyaluronic acid, and chitosan. Hyaluronic acid is of particular interest because of its extracellular matrix origin and critical role in wound healing (Yoon & Fisher, 2009). Polypeptide examples include gelatin, silk, and the commonly used collagen for its impact on cell function and strength.

Current research is exploring the use of the extracellular matrix as a natural material due to its assortment of biological and wound healing properties. The ECM already has innate adhesion domains, diverse molecules, and the signaling needed to support cellular processes. The ECM can provide structure and constructive remodeling in tissue engineering applications, similar to its native functions within tissue. Stephen Badylak, a leader in ECM research, suggests that the extracellular matrix is “nature’s ideal biologic scaffold material” (Badylak, 2007). Using ECM as a scaffold is discussed further in section 2.6.

There are unfortunately several concerns when using natural materials. One of the main drawbacks of natural materials is that their mechanical properties are outperformed by both synthetic polymers and native tissue (Liu et al., 2007). Unlike synthetic materials, natural materials cannot be easily processed or reproduced, and there is little flexibility in varying mechanical and structural properties (O'Brien, 2011). Also, the in vivo rate of degradation cannot be controlled as easily as in synthetic materials, and there is difficulty in accurately quantifying the expected lifespan of these materials after implantation (Yoon & Fisher, 2009). There is also the concern of antigenicity and immunogenicity. Depending on the host organism, there is the potential for pathogen transmission and consequently immune reactions (Liu et al., 2007).

2.2 Skin

Skin is the largest organ of the human body, occupying over 2.0m² in (Rouabhia, 1997) and more mass than all other organs (Goldsmith, 1983). Integument, or skin, is multifunctional, with its primary functions in thermoregulation, physical protection from external stimuli, and

sensation. Skin helps to maintain internal stability and regulates the dilation of blood vessels, as well as the secretion of sweat. It acts as a barrier from the external environment to protect the body from mechanical and thermal insults, UV irradiation, hazardous chemicals, water and ionic loss, and very importantly, infection. Skin also acts in the production of vitamin D, waste and glandular secretions, and sensing for touch, pain, heat, and cold (Flynn & Woodhouse, 2009).

2.2.1 Structure and Composition

Skin is organized into three distinct layers (see Figure 1). The outermost layer is the epidermis and protects the body against external factors. The middle layer is the dermis, which is a layer of dense connective tissue. The inner layer is the hypodermis, also known as subcutaneous fat, and consists of loose fatty connective tissue (Hendriks, 2005). A basement membrane binds the epidermal and dermal layers (Shier, Butler, & Lewis, 2009)

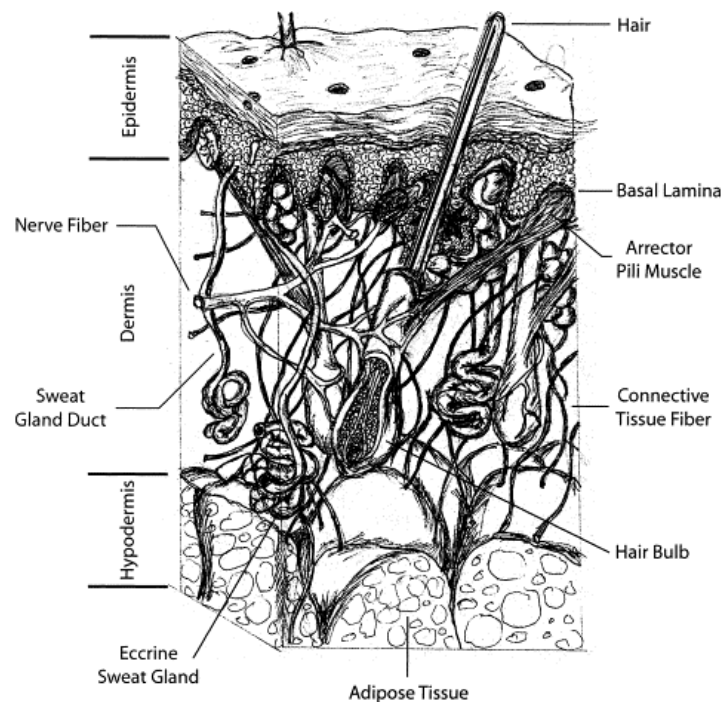


Figure 1: Three-Dimensional View of Skin (Seal, Otero, & Panitch, 2001)

2.2.1.1 Epidermis

The epidermis is the outermost part of the skin and is roughly 75-150µm in thickness (Goldsmith, 1983). The epidermis is mainly cellular with little vasculature and consists of several layers: the stratum corneum, the stratum granulosum, the stratum spinosum, and the stratum germinativum. Keratinocytes reside in the deeper regions of the epidermis, whereas cornified cells predominate in the upper regions (Rouabhia, 1997). Together, these continually renewing compacted layers act in the protective functions of skin.

2.2.1.2 Dermis

The dermis is a fibroelastic layer approximately 1-4mm in thickness and consists of the extracellular matrix of cells, primarily collagen fibers. The dermal layer comprises the majority of skin and has various irregularities within the layer, as well as protruding from the layer. These components include blood and lymph vessels, nerve endings, hair follicles, and glands (Hendriks, 2005). The blood vessels in the dermis supply nutrients to both the dermal and epidermal layers. The dermis is mostly acellular and the few residing cells are fibroblasts, which synthesize the extracellular matrix (ECM) that constitutes the dermal layer (Zhong, Zhang, & Lim, 2010).

The dermis consists of the three fibrous proteins collagen, elastin, and reticulin, as well as surrounding glycosaminoglycans (GAGs) and polysaccharides. Collagen bundles run almost parallel to the epidermis in an irregular network, occupying roughly 75% of dermal volume. Elastin occupies only about 1% of the dermal volume, but it provides the recoiling capacity of the tissue after deformation from external mechanical stresses. These fibers are positioned amongst the collagen bundles. The collagen is responsible for the strength of the skin and elastin is responsible for preventing permanent deformation when stresses are applied (Hendriks, 2005).

The dermal layer is composed of two regions: the papillary dermis and the reticular dermis. The papillary layer is the thin, outermost (upper) layer of the dermis and interacts with the epidermis through the basement membrane (Rouabhia, 1997). Constituting about 10% of the full dermal thickness, the collagen fibrils in this region are typically type III collagen and are packed into fibers of 0.3um-3um in diameter (Silver, Freeman, & DeVore, 2001). The fibers are loosely distributed within the layer, along with the elastin fibers (Goldsmith, 1983). The bulk of the dermis is the reticular layer, which lies beneath the papillary region and above arteries and postcapillary venules (Rouabhia, 1997) contains collagen fibers 10-40um in diameter (silver). These fibrils are predominately type I collagen, which are stronger than the type III collagen, providing the majority of dermal strength (Silver et al., 2001).

2.2.2 Mechanical Properties

Several studies were completed in the 1970's to the mid-1980's by Cook, Wan Abas, Barbanel, and many others, who collectively found that human skin is nonhomogeneous and also anisotropic (Alexander & Cook, 1977; Wan Abas & Barbanel, 1982). The mechanical properties of skin can differ based on various factors, including the location on the body where the skin is tested/derived from (ex. abdomen, leg, upper arm, etc.), the type and method of testing, temperature, humidity, and the age and health of the patient. Although values of skin have been published, these factors make it difficult to determine one exact value for the properties of skin, including strength, stiffness, and shear resistance (Hendriks, 2005; Lacroix & Planell, 2009).

Skin is a viscoelastic material with an internal framework designed to minimize strain. Skin exhibits creep, in which strain increases at a constant stress, and relaxation, in which the stress required to maintain a constant strain is reduced (Edwards & Marks, 1995). However, creep and relaxation resistance decreases with age, as explained in the following paragraphs.

Common mechanical testing methods for skin include tensile testing, torsion testing, suction, and indentation. Tensile testing is a widely used method where the skin is loaded parallel to its surface and a tab is attached to either side of the sample, pulling the sample outward. In torsion testing, a guard ring and intermediary disc are attached to the skin and a constant torque/rotation is applied. The suction method applies a partial vacuum to the sample and measures the resulting elevation. For indentation experiments, an indenter is applied to the sample at a known force (Hendriks, 2005).

Damien Lacroix and Josep Planell stretched skin at a slow rate of 5 cm/min and found that the tensile strength of skin ranges from 5-30MPa (Lacroix & Planell, 2009). The average of the experiments showed a maximum of 21MPa at 8 years of age that decreased to 17MPa for 95 years of age. The ultimate strain varied from 35-115% with a mean value around 70% (Lacroix & Planell, 2009). The shear modulus ranges from 435-6620 Pa (Holt, Tripathi, & Morgan, 2008) and the ultimate modulus of elasticity ranges from 15-150MPa, with a mean value of 70MPa at 11 years of age and a value of 60MPa at 95 years of age (Edwards & Marks, 1995). Manschot and Brakkee performed uniaxial tensile tests on human calf skin and concluded a maximum strain of 32% and Young's modulus of 4MPa across the tibia axis; a maximum strain of 30% and Young's modulus of 20MPa was found across the tibia axis (Manschot & Brakkee, 1986). Silver and Freeman reported a similar modulus of 18.8MPa for human skin obtained from the thoracic and abdominal areas in patients 47-86 years of age (Silver et al., 2001). Other testing methods produce significantly lower values for the modulus. For the torsion tests, Agache et al. reports stiffness values of 0.42-1.12MPa, which is supported by similar values of 0.4-0.85 MPa from other literature (Agache, Monneur, Leveque, & De Rigal, 1980). Barel et al. reported a stiffness of 1.12 MPa for suction testing, which is slightly greater than other values of literature (Hendriks, 2005; Zahouani et al., 2009). However, the values obtained were based on locations dissimilar than the tensile experiments. These reports confirm the

anisotropic properties of skin as determined years ago, which is demonstrated by differing strengths with different force directions.

2.3 The Extracellular Matrix

The extracellular matrix (ECM) is a dynamic, biological substance composed of fibers and an interfibrillary matrix of glycosaminoglycans (GAGs) and proteoglycans, adhesive glycoproteins, solutes, and water. The ECM is synthesized by cells and deposited in the intracellular space so that it resides amongst the cells. The ECM structurally supports cells, provides a matrix to which cells can adhere, and provides biological cues and signaling that can influence cell behavior (Badylak, 2007). According to Schoen and Mitchell, the ECM has seven principle functions: (1) mechanical support for the cell, (2) determination of cell orientation, (3) control of cell growth, (4) maintenance of cell differentiation, (5) scaffolding for orderly tissue renewal, (6) establishment of tissue microenvironment, and (7) sequestration, storage, and presentation of soluble regulatory molecules (Schoen & Mitchell, 2004).

The cells within the tissues not only synthesize and secrete the matrix, but they also remodel it. The composition of the ECM is modified according to stimuli that instruct the cells to reorganize and reconstitute the matrix. Fibroblasts and smooth muscle cells predominately synthesize interstitial ECM, and epithelial cells typically synthesize the matrix for the basement membrane of the tissue. Almost all cells, however, are capable of secreting and breaking down ECM, to an extent (Schoen & Mitchell, 2004)

Cell-cell and cell-ECM communications are crucial for cellular survival and tissue formation. The matrix can be characterized by the secreted constituents that contribute to this cell-ECM signaling; they are collagen, elastin, glycosaminoglycans (GAGs) and proteoglycans, and adhesive glycoproteins (Rosso, Giordano, Barbarisi, & Barbarisi, 2004). Collagen is the dominant protein within the ECM (Badylak, 2002) and provides the extracellular framework for all multicellular organisms. Collagen not only serves as the mechanical strength and structural

organization of the matrix, but it also influences cell spreading and movement (Rosso et al., 2004). Elastin is also present in the matrix and gives tissues the ability to passively recoil due to its capability to stretch. Although minute quantities exist in the matrix of most tissues, elastin is typically found in larger quantities in the matrix of heart valves, the aorta, and in the walls of arteries (Schoen & Mitchell, 2004).

The nonfibrillar components (GAGs, proteoglycans, and adhesive glycoproteins) of the matrix have various functions, including lubrication, cell movement and differentiation, cell growth, and cell attachment (Rosso et al., 2004; Schoen & Mitchell, 2004). GAGs are long-chained polysaccharides, that when bound to proteins, are termed proteoglycans (Schoen & Mitchell, 2004). They contribute to pressure resistance, water retention, and very importantly, the binding of growth factors and cytokines (Badylak, 2002). Common GAGs include hyaluronic acid, chondroitin sulfate and dermatan sulfate, heparin sulfate and heparin, and keratin sulfate (Schoen & Mitchell, 2004). Without the signaling from the growth factors and cytokines, cellular processes would be impeded.

Fibronectin and laminin are two very common adhesive proteins within the matrix. Fibronectin is no longer purely characterized by its structural properties, but also by its ability to facilitate cell behavior (Badylak, 2002). Fibronectin is of significant importance in binding cells to the matrix and is essential for cell movement, and differentiation (Rosso et al., 2004; Schoen & Mitchell, 2004). It also helps form fibrin clots (Schoen & Mitchell, 2004), making it a crucial component of wound healing and necessary for an ECM scaffold for dermal wound healing. Laminin, on the other hand, not only assists in cell sitting and tissue remodeling (Schoen & Mitchell, 2004), but it is paramount for the formation and regulation of vascular constructs within the matrix (Badylak, 2002). As will be discussed later, vascularization in TE-scaffolds is a complex challenge; laminin provides one technique to help induce this property.

2.4 Dermal Injury

In fulfilling its role as a barrier between the body and the environment, skin is exposed to many external insults. The most common causes of cutaneous wounds are burns, physical trauma, surgery, and pathologically induced chronic ulcerations (Macri & Clark, 2009). It is estimated that there are approximately 35 million cases of significant skin loss annually which require clinical intervention (Clark et al., 2007). Of these, 20% develop into chronic, difficult-to-heal, wounds. In the United States alone, approximately 6.5 million patients suffer from chronic wounds, and it is estimated that more than \$25 billion is spent annually for the treatment of chronic wounds in the US (Sen et al., 2009).

2.4.1 Natural Course of Wound Healing

When a wound occurs and the epidermal barrier is broken, the body responds by initiating a cascade of events to maintain homeostasis. If it is an acute wound, it tends to undergo a natural, non-pathological course of repair. The natural process of wound healing is a highly organized and dynamic series of events involving three interdependent stages: inflammation, tissue formation/proliferation, and tissue remodeling. Each phase is marked by a series of complex interactions between different cells and biochemical signals (Freinkel & Woodley, 2001).

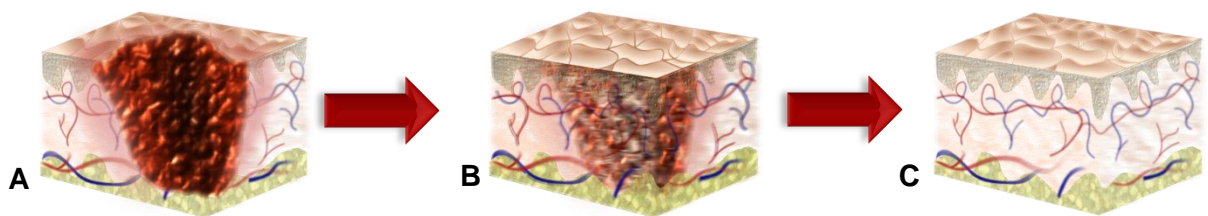


Figure 2: Three phases of natural wound healing. (A) Inflammation, (B) tissue formation/proliferation, and (C) tissue remodeling

2.4.1.1 Inflammation

The phase of inflammation (see Figure 2) begins immediately after an injury and often lasts for 4-6 days (Shai, 2005). The cascade of events is initiated by the disruption of blood vessels and the subsequent accumulation of platelets in the site of the injury. The platelets are responsible for forming a fibrin-rich clot to act as a barrier between the blood stream and the external environment. The fibrin clot also acts as a provisional matrix for supporting the later phases of wound healing (Freinkel & Woodley, 2001). The activated platelets also play a major biochemical role by releasing numerous growth factors and cytokines to recruit and activate neutrophils, monocytes, keratinocytes, and fibroblasts to the wound site (Macri & Clark, 2009). The structural cues and chemoattractants which are presented by the provisional matrix are thus crucial for initiating a natural course of wound healing.

Neutrophils migrate into the wound scene within minutes of the injury and remain there for 1-2 days, clearing infections and cellular debris by phagocytosis. As the wound is cleared, neutrophils reduce in number and slowly recruit macrophages. Both neutrophils and macrophages are responsible for releasing many cytokines and chemoattractants into the wound, including tumor necrosis factor- α (TNF- α), transforming growth factor- α (TGF- α), TGF- β , interleukin-1, and fibroblast growth factor (Freinkel & Woodley, 2001). These chemical signals bring in keratinocytes and fibroblasts for re-epithelialization and matrix synthesis.

2.4.1.2 Tissue Formation and Proliferation

The tissue formation phase involves many major events including re-epithelialization, extracellular matrix formation, and angiogenesis. The main contributors of this phase are the keratinocytes and fibroblasts. Re-epithelialization overlaps greatly with the inflammatory phase, beginning within hours of the injury. Re-epithelialization is marked by the migration of keratinocytes from the surrounding epidermis to the surface of the wound. Keratinocytes express integrins $\alpha_5 \beta_1$ and $\alpha_2 \beta_1$, which are important for their migration onto fibronectin and

collagen filaments, respectively. Ideally, the body seeks to close the wound with an epithelial layer before it begins to structurally rebuild the inner dermal tissue (Shai, 2005). One or two days after the injury, the surface keratinocytes begin to proliferate and cover the wound (Freinkel & Woodley, 2001). Fibroplasia begins within 2 days of the injury. It is characterized by the formation of granulation tissue and reconstruction of the dermal matrix (Macri & Clark, 2009). Fibroblasts are the main directors of this process, replacing the fibrin-fibronectin provisional matrix with more stable extracellular components. Upon migrating and repopulating the wound, they begin to reconstitute the dermal matrix and synthesize numerous extracellular components including types I and III collagen, elastin, glycosaminoglycans, and proteoglycans (Freinkel & Woodley, 2001).

Angiogenesis refers to the process of new vessel formation and is also known as neovascularization. This process occurs simultaneously with fibroplasia and is directed by endothelial cells. The migration and proliferation of endothelial cells in the wound site is dependent on several chemotactic signals. Fibronectin and heparin are responsible for the migration of the cells into the wound, while TGF- β , FGF, and VEGF stimulate angiogenesis (Freinkel & Woodley, 2001). The TGF- β family of growth factors is in part responsible for many of the physiologic processes during wound healing. It plays a role in fibroblast proliferation and ECM production, mediates the differentiation of fibroblasts, and enhances angiogenesis (Shai, 2005).

After the reconstitution of much of the matrix, the wound begins to contract. Contraction is mediated by fibroblasts which undergo a phenotypic change into myofibroblasts. These cells are actin-rich and morphologically similar to smooth muscle cells. Their contraction of the wound is the primary factor responsible for wound closure. Depending on the depth of the wound, contraction can contribute to approximately 40% reduction of wound size (Freinkel & Woodley, 2001).

2.4.1.3 Tissue Remodeling

The third and final stage of wound healing is tissue remodeling. It begins at the same time as tissue formation and continues for months. During this time, type I collagen replaces the type III collagen of granulation tissue, eventually forming more stable scar tissue. Within one month, the tissue will have regained 40% of its original strength, and over time it can regain as much as 70-80% of its tensile strength as compared to pre-injured skin (Shai, 2005). The remodeling phase is directed by both matrix-degrading metalloproteinases (MMPs), which break down collagen, and by fibroblasts, which replace the type III collagen with type I. The actions of these contributors are dependent on a number of growth factors, as well as the ECM itself. Interleukin-1 stimulates the synthesis of MMPs, while natural polymers such as fibronectin and hyaluronic acid provide a foundation for the production of collagen and cellular locomotion (Freinkel & Woodley, 2001).

2.4.2 Chronic Wounds

A chronic wound is defined as any wound which fails to progress through the natural phases of wound healing, and therefore remains in a pathologic state of inflammation (Menke, Ward, Witten, Bonchev, & Diegelmann, 2007). The degree of chronicity of a wound is defined by many factors, but it is generally agreed upon that if a wound does not heal within 3-4 months, then it can be defined as a “chronic cutaneous ulcer” (Shai, 2005). In contrast to an acute wound, a chronic ulcer occurs as a result of an underlying pathology. Acute wounds can develop into chronic non-healing ulcers in patients with diabetes mellitus, venous insufficiency, or immobility (Macri & Clark, 2009; Shai, 2005). In the United States 2-3 million individuals are at risk of developing chronic diabetic ulcers; 600,000 of developing venous leg ulcers; and 2-3 million of developing pressure ulcers as a result of immobility (Macri & Clark, 2009).

2.4.3 Wound Infection

Infection is a major problem faced by patients with chronic wounds, often leading to morbidity and mortality (Siddiqui & Bernstein, 2010). It is responsible for 75% of all deaths in patients with burns wounds exceeding 40% TBSA (Rode, Vale, & Millar, 2008).

The presence and activity of various microbes on a wound determines whether or not an infection will occur. The concentration of bacteria and the significance of their proliferation results in different levels of chronicity, as shown on Figure 3 (Siddiqui & Bernstein, 2010). Contamination is the transient presence of non-multiplying bacteria on a wound. This can occur in almost all wounds. Colonization occurs when bacteria are multiplying but do not initiate any pathogenic response from the host. Critical colonization is the point at which the bacteria contact healthy tissue, initiating a host response and causing the wound to enter a non-healing, chronic inflammatory state. Symptoms of critical colonization include deterioration of granulation tissue, discoloration of tissue to deep red or gray color, increased wound friability, and increased drainage (Siddiqui & Bernstein, 2010). Infection occurs when the bacterial proliferation rate surpasses host response, resulting in direct injury to the deep tissues of the host. Clinically, infection is defined by a deep tissue quantitative microbial count of $>10^5$ cfu/ml (colony-forming units/ml tissue) (Landis, 2008).

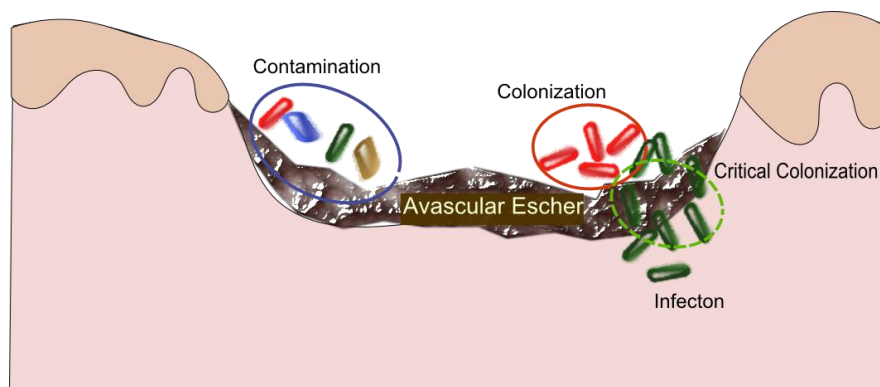


Figure 3: Spectrum of Bacterial Contamination-to-Infection (adapted from Siddiqui & Bernstein, 2010)

The necrotic tissue in wounds provides a favorable niche for bacterial colonization and proliferation. The dead tissue provides a rich source of protein for bacterial growth and is inaccessible by both the circulatory and immune systems, allowing infections to develop undetected. The colonized bacteria may produce biofilms which further protect them from host defense mechanisms. These biofilms can develop within 10-72hrs (Rode et al., 2008).

In burn wounds, gram-positive bacteria, including *Staphylococcus* and *Enterococcus* strains, are the first to colonize because they are normally present in the glands and hair follicles of healthy skin (Landis, 2008). Within one week, gram-negative bacteria, such as *Pseudomonas*, *Klebsiella* and *Escherichia* species can overpopulate the wound. These species are natively in the respiratory and gastrointestinal tracts, but tend to spread in the hospital environment. They present the most concerning clinical burden in wounds, as they often have high virulence and possess antimicrobial resistant traits (Church, Elsayed, Reid, Winston, & Lindsay, 2006).

Table 1: Microorganisms Causing Invasive Wound Infections (adapted from Church et al., 2006)

Group	Species
Gram-positive	<i>Staphylococcus aureus</i>
	Methicillin-resistant <i>S. aureus</i>
	Coagulase-negative staphylococci
	<i>Enterococcus</i> spp.
	Vancomycin-resistant enterococci
Gram-negative	<i>Pseudomonas aeruginosa</i>
	<i>Escherichia coli</i>
	<i>Klebsiella pneumoniae</i>
	<i>Serratia marcescens</i>
	<i>Enterobacter</i> spp.
	<i>Proteus</i> spp.
	<i>Acinetobacter</i> spp.
	<i>Bacteroides</i> spp.
Fungi	<i>Candida</i> spp.
	<i>Aspergillus</i> spp.
	<i>Fusarium</i> spp.
	<i>Alternaria</i> spp.
	<i>Rhizopus</i> spp.
	<i>Mucor</i> spp.
Viruses	Herpes simplex virus
	Cytomegalovirus
	Varicella-zoster virus

The prevalent bacterial species found in wounds are *Staphylococcus aureus*, present in 93.5% of wounds; *Enterococcus faecalis*, present in 71.7% of wounds; and *Pseudomonas aeruginosa*, present in 52.2% of wounds (Gjodsbol et al., 2006). Fungal wound infections also occur, and are most commonly caused by *Candida* species. Fungal infections occur in 30% of burn wounds, and are usually prevalent after patients have undergone treatment with broad-spectrum antibiotics. Their presence in wounds increases the risk of mortality for the patient (Rode et al., 2008). Other species of microbes which contribute to wound infections are listed in Table 1.

2.5 Current Treatments

In choosing the proper treatment for a wound, the wound depth is one of the most important factors to be considered (James, 2009). Wounds can be classified as either partial-thickness, where the injury extends through a portion of the dermis, or full-thickness, where the entire dermis and parts of the subcutaneous layers are damaged. While most acute and superficial wounds can be treated with topical medication and dressings, full-thickness wounds and chronic ulcers require more localized regenerative therapies to achieve healthy wound healing (Téot, 2010). If left untreated, the damaged tissue of a full-thickness wound begins to break down within 24-48h and becomes highly susceptible to bacterial infection (James, 2009). Depending on the condition of the wound and whether or not necrotic and infected tissue is present, the physician may need to debride the wound.

2.5.1 Debridement

Debridement involves the removal of devitalized and infected tissue to stimulate wound healing (Shai, 2005). Common methods of debridement include surgical removal, hydration or absorption to control the moisture of the wound, and enzymatic or chemical break down of necrotic material (Shai, 2005). Following debridement, the wound is left clean with the potential to undergo a natural course of repair. The use of skin substitutes and grafts is often required to support the normal wound healing process (Shai, 2005).

2.5.2 Antimicrobial Treatments

As mentioned earlier, the presence of necrotic tissue is the major predisposing factor for the onset of bacterial wound infections. Thus, when a wound contains devitalized tissue, topical antimicrobial treatments alone are not always effective. Wound site excision or debridement is often required to clean the wound and expose living and active dermal tissue. Antimicrobial treatments are only applied once the wound has been cleaned and excess surface bacteria is removed (Rode et al., 2008).

Antimicrobial treatments can be categorized into two types: antiseptics and antibiotics. Antiseptics are chemicals which have a broad spectrum of toxicity against microbes, whereas antibiotics are characterized by more specific mechanisms of action which target a narrow-spectrum of microbes (Siddiqui & Bernstein, 2010). Antiseptics, usually used topical treatments, are usually alcohols (ethanol, isopropanol), biguanides (chlorhexidine, polyhexadine), sodium hypochlorite solutions, halogen compounds (pyrrolidone iodine), heavy metals (silver), or peroxygens (hydrogen peroxide). Topical antiseptics are used in fresh wounds to prevent infection, or in more established wounds to reduce bacterial count below 10^5 cfu/mL of tissue (Rode et al., 2008). A list of commonly used antiseptics is summarized in Table 2. These antimicrobial treatments are not universally effective; each treatment having its own spectrum of activity, as well as corresponding limitations. Although they can reduce microbial burden, these treatments are not able to sterilize the wound. Use of any one agent for an extended period of time can often cause bacterial resistance, so it is usually recommended that patients rotate between using different agents. Because of this, antimicrobial therapies often require the use of multiple types of antiseptic agents. Finally, a closed dressing is required to maintain continuous contact between the antimicrobial agent and the burn wound (Rode et al., 2008).

Table 2: Types of Topical Antiseptic Treatments (adapted from Rode et al., 2008)

Agent	Application Frequency	Escher Penetration	Action
Sodium hypochloride (NaOCl 0.025%)	Daily for 20 - 30 minutes	Surface action	Bactericidal to Gram (+) and (-) organisms including MRSA and <i>Pseudomonas</i>
Silver-sulphadiazine 1%	12-hourly liberal application	Limited	Bactericidal for many Gram (+) and (-) organisms including yeasts
Povidine iodine	6 hourly	Limited	Bactericidal, broad-spectrum bacterial and antifungal activity
Mupirocin	Daily	Excellent	Bactericidal, broad-spectrum bacterial and antifungal activity
Chlorhexidine	Daily		Bactericidal, especially against <i>Pseudomonas</i>
Nanocrystalline silver	3 - 4 days	Excellent	Bactericidal to more than 150 bacteria and yeasts

Systemic antimicrobial treatments, or antibiotics, have received some controversy in relation to their effectiveness and accompanying risks. Although antibiotics are often used to treat or prevent invasive systemic infections, they have not proven to be any more effective than topical antiseptics in treating the actual wound site (Rode et al., 2008). In addition to this doubt, there is the concern associated with the risk of producing antimicrobial resistant bacteria. Because wounds host an environment for polymicrobial growth, there is ample opportunity for microbes to share genes for antimicrobial-resistance. This issue is a growing concern for public health, and thus use of systemic antibiotics is under more regulation. Systemic antibiotics are only used in cases where wound infection cannot be controlled by topical intervention. These cases include sepsis, cellulitis, lymphangitis, abscess formation, and when tissues present signs of an invasive microbial species (Siddiqui & Bernstein, 2010).

2.5.3 Skin Grafting

Full-thickness wounds with large voids and extensive tissue loss exhibit impaired wound healing because the native parenchymal cells cannot completely rebuild the original structure of the tissue. Instead, a large amount of granulation tissue is applied to fill the defect. If left to heal naturally, the granulation tissue leads to scar formation and hypercontraction (Morgan et al., 2004), leaving the wound site mechanically compromised. In the case of wounds near joints, such as the wrist or hand, the contracted scar tissue can distort the natural position of the joint and even limit its mobility (Klein, 2010).

In order to reduce scar formation and support functional regeneration of the dermis, skin grafts are often recommended for use in full-thickness wound healing. Skin grafts are referred to as “biological dressings” used for wound coverage, wound closure, or both. Epidermal grafts are developed for partial thickness coverage, while dermal grafts are intended for full-thickness wound closure. For purpose of this review, dermal substitutes are described in context of their general use for wound closure. There are currently several substitutes commercially available for patients. These products range in functional depth, source type, duration of coverage, and overall composition. The most common types are listed in Table 3.

2.5.3.1 Autografts

The gold standard for dermal substitution is via an autograft, where healthy skin is harvested from a patient’s own body and transplanted to the wound site. Using autologous skin eliminates both the search for a donor and the possibility of immunological rejection. A drawback with using a patient’s own skin arises when wounds cover more than 50% of the total body surface area such as in burn victims (Klein, 2010). Another limitation with transplanted skin flaps is its conditional success. In order for an autograft to be successful, the transplanted skin needs to be re-vascularized at the wound site. If the transplant does not “take,” or become incorporated with its new environment, then the tissue will become necrotic. The use of

autologous grafts can create multiple wound sites, results in slow recovery in areas with high mesh expansion ratios, and ultimate scarring and disfiguration of the skin (James, 2009).

Other, similar options include autologous cultured skin substitutes, such as Epicel (Genzyme Biosurgery). Autologous based cell-derived products require a skin biopsy, as well as several weeks of culturing (Shores, Gabriel, & Gupta, 2007).. Leaving a full-thickness wound untreated for more than 48 hours, however, can result in the breakdown of damaged tissue, and an increased risk of infection (James, 2009). Another disadvantage is the high cost associated with the customized treatment;~\$13,000 per 1%TBSA (Clark et al., 2007). Despite, the apparent advantages of using one's own skin for regeneration, patients with pathological or extensive wounds are often prompted to choose from several other clinically available substitutes.



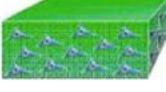











2.5.3.2 Allogeneic Grafts

Allogeneic grafts are donated from individuals for transplanation onto another pateint's wound site. Using *living* cadaver skin as an allograft provides natural qualities, however these kinds of substitute need to be removed 10-21 days after application because they tend to elicit an immune response.In order for these products to be successfully accepted by the host, they need to be processed and decellularized prior to transplantation. (Van der Veen, 2011). Some commercially available human allografts include AlloDerm (Life Cell), and GraftJacket (Wright Medical Technology).

Acellular dermal allografts consist of decellularized dermis obtained from human cadaveric donors. The scaffolds are cryopreserved, lyophilized and glycerolized to reduce immunogenic response, but preserve the structural and functional integrity of the graft. In a wound, they serve as a template for the ingrowth of fibroblasts, as well as vascularization. These products are available commercially from skin-banks. The drawback with these products is that they are dependent on the availibility of cadaveric donors (James, 2009). There is also the risk of infectious disease transmission and immunorejection from cellular remnants. Both

Alloderm and GraftJacket show remnants of donor DNA, which could result in disease transmission (Shores et al., 2007).

Table 3: Dermal Substitutes (James, 2009)

Brand Name / Manufacturer	Schematic Representation	Incorporated Human Cells	Cell/ Scaffold Source	Scaffold Material
AlloDerm[®] LifeCell Corporation, Branchburg, NJ, USA		—	— / allo	human acellular dermal matrix
Biobrane[®] / Biobrane[®]-L UDL Laboratories, Inc., Rockford, IL, USA		—	— / xeno	silicon film, nylon fabric + collagen
Demigraf[®] Advanced BioHealing, Inc., New York, NY and La Jolla, CA, USA		Cultured neonatal fibroblasts from foreskin tissue	allo / —	PGA/PLA + ECM
EZ Derm[™] Brennen Medical, Inc., MN, USA.		—	— / xeno	aldehyde crosslinked porcine dermal collagen
GraftJacket[®] Wright Medical Technology, Inc., Arlington, TN, USA		—	— / allo	human acellular dermal matrix
Hyalograft[®] 3D Fidia Advanced Biopolymers, Abano Terme, Italy		Cultured fibroblasts	auto / —	HAM
Hyalomatrix[®] PA Fidia Advanced Biopolymers, Abano Terme, Italy		—	— / —	HYAFF layered on silicone membrane
Integra[®] Dermal Regeneration Template Integra NeuroSciences, Plainsboro, NJ, USA		—	— / xeno	polysiloxane (silicone), cross-linked bovine tendon collagen + GAG
Matriderm[®] Dr. Suwelack Skin & Health Care AG, Billerbeck, Germany		—	— / xeno	bovine collagen and elastin
OASIS[®] Wound Matrix Cook Biotech Inc., West Lafayette, IN, USA		—	— / xeno	porcine acellular small intestine submucosa
Permacol[®] Surgical Implant Tissue Science Laboratories plc, Aldershot, UK		—	— / xeno	cross-linked porcine acellular dermal collagen
SureDerm[™] HANS BIOMED Corporation, Seoul, Korea		—	— / allo	human acellular dermal matrix
Terudermis[®] Olympus Terumo Biomaterial Corp., Tokyo, Japan		—	— / xeno	silicone, lyophilized collagen sponge of heat-denatured bovine atelocollagen
TransCyte[®] Advanced BioHealing, Inc., New York, NY and La Jolla, CA, USA		cultured neonatal fibroblasts	allo / xeno	silicon film, nylon mesh, porcine dermal collagen

PGA – polyglycolic acid (Dexon[™]); PLA – polylactic acid (Vicryl[™]); ECM – extracellular matrix, derived from fibroblasts; HAM – Hyaluronic Acid Membrane (microperforated); HYAFF[®] – a derivative of hyaluronan; GAG – glycosaminoglycan.

2.5.3.3 Xenografts

Xenografts are tissues obtained from other species. Most commonly, dermal substitutes are isolated from porcine and bovine tissues. Some commercially available xenografts include OASIS (Healthpoint Ltd) and Permacol (Tissue Science Laboratories). OASIS is decellularized porcine submucosa, while Permacol is decellularized and crosslinked porcine collagen dermis. Xenografts are usually temporary grafts and require changing every 2-4days (Shores et al., 2007).

2.5.3.4 Natural and Synthetic Scaffolds

Other commercially available products, include natural and synthetic scaffolds such as Apligraf (Organogenesis) and Integra (Integra Neurosciences) are aimed at providing a structural base for dermal regeneration. Both of these products use bovine collagen. Integra includes a synthetic silicone layer to act as a permanent barrier at the wound site. Apligraf is seeded with both neonatal fibroblasts and neonatal keratinocytes, giving it a shelf life of approximately ~5days. Because of its living components, the cost of this graft is among the highest, ~\$30/cm². In addition, it often requires multiple applications for wound treatment every 4-6 weeks (Shores et al., 2007).

2.6 ECM Scaffolds for Dermal Regeneration

The extracellular matrix (ECM) is an appealing alternative material for scaffolds over many other biological and synthetic polymers for skin therapies. Not only does the ECM provide structural support in the wound bed for cell proliferation, migration, and differentiation, but it also has mechanical properties and fiber orientation that matches the native tissue. Furthermore, ECM scaffolds provide the biological growth factors and cytokines that modulate and propagate signals of the wound healing response (Liu et al., 2007; Lu, Hoshiba, Kawazoe, Song, & Chen, 2011; Macri & Clark, 2009).

2.6.1 Decellularized Tissue-Derived ECM

The initial and most widely used method to isolate ECM for acellular scaffolds is the decellularization of tissues and organs. Many of these tissue-derived ECM scaffolds have been successfully applied in human clinical applications, including but not limited to scaffolds for tissue reconstruction, urethral repair, tendon ruptures, rotator-cuff repairs, and for full-thickness burns (Gilbert, Sellaro, & Badylak, 2006). Extensive research has also been conducted using decellularized heart valves, blood vessels, urinary bladder, small intestine submucosa, and liver (Gilbert et al., 2006). For skin, cadaver or bovine skin is commonly decellularized to create an ECM scaffold (Zhong et al., 2010). The assumption for animal skin is that extracellular components are conserved among species, allowing the acellular graft to be tolerated by xenogeneic graft recipients. The goal of decellularization is to remove all of the cellular and nuclear components of the tissue to circumvent the foreign body response that plagues many of the synthetic materials and allogenic or xenogenic grafts used for therapeutic regeneration (Gilbert et al., 2006).

2.6.2 Decellularization Process

There are varieties of different decellularization techniques that can be used to isolate the extracellular matrix from the cellular components in tissues (Table 4). Each step of the process has the potential to impact the composition or structure of the desired ECM; therefore, depending on the desired biochemical composition and structure, biological activity, and mechanical behavior to be retained in the scaffold, techniques that minimize damage to these properties should be selected (Gilbert et al., 2006). The method proceeds by disrupting the cell membrane, separating the cellular components, and then removing the cellular debris. Physical, chemical, and enzymatic treatments are used to ensure that all cells are adequately exposed and removed from the scaffold (Gilbert et al., 2006).

Table 4: Various Decellularization Methods (Gilbert et al., 2006)

Technique	Mode of action	Effects on ECM
Chemical Agents		
Sodium dodecyl sulfate (SDS) – Ionic detergent	Solubilize cell and nucleic membranes, can denature proteins	Effectively removes nuclear remnants and cytoplasmic proteins from dense tissues, removes GAG and growth factors and damages collagen
Hypertonic / Hypotonic Solutions	Cell lysis by osmotic shock, disrupts DNA-protein interactions	Effectively lyses cells Does not effectively remove cellular residues
Triton X-100 (Non-ionic detergent)	Disrupt DNA-protein interactions, disrupt lipid-lipid and lipid-protein interactions, and sometimes protein-protein interactions	More effective cell removal on thin tissues, some disruption of ultrastructure and removal of GAG, less effective than SDS
Biologic Agents		
Nucleases (enzyme)	Catalyze the hydrolysis of ribonucleotide and deoxynucleotide chains	Mixed results with efficacy dependent on tissue, dense tissues lost collagen but impact on mechanical strength was minimal
Trypsin (enzyme)	Cleaves peptide bonds on the C-side of Arg and Lys	Prolonged exposure can disrupt ECM ultrastructure, removes ECM constituents (collagen, laminin, fibronectin, elastin, and GAG), slower removal of GAG compared to detergents
Chelating Agents (EDTA)	Bind metallic ions to disrupt cell adhesion to the ECM	Ineffective when used alone
Physical Agents		
Temperature (Freezing and thawing)	Intracellular ice crystals disrupt cell membrane	Can disrupt or fracture ECM
Direct application of force	Removal of tissue eliminates cells and force can burst remaining cells	Can directly damage ECM
Pressure	Burst cells and aid in cellular removal	Can disrupt ECM
Electroporation (Pulsed electrical fields)	Disrupt cell membranes	Can disrupt ECM

The purpose of physical decellularization treatments is to disrupt the cell membrane so that cellular components are released and washed away. Agitation, sonication, mechanical pressures, or freeze and thaw cycles can cause physical disruption. Physical treatments do not

remove all of the cellular components and must be combined with chemical treatments for complete decellularization. Enzymes, such as trypsin, and chemicals, including ionic solutions, detergents, and chaotropic agents, are used to disrupt the membranes and break the bonds between intracellular and extracellular components (Gilbert et al., 2006). It is extremely important that none of the chemicals remain in the tissue after treatment. A high concentration of chemical residues will cause the scaffold to be toxic to the host (Gilbert et al., 2006).

Unfortunately, both physical and chemical treatments used to remove the cells have the potential for disrupting the 3D architecture of the scaffold (Gilbert et al., 2006). A variety of histological stains can be used to verify the preservation of tissue architecture as well as the removal of cellular components. Hematoxylin and Eosin (H&E) can be used to validate the removal of nuclear structures as well as observe the structure of the tissue. Masson's Trichome, Movat's Pentachrome, or Safrin O can be used to identify cytoplasmic and extracellular molecules remaining in the matrix. Picrosirius Red can be used to observe and subsequently verify the amount of collagen retained in the decellularized tissue. DNA can be identified using the fluorescent molecules DAPI or Hoechst, which have an affinity for double stranded DNA (Gilbert et al., 2006).

Similarly, a variety of techniques are needed to quantify the retention of components in the matrix. This data can be achieved by using identification assays for GAGs, growth factors, adhesion proteins, elastin, and collagen. The integrity of the ECM structure can also be examined using mechanical testing (Gilbert et al., 2006).

Typically, the best strategy is to use the mildest available decellularization approach first to minimize disruption of the extracellular matrix (Gilbert et al., 2006) These include hypotonic or hypertonic solutions. For the decellularization of fibroblasts for cell-derived ECM scaffolds, Lu et al. used freeze-thaw cycling and NH_4OH aqueous solution treatment (Liu et al., 2007; Lu et al., 2011). The freeze-thaw cycles create intracellular ice crystals that disrupt the cell membrane, and

the ammonium hydroxide solubilizes cytoplasmic components of the cell and disrupts nucleic acids (Gilbert et al., 2006).

However, decellularizing tissue to derive ECM scaffold has limitations. When allogenic or xenogenic tissue are used, there is the potential for host rejection or the transfer of pathogens from the host to the patient (Gilbert et al., 2006; Lu et al., 2011).

2.6.3 Advantages of cultured cell-derived extracellular matrix scaffolds

Cultured cells provide an alternative source of tissue for therapeutic scaffolds. These cell-derived tissues can be decellularized to isolate the extracellular matrix produced by the cells. Preparing ECM in this way provides numerous advantages over using decellularized human or animal skin. First, the three-dimensional architecture of the scaffold enhances the activity of the cells seeded on to it. Cukierman et al. showed that cell-derived 3D matrices were more effective than 2D substrates for fibroblast attachment, migration, proliferation, and characteristic in vivo morphology. Additionally, there are techniques available for screening cultured cells for pathogens and maintaining them in a pathogen-free condition. Cell-derived ECM scaffolds also provide the option of using the patient's own autologous cells, which can be expanded in the laboratory for scaffold fabrication. Although the decellularization method should be sufficient to remove foreign material, these autologous cell-derived ECM scaffolds avoid any undesired host responses that can be induced by allogenic or xenogenic materials. In addition, the procedure for isolating patient cells is much less invasive than taking an autologous graft, and can be beneficial for patients with limited undamaged donor sites. Therapeutic ECM scaffolds are not limited to autologous cells; a variety of cell types including mesenchymal stem cells (MSC), chondrocytes, and fibroblasts have been explored for their ECM matrix effects on cell function and tissue regeneration (Lu et al., 2011). However, there are still limitations with cell-derived matrixes. Fabricating the scaffolds from cells takes more time than decellularizing

tissue. Additionally, the decellularization and processing methods can affect the structure and mechanical strength of the scaffold (Gilbert et al., 2006).

2.6.4 Strategies for enhancing extracellular matrix scaffolds

Many techniques have been explored to enhance the wound regeneration capabilities of both synthetic and natural scaffolds. These techniques can be applied to tailor ECM scaffolds to enhance their therapeutic efficiency.

2.6.4.1 Growing cell-derived scaffolds on 3D matrices

One of the desired characteristics of a scaffold includes the formation of a physiologically and anatomically similar architecture to native skin. For cell-derived tissues, removable substrates can be used as a templates to encourage three-dimensional (3D) cell culture (Lu et al., 2011). The three-dimensional architecture has numerous advantages over a scaffold produced by two-dimensional growth on a flat surface. In the case of skin, three-dimensional substrates affect the presentation of fibroblast focal adhesions, and subsequently keratinocyte attachment, proliferation, and differentiation. The limitation with two-dimensional growth of fibroblasts is the production of an artificial polarity that is not normally present, affecting the morphology and migration of the fibroblasts (Cukierman, Pankov, Stevens, & Yamada, 2001). Cukierman, et al. tested a variety of 2D and 3D matrices to determine which was the most effective at mediating cell adhesion, enhancing migration and proliferation rates, and achieving an accelerated rate of fibroblastic spindle-shaped morphology. The substrates that were tested were cell-derived 3D matrices, tissue-derived 3D matrices, 3D collagen gels, and 2D ECM substrates of fibronectin, laminin, and collagen I. After exploring their interaction with fibroblasts, cell-derived 3D matrices were the most effective at the abovementioned tasks. In these three-dimensional cell-derived structures, α_5 integrin, paxillin, and fibronectin triple co-localize; this may be a more physiologically similar matrix adhesion, which accounts for the

enhanced cell interactions seen on the cell-derived 3D matrices as opposed to matrices derived from tissue, collagen, or 2D ECM substrates (Cukierman et al., 2001).

2.6.4.2 Cell-specific ECM Production

The most common cell types used for skin scaffold fabrication are skin cells themselves: the keratinocytes of the epidermal layer and the fibroblasts of the dermis. Using the cell type naturally found in the tissue of interest will provide the most natural three-dimensional structure, mechanical properties, and chemical cues to promote proper regeneration. Researchers have used fibroblasts to make cell-derived dermal substitutes as well as acellular scaffolds (Lu et al., 2011; Tremblay, Hudon, Berthod, Germain, & Auger, 2005). Dermal fibroblasts are not only easily isolated from neonatal foreskin, but they also maintain steady collagen synthesis and growth rate until passage 14 (Ahlfors & Billiar, 2007; Lu et al., 2011).

One of the advantages of using cell-derived tissues is that a variety of cells can be used to obtain the optimal scaffold. ECM production can be mixed by the in vitro culture of different cell types to produce the desired ECM proteins (Lu et al., 2011).

2.6.4.3 Pre-vascular Networks

Multiple strategies have been used to induce angiogenesis in scaffolds. Delayed vascularization is one of the leading problems with skin substitutes that are currently used for full-thickness wounds (Tremblay et al., 2005). A lack of vasculature leads to poor graft take and ultimately graft necrosis. In fact, when Krejci et al. implanted decellularized dermis with keratinocytes into mice, they found that it took up to 15 days for neovascularization to occur (Krejci, Cuono, Langdon, & McGuire, 1991). This process is limited by the thickness of the graft, and relies on passive diffusion of nutrients from the wound bed to the graft to be sufficient for graft survival. To solve this problem, researchers have been exploring methods to create a prevascular network in scaffolds that can promote blood supply through faster connection to the host's vascular system. This fact makes decellularized tissue an appealing therapy, because of

the pre-existing capillary network. It also brings forth the possibility of encouraging the growth of a vascular network during the culture of cell-derived tissues. Tremblay et al. proved that this method is possible. The researchers seeded a 1:1 ratio of human fibroblasts and human umbilical vein endothelial cells onto a collagen/glycosaminoglycan/chitosan biopolymer scaffold. After 5 days, keratinocytes were added to the culture. When these living cellular grafts were implanted into mice wounds, Tremblay et al. showed that complete inosculation of human vessels from the graft to mice vessels in the wound bed occurred within 2 to 5 days. Their study highlights the significance of growing an in vitro capillary network prior to scaffold implantation.

Because cell-derived ECM scaffolds are cultured in vitro, methods for the growth of a vascular network should be taken into consideration. Success would make the cell-derived ECM just as capable of rapid revascularization as decellularized cadaver skin. The addition of angiogenic growth factors, such as VEGF, may not lead to proficient vascularization, since the thickness of the dermal component will deter growth factor diffusivity (Tremblay et al., 2005). To date, no cell-derived ECM scaffold has been created with a prevascular network for improved angiogenesis.

2.6.4.4 Antimicrobial Peptides

Antimicrobial peptides (AMPs) are an emerging source for treatment of infections (Hancock & Sahl, 2006). AMPs are naturally occurring small molecular weight proteins, which possess a broad spectrum of antimicrobial activity against bacteria, fungi, and viruses (Izadpanah & Gallo, 2005). They are usually between 10 and 50 amino acids long, and overall cationic. Their amphiphilic structures allow them to target a broad range of microbes by electrostatically attaching to their surfaces (Hancock & Sahl, 2006).

Mammals produce a variety of AMPs which mostly fall into the categories of defensins or cathelicidins (Yang, Biragyn, Hoover, Lubkowski, & Oppenheim, 2004). These AMPs are most often expressed by epithelial cells as host-defense molecules. The human cathelicidin peptide,

LL-37, encoded by hCAP-18 has drawn considerable interests because of its expression by epidermal keratinocytes. In particular, the expression of LL-37 is upregulated in keratinocytes after a skin injury (Heilborn et al., 2003).

All cathelicidins contain an N-terminal signal peptide (pre-region), a conserved cathelin-like domain (proregion), and a microbiocidal peptide sequence along their C-terminus. “LL-37” refers to the microbiocidal domain of the human cathelicidin. After the expression and secretion of cathelicidin, proteinase-3 acts to cleave the proregion, leaving behind the cationic alpha helical LL-37. The broad range of bacteriocidal activities of LL-37 are summarized in Table 5. Cathelicidin is effective against a variety of both Gram-positive and Gram-negative bacteria, as well as *Candida* species of yeast.

Table 5: Range of Microbiocidal Activity of LL-37 (adapted from De Smet & Contreras, 2005)

Peptide	Organism	Gram-Stain	MIC (µg/ml)
LL-37	<i>Listeria monocytogenes</i>	Positive	1.5
	<i>Staphylococcus epidermis</i>	Positive	7.6
	<i>Staphylococcus aureus</i>	Positive	3.6
	MRSA	Positive	3.4
	<i>Bacillus subtilis</i>	Positive	2.7
	VREF	Positive	3.5
	<i>Escherichia coli</i>	Negative	0.1
	<i>Salmonella typhimurium</i>	Negative	0.4
	<i>Pseudomonas aeruginosa</i>	Negative	4.7
	<i>Burkholderia cepacia</i>	Negative	>79.1
	<i>Stenotrophomonas maltophilia</i>	Negative	1.9
	<i>Proteus mirabilis</i>	Negative	5.7
	<i>Proteus vulgaris</i>	Negative	2.5
	<i>Candida albicans</i>	Yeast	>250

In addition to its antimicrobial properties, it has been determined that LL-37 also promotes wound healing (Carretero et al., 2007). It acts as a chemoattractant for immune cells and has shown to directly induce chemokines on macrophage receptors. It also increases the production of several cytokines, including IL-6, IL-8, and TNF- α (Carretero et al., 2007). Several studies have determined that LL-37 also contributes to neovascularization, as well as cellular

growth (Bucki, Leszczynska, & Namiot, 2010). These unique properties show that cathelicidin has the potential to be used as a powerful tool in dermal regeneration.

The previous literature review was conducted to gain insight on dermal wound healing and the advantages and limitations of current therapies. Understanding the components of the ECM and the wound healing response is critical to fabricating a successful dermal template for tissue regeneration. The literature review will serve as the foundation for the design and fabrication an extracellular matrix scaffold that surpasses current limitations in dermal wound healing skin substitutes.

3 Project Definition and Strategy

In the United States alone, approximately 6.5 million patients suffer from chronic wounds, and it is estimated that more than \$25 billion is spent annually for the treatment of chronic wounds in the US (Sen et al., 2009). There are currently numerous dermal substitutes commercially developed for healing full-thickness wounds; however, these products are limited by donor supply, potential for transmission of disease, and are not cost-effective. There is currently a need for an ideal scaffold which is durable, cost effective, biocompatible, while also promoting regeneration, providing a barrier against water loss and microbes, promoting a new vascular network, and having the mechanical integrity and structural composition of the native dermis. The ultimate goal of our project is to meet these needs by developing a novel scaffold for dermal regeneration.

3.1 Initial Client Statement

At the start of this project, the client presented the design team with the following initial client statement:

“Design and fabricate a series [of] protocols and devices to produce a novel cell-derived matrix scaffold with structural, mechanical and biochemical properties that emulates the properties of a highly functional dermal regeneration scaffold.”

The goals of the project are to (1) design and create an experimental approach for fabricating a cell-derived matrix (CDM) with mechanical properties that mimic those of the natural dermis; (2) design the CDM to include angiogenic and antimicrobial properties that promote dermal regeneration with the scaffold; and (3) design a series of in vitro assays for analyzing the mechanical, angiogenic, and antimicrobial properties of the novel CDM scaffold.

3.2 Initial Approach

The design team first sought to gain a better understanding of the client statement. One of the first approaches the team used was to gather a large amount of background information.

The team used multiple sources to gain knowledge about extracellular matrix scaffolds, its importance to the tissue engineering field, its current use, and existing limitations with its design for dermal wound therapies. To achieve this goal, the team performed an extensive literature review by searching through electronic search engines such as Science Direct, Pubmed, and Google Scholar. These databases were used by searching keywords such as “extracellular matrix,” “dermal,” “scaffold,” “design,” “cell-derived,” “decellularized,” “regeneration,” “wound healing,” or any combination of those terms. The team also used the library catalogue to explore books related to scaffolds for tissue engineering, as well as two initial meetings with the client to gain an in-depth understanding of the goals of the design project.

3.3 Attributes List

After conducting the scientific literature review and initial meetings with the client, the design team approached the client’s problem statement by brainstorming the objectives of the design project. According to Dym and Little, an objective is “something toward which effort is directed” or “an aim or end of action.” In other words, objectives can be thought of as goals for the behavior or features that the client or user desires for the device. With this in mind, the design team formulated an initial attributes list for the bioactive scaffold described by the client statement.

List 1: Biological Scaffold Attributes List

- Non-viable scaffold
- Angiogenic
- Antimicrobial
- Structurally similar to native dermis
 - Porosity
 - Density
 - Thickness
 - Degradation rate
- Mechanical similar to native dermis
 - Tensile strength
 - Stiffness
 - Shear resistance
- Preservable

- Can be stored for extended time periods (up to years)
- Can be handled without fracture
- Simple in-vivo attachment/easy implantation
- No rejection
- Improved healing quality
- Quick wound healing
- Undergoes constructive/uniform remodeling
- Decreases formation of granulation tissue and scar formation
- Induces cellular migration
- Minimal preparation from shelf to body
- Non toxic
- Incorporation into native tissue
- Tailorable (shape, matrix components) to various wounds
- Only requires one application
- Human cell derived
- Low cost production
- Easy manufacturability

3.3.1 Pruned Objectives

The list was brought to the client for feedback and discussion. The client and design team eliminated the attributes which were constraints or functions and decided on five major goals for the characteristics of the ECM scaffold. These higher level objectives revert back to the original client statement, while the sub-objectives better define the major goals.

List 2: Biological Scaffold Attributes Indented Objectives List

0. *A novel cell-derived matrix scaffold for wound healing*
1. **Ease of production**
 - 1.1 Can be manufactured in large quantities
 - 1.2 Minimize production costs
 - 1.2.1 Minimal use of materials for scaffold production
 - 1.2.2 Minimal time required to complete all steps for fabricating matrix scaffold
2. **Structurally and mechanically similar to native dermal tissue**
 - 2.1 Permeable to cells
 - 2.2 Thickness of dermis
 - 2.3 Biomolecules should be able to diffuse at natural rate
 - 2.4 Tensile strength
 - 2.5 Stiffness
 - 2.6 Shear resistant
 - 2.7 Suture pullout strength
 - 2.8 Adhesion to wound bed
3. **Clinical Ease of Use**
 - 3.1 Ease of implantation

- 3.1.1 Minimal preparation from shelf to body
- 3.1.2 Can be handled without tearing
- 3.1.3 Simple in-vivo attachment to wound bed
- 3.2 Minimal number of applications
- 3.3 Applicable to various wound sizes and shapes
- 3.4 Can be stored for extended time periods (up to years)
- 4. Ease of Laboratory Processing**
 - 4.1 Minimize the difficulty of process steps
 - 4.2 Minimize the equipment and technology required
 - 4.3 Minimize the production area (laboratory/bench space)
 - 4.4 Minimize production costs
 - 4.4.1 Minimal use of laboratory consumables for cell culture
 - 4.4.2 Minimal time required to complete all steps for fabricating matrix scaffold
 - 4.5 Repeatable process to minimize variation in results
- 5. Bioactive**
 - 5.1 Promotes angiogenesis
 - 5.2 Actively inhibits microbial infections
 - 5.3 Improved wound healing
 - 5.3.1 Incorporation and attachment into native tissue
 - 5.3.2 Permeable to migrating cells
 - 5.3.3 Heals with uniform surface topography
 - 5.3.4 Uniform rate of wound healing
 - 5.3.5 Decreases formation of granulation tissue and scar formation
 - 5.3.6 Similar degradation rate to rate of wound healing

From the indented objectives list, five major objectives were identified for the desired behavior of the client's proposed scaffold design. These objectives include ease of production, structurally and mechanically similar to native dermal tissue, clinical ease of use, ease of laboratory processing, and bioactive. The hierarchy of the objectives can be visualized in the following objectives tree (see Figure 4).

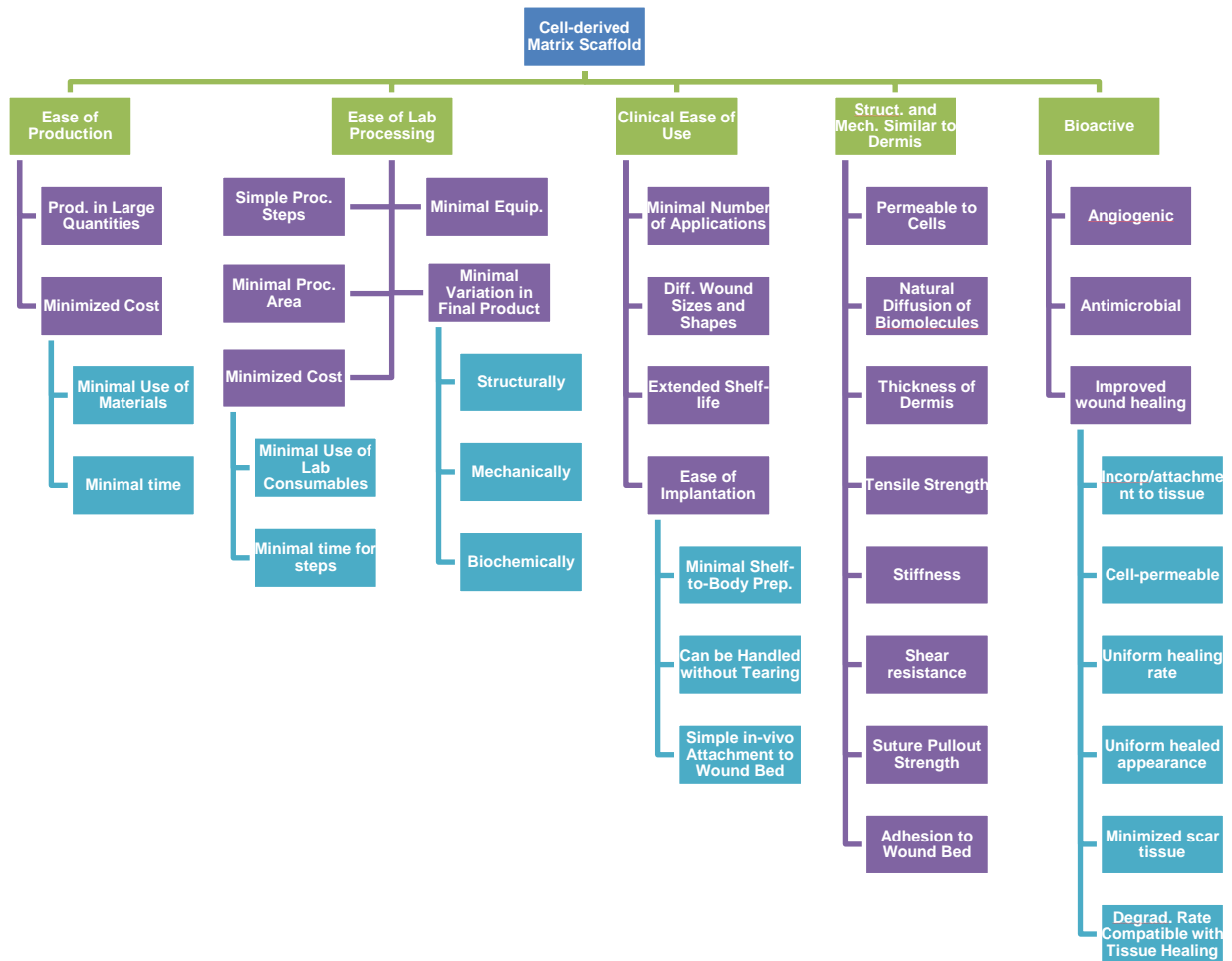


Figure 4: The Objectives Tree for the Design of a Novel ECM Scaffold

It was also noted that one of the client's goals was to create a series of in vitro assays for analyzing the device. After discussion, brainstorming, and pruning, the design team created an indented objectives list for the goals pertaining to the in vitro assays. The hierarchy of these objectives can be visualized in the following objectives tree (see Figure 5).

List 3: In Vitro Assays Indented Objectives List

0. *In vitro* assays to analyze the mechanical, angiogenic and antimicrobial properties of the ECM scaffold
 1. **Should be low in cost**
 2. **Should require attainable supplies**
 3. **Should be feasible**
 - 3.1 Should be achievable in short periods of time
 - 3.2 Should not require extensive training or expertise
 4. **Should be accurate**
 5. **Should be precise**

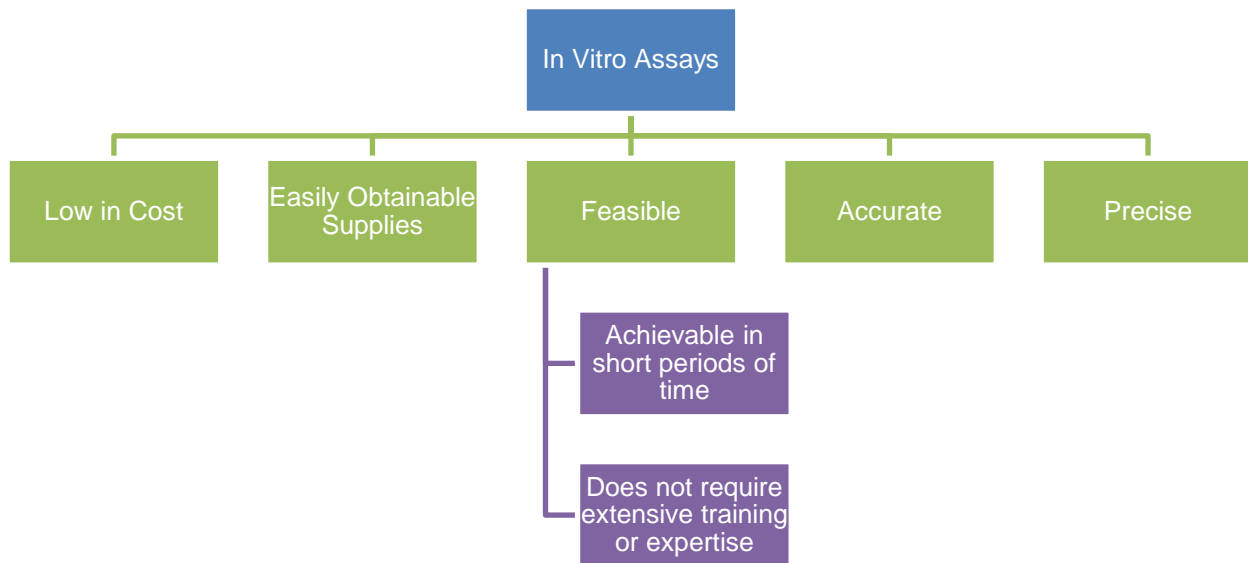


Figure 5: The Objectives Tree for the Design of in vitro Assays to Analyze the Properties of the Novel ECM Scaffold

3.3.2 Ranking the Objectives

To better understand the client’s and the design team’s expectations for the scaffold, the two stakeholders filled out separate pairwise comparison charts (PCCs) to numerically rank the objectives based on importance. PCCs were completed for the five top-tier objectives of the bioactive scaffold characteristics, the sub-objectives for each of those top-tier objectives, and the objectives for the in vitro assays.

Bioactive (see Table 6) includes the angiogenic and antimicrobial properties that are outlined in the client goals, as well as improved wound healing. Angiogenic properties should speed up the rate at which the scaffold is vascularized once implanted into the wound bed. Antimicrobial properties should protect the wound against infection. Improved wound healing includes incorporation and attachment into native tissue the following characteristics which promote successful dermal regeneration: permeable to migrating cells, heals with uniform

surface topography, uniform rate of wound healing, decreases formation of granulation tissue and scar formation, and similar degradation rate to rate of wound healing.

Table 6: Overall Scaffold Characteristics PCC Results

Overall Scaffold Characteristics		
	Design Team	Client
Bioactive	3	3
Structurally and mechanically similar to native dermis	4	4
Clinical ease of use	2	1
Ease of lab processing	1	2
Ease of production	0	0

Ease of production (see Table 7) includes minimized production costs and manufacturability in large quantities. Costs that should be minimized include the use of materials to produce the scaffold as well as the time required to complete all steps for fabricating the matrix scaffold. The scaffold should have the ability of being manufactured in large amounts for successful sales and distribution.

Table 7: Ease of Production PCC Results

Ease of Production		
	Design Team	Client
Minimize production costs	1	1
Can be manufactured in large quantities	0	0

The scaffold should be structurally and mechanically similar to the native dermis such that the tensile strength, shear resistance, stiffness, thickness, diffusivity of biomolecules, and permeability for infiltrating cells are the same or close to the properties of native dermis (see Table 8). The scaffold should also have reliable suture pull-out strength for successful clinical use, as well as proper adhesion to the wound bed.

Table 8: Structurally and Mechanically Similar to Native Dermal Tissue PCC Results

Structurally and Mechanically Similar to Native Dermal Tissue		
	Design Team	Client
Tensile Strength	6.5	6.5
Shear resistance	6.5	4.0
Adhesion to wound bed	5	0.5
Permeability	4	3.5
Diffusivity	3	3.5
Stiffness	2	6.5
Thickness	1	3.0
Suture pull-out strength	0	0.5

The scaffold should be able to be used for clinical applications such that it is easy to implant, it does not require a number of applications or surgeries, and it can be applied to various wound sizes and shapes (see Table 9). The scaffold should be able to be stored for extended periods of time so that it can be used immediately.

Table 9: Clinical Ease of Use PCC Results

Clinical Ease of Use		
	Design Team	Client
Ease of implantation	3	2.5
Can be stored for extended time periods	2	0.0
Minimal number of applications	1	1.0
Applicable to various wound sizes and shapes	0	2.5

The scaffold should be able to be fabricated easily in the laboratory (see Table 10). This includes minimizing the difficulty of fabrication steps, minimizing the equipment and technology required for production, minimizing the area over which production will occur, and minimizing the variation in the resulting scaffold by creating a repeatable process. Laboratory production costs should also be minimized such that fabrication requires the minimal use of laboratory consumables for cell culture and minimal time required to complete the fabrication steps.

Table 10: Ease of Laboratory Processing PCC Results

Ease of Laboratory Processing		
	Design Team	Client
Repeatable to minimize variation	4	4.0
Minimize equipment and technology required	3	1.0
Minimize difficulty of steps	2	0.0
Minimize production costs	1	3.0
Minimize production area	0	2.0

The scaffold should be bioactive (see Table 11) such that it promotes angiogenesis, it actively inhibits microbial infections, and it enhances the wound healing response. To enhance wound healing, the scaffold should incorporate and attach into the native tissue, it should be permeable to migrating cells, it should heal with uniform surface topography at a uniform rate, it should degrade with a degradation rate comparable to the rate of regeneration, and it should decrease the formation of granulation tissue and scar formation.

Table 11: Bioactive PCC Results

Bioactive		
	Design Team	Client
Inhibits microbial infections	2	1
Improved wound healing	1	0
Promotes angiogenesis	0	2

The in vitro assays (see Table 12) used to analyze the scaffold should be precise, accurate, and low in cost. The assays should be feasible such that they do not require long periods of time or extensive training. The supplies required for the assays should be easily obtainable.

Table 12: In Vitro Assays Characteristics PCC Results

In Vitro Assays Characteristics		
	Design Team	Client
Feasible	3	3.5
Precise	3	3.5
Accurate	3	1.0
Easily Attainable Supplies	1	0.0
Low in cost	0	2.0

3.3.3 Finalizing the Priority of Objectives

After discussing the ranked objectives with the client, compromises were made to decide the final ranking of the objectives. Both the client and the design team discussed their rationale behind their ranking, which led to an in-depth discussion of the importance of each objective relative to the client statement.

The client and the design team agreed that a successful scaffold must have the proper mechanical and structural properties to be handled properly; this is the most important objective of the project. Bioactive was the next ranked objective, since bioactivity lends itself to the overall purpose of the scaffold, which is a reliable wound healing response. Within the bioactive objective, however, the design team felt that antimicrobial was the most important component, whereas the clients felt that angiogenic was the most important component. After discussion, both parties agreed that antimicrobial was more significant because proper wound healing cannot occur in infected tissues. In addition, the design team felt that the client was correct when proposing that ease of production and clinical ease of use were beyond the scope of this design project. The design team gave these two objectives the lowest ranking.

The results of the finalized priority of objectives that have been approved by the design team and the clients (see Table 13).

Table 13: Summary of Overall Prioritized Objectives

Summary of Prioritized Objectives – Design Team & Clients							
	Scaffold Characteristics	Structurally and Mech. Similar	Bioactive	Clinical Ease of Use	Ease of Laboratory Processing	Ease of Production	In Vitro Assays
Highest Priority	Structurally and Mech. Similar	Tensile Strength, Stiffness	Inhibits Microbial Infections	Repeatable to Minimize Variation	Ease of Implantation, Applicable to Wound Sizes/Shapes	Minimized Production Costs	Feasible, Precise
	Bioactive	Shear Resistance	Promotes Angiogenesis	Minimize Production Costs	Minimal Number of Applications	Can be Manufactured in Large Quantities	Low in Cost
	Ease of Lab Processing	Permeable, Diffusivity	Improved Wound Healing	Minimize Production Area	Stored for Long Periods of Time		Accurate
	Clinical Ease of Use	Thickness of Dermis		Minimized Equipment and Technology Required			Easily Attainable Supplies
	Ease of Production	Suture Pullout Strength, Adhesion to Wound Bed		Minimize Difficulty of Process Steps			
Lowest Priority							

3.4 Constraints

There are several constraints that limit the design space and that the team must consider through the design of the product. A brief list is presented below. These constraints not only minimize the design space, but correspond to the success of the final product. If the binary constraints of cell-derived, acellular, biodegradable, and biocompatible are not followed, the design will fail.

List 4: Constraints

- Budget (\$368 USD)
- Time (21 weeks)
- Must be a cell-derived tissue
- Must be acellular
- Must be biodegradable
- Must be biocompatible
- Assays must not harm scaffold

From a logistics point of view, the design team is limited by a budget of \$156 per team member, minus \$100 for usage fees, leaving a total of \$368 total for all design, fabrication, and testing needs. The team is also restricted to a timeline of 21 weeks, from A Term beginning in August 2011 through the end of C Term in the first week of March 2012. The scaffold design is limited by how it will respond in vivo. It must be biodegradable so that the scaffold material degrades as new matrix and tissue is established, and the release by-products must not be toxic to the surround cells or remaining tissue. It must be biocompatible such that a chronic inflammatory or immune response is not provoked, cell adhesion and growth is not reduced, and toxic components are not included. For the scaffold source, the initial tissue must be cell-derived, but the final scaffold must be acellular and free of cells. A final constraint corresponds to the validation of the final product; the in vitro assays for product verification must not injure the scaffold such that data is compromised.

3.5 Revised Client Statement

In order to clarify the initial client statement, the design team reviewed current literature, conducted a series of client interviews, and developed a list of ranked objectives. Based on the analysis of design requirements and considering the priorities set by the client, a revised client statement was developed:

“Design and fabricate a highly functional and bioactive cell-derived matrix scaffold with antimicrobial and angiogenic properties as an enhanced dermal regenerative therapy for full-thickness wounds. Design the scaffold with structural, mechanical, and biochemical properties that emulate those of the native dermis; and devise protocols and devices for scaffold fabrication, as well as a series of in vitro assays to analyze and verify the scaffold’s properties.”

The revised client statement represents a more specific scope of the project.

3.6 Project Approach

Figure 6 illustrates the basic approach to the project. The black boxes represent the sequential milestones to create the final product. Functions will be developed for each of these

stages. The triangles represent the processes required to achieve each milestone. These processes are tools that are related to the objectives of the project and can be used to achieve the goals of the project, as shown below. Means will be established for each process in order to determine the most appropriate methods to achieve the corresponding milestones.

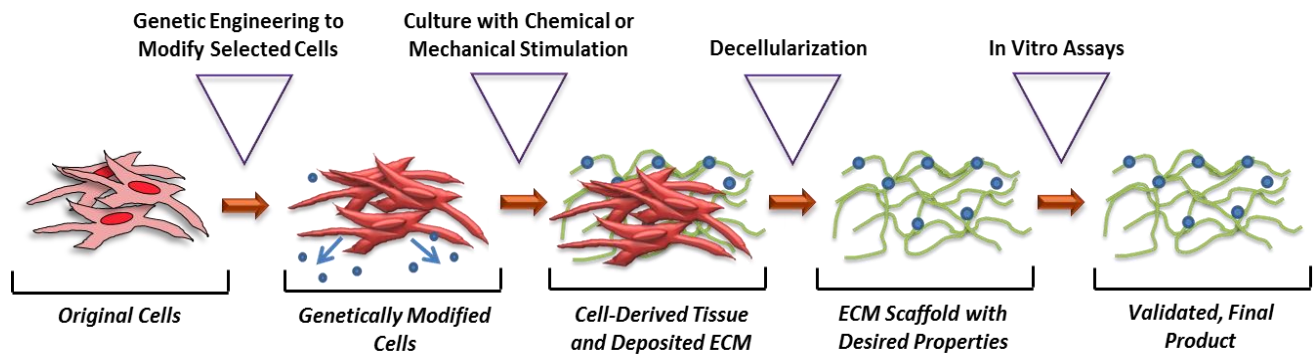


Figure 6: Project Approach

Genetic engineering can be used to accomplish goals 1 and 2. This technique can be potentially used to modify cells for improving mechanical and structural properties, inducing antimicrobial responses, or improving angiogenic properties. Cell culture can also be used to accomplish the first goal, such that cell type of choice will produce an ECM scaffold with the desired mechanical and structural properties. Using decellularization as a method to isolate the ECM will achieve the overall production goal of an acellular scaffold. Finally, a proper set of in vitro assays will provide validation of the design and its achievement of meeting the prioritized objectives. In Appendix A, a Gantt chart shows the sequence of steps for this approach for the following 7 week design period (October-December).

4 Alternative Designs

4.1 Generation of Alternative Designs

After ranking the design objectives and developing the client statement, the design team began to organize a list of functions for the scaffold that would satisfy the desired objectives. The team began by drawing from the literature review to brainstorm an initial list of functions and design specifications. Brainstorming with the client was used to inspire means and approaches to the conception of the scaffold. Afterwards, a preliminary functions and means list was generated and eventually pruned to better fit the client objectives.

4.1.1 Initial Functions List

The design team created an initial functions list for the actions of the scaffold that meet the designed design objectives. To stay within the scope of the deliverables for the client, functions were identified that complement the two highest-ranked objectives: structurally and mechanically similar to native dermal tissue and bioactive.

List 5: Initial Functions List

1. Resists comparable mechanical forces to which the native dermis is subjected
2. Actively inhibits microbial infection
3. Actively establishes new blood vessel formation
4. Discourages foreign body response
5. Actively promotes cellular migration

In order for the scaffold to be structurally and mechanically similar to native dermis, the design team felt that the scaffold must be as robust as native dermis by resisting comparable mechanical forces to which the dermis is subjected. To address the bioactive objective and sub-objectives, four more functions were conceptualized. To resist infection, the scaffold should actively inhibit microbial growth. To promote angiogenesis, the scaffold should actively establish new blood vessel formation when it implanted in the patient. This will also assist in enhancing the wound healing response. To improve wound healing, the scaffold must not elicit a foreign

body response as well as actively promote fibroblast and keratinocyte migration for enhanced healing.

4.1.2 Initial Specifications/Requirements

Drawing from the literature review and laboratory experience, the design team created a list of prescriptive and performance requirements for the acellular scaffold. Prescriptive requirements describe the characteristics of the scaffold. Performance requirements dictate the specific actions of the scaffold.

The design team brainstormed prescriptive requirements to conceptualize what the scaffold will look like. Since the normal thickness of the dermis is 1mm, the design team decided that the acellular scaffold should attain a thickness of 1mm as well. Ultimately, the design team imaged the scaffold as being any length and width so that it could be applied to all sizes of skin injuries. Looking ahead to in vitro testing of the scaffold, the design team came up with two possible diameters. If the final design includes using a cyclic biaxial stretch machine to cyclically condition the tissue, the tissue will need a diameter of 35 mm (Balestrini & Billiar, 2006). If the scaffold is subjected to biaxial inflation testing to measure mechanical properties, the scaffold must have a diameter of at least 1 cm (Billiar, Throm, & Frey, 2005). The design team felt that the scaffold should have porosity similar to that of native dermis. Therefore, pore size should be between 20-125 μm to promote fibroblast and endothelial cell in-growth (Yannas, Lee, Orgill, Skrabut, & Murphy, 1989). The composition of the scaffold should also mimic that of native dermis. The scaffold should have at least 70% of its protein content as collagen type I (Mansbridge et al., 1999).

Prescriptive requirements for the scaffold aim to surpass the properties of current dermal scaffolds. The tensile strength of the scaffold should be within 5-30 MPa (Edwards & Marks, 1995) and the shear strength should be within 435-6620 Pa (Holt et al., 2008). The scaffold should encourage typical speeds of cellular migration, including fibroblasts at 0.5 $\mu\text{m}/\text{min}$ and

endothelial cells at 300 $\mu\text{m}/\text{min}$ (Saltzman, 2004). Additionally, the scaffold should be able to kill 99.9% (minimum bactericidal concentration) of streptococcus aureus, enterococcus faecalis, and pseudomonas aeruginosa to effectively inhibit microbial infection (Dowling, 2012).

4.1.3 Development of Conceptual Designs

The team conducted a brainstorming session with the client to produce conceptual designs for the scaffold (see Figure 7 and Figure 8). One person started a design, and others added to the idea as they saw fit. This resulted in the accumulation of a number of conceptual designs to address the initial functions list. The following figures show the progression of conceptual designs during the brainstorming session, including 15 different designs that are described below. The conceptual designs are organized with pictures and descriptions in Appendix D: Conceptual Designs.

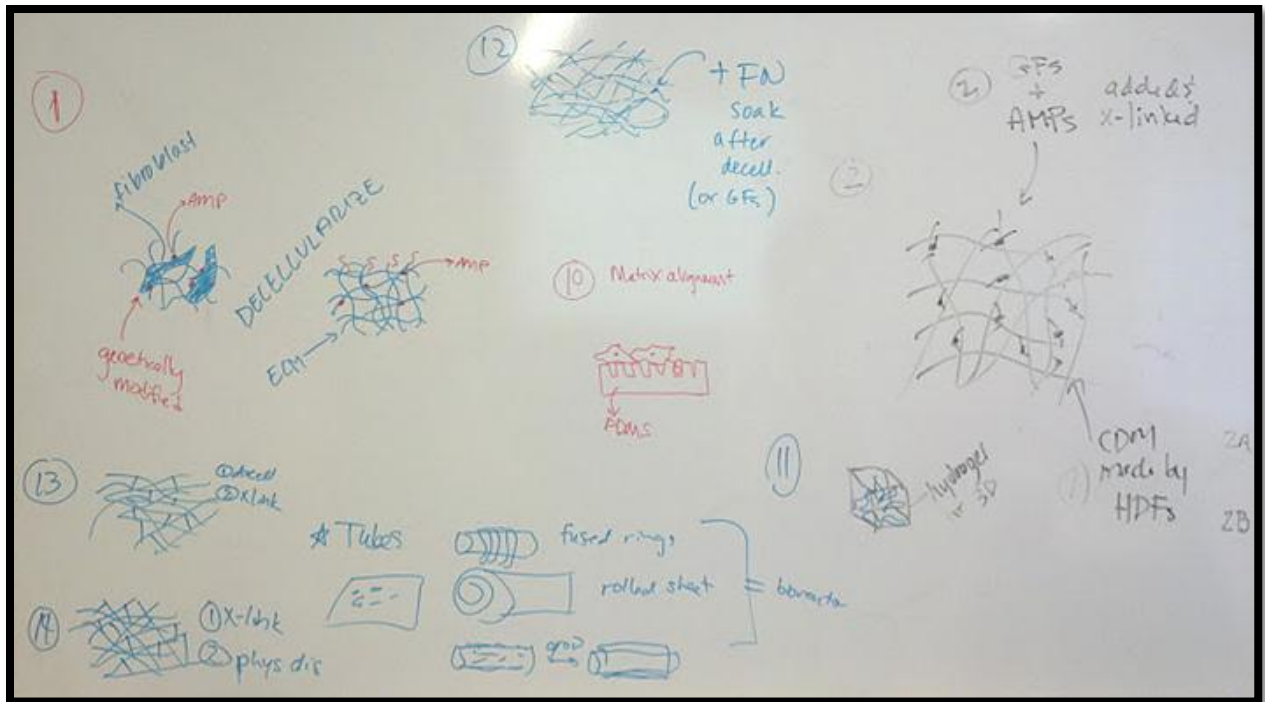


Figure 7: Brainstorming Session (a)

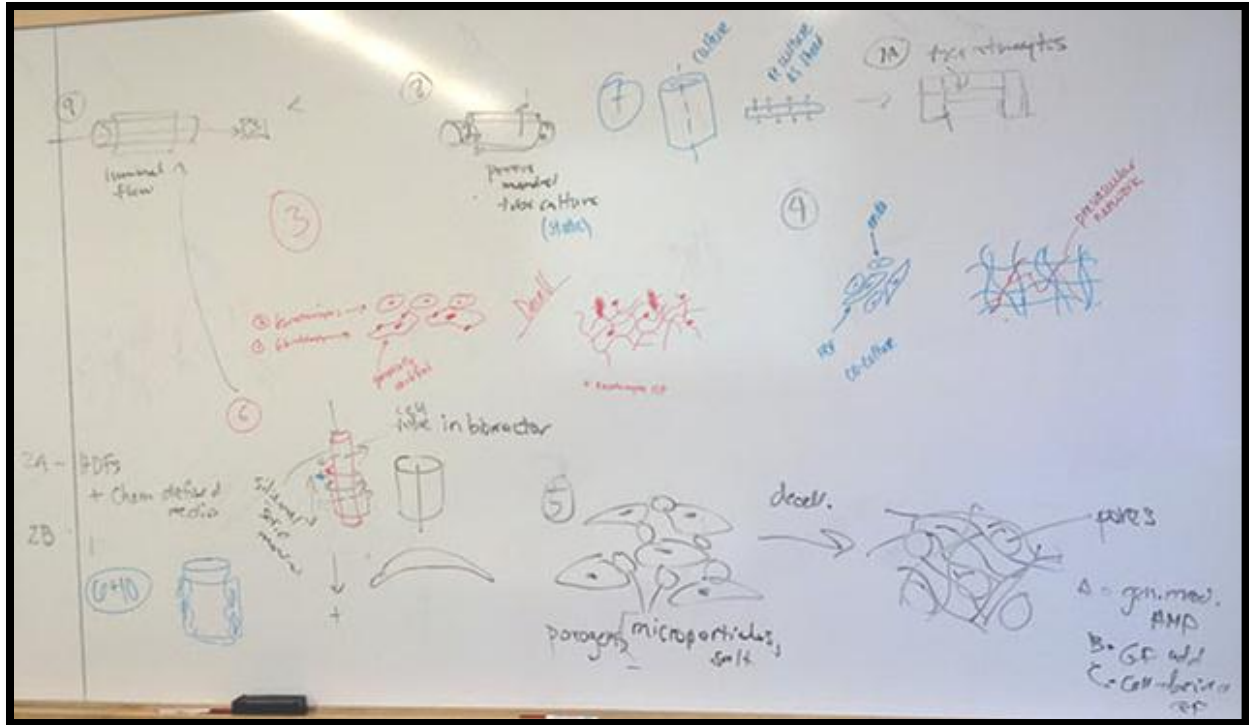


Figure 8: Brainstorming Session (b)

Design number 1 shows AMP-producing fibroblasts. Genetically modified human dermal fibroblasts produce antimicrobial peptides that bind to the extracellular matrix. The tissue is then decellularized, resulting in a cell-derived matrix (CDM) with bound anti-microbial peptides (AMPs).

Design number 2 shows the exogenous addition of AMPs to the CDM. Human dermal fibroblasts (HDFs) produce a CDM. After decellularization, growth factors and AMPs are cross-linked to the matrix. Additionally, the fibroblasts can be cultured in chemically defined media to increase matrix production.

Design number 3 shows a CDM with enhanced keratinocyte binding sites. Genetically modified fibroblasts that produce AMPs and keratinocytes are co-cultured until they form a tissue. The tissue is then decellularized. Keratinocytes may deposit proteins or encourage the formation of binding sites that are conducive to their attachment.

Design number 4 shows a prevascular network in the CDM. The HDFs and endothelial cells are co-cultured until they form a tissue. The tissue is then decellularized. The addition of endothelial cells may form tubular constructs (the prevascular network) that will enhance angiogenesis during implantation.

Design number 5 shows the addition of porogens. Microparticles are added to the cells, which are cultured until they form a tissue. The tissue is decellularized, and the microparticles are removed. This may retain a pore size in the matrix that is conducive to cellular migration.

Design number 6 shows the tissue being grown as a cellular tube in a bioreactor. The cells are grown in a sheet around a silicone solid mandrel in a bioreactor. The sheet is cut to flatten out, and then the tissue is decellularized. The bioreactor may increase matrix production and strength. Cell tubes for bioreactor conditioning can be constructed by fusing rings, rolling tissue sheets, or growing cells directly on the mandrel.

Design number 7 shows a two-layer cell tube. The HDFs are cultured around a tubular bioreactor to benefit from mechanical conditioning. The tissue is cut, flattened, and continued to culture as a sheet to encourage planar formation. Keratinocytes are added at this point and allowed to culture. The tissue is then decellularized.

Design number 8 shows cells being cultured around a porous mandrel tube in static conditions. The tissue is then cut, flattened, and decellularized to produce the CDM.

Design number 9 shows cells being cultured around a luminal flow tube in dynamic conditions. The tissue is then cut, flattened, and decellularized to produce the CDM.

Design number 10 shows the 3D culture of the tissue on a micro-patterned substrate. The cells are grown on a micro-patterned PDMS substrate. The substrate may influence matrix alignment that is conducive to fibroblast re-population.

Design number 11 shows the 3D culture of the tissue in a hydrogel. The hydrogel is removed after culture, and the tissue is decellularized.

Design number 12 shows a growth factor soak. The tissue is first decellularized, and then submerged in fibronectin or another desired growth factor.

Design number 13 shows crosslinking. The tissue is first decellularized. Then the CDM is crosslinking using chemical or physical methods

Design number 14 also shows crosslinking, but before decellularization. A chemical or enzymatic crosslinking agent is added to the tissue to crosslink the ECM. The tissue is then decellularized. Crosslinking the tissue beforehand may allow for the use of harsher methods of decellularization, such as physical methods, that might greatly disrupt the matrix.

Design number 15 shows cells grown on a micro-patterned silicone solid mandrel in a bioreactor. After the tissue forms, the sheet is cut, flattened, and then decellularized.

Brainstorming conceptual designs in the manner opened the design space for the team, and allowed the team to delve into creative solutions. These designs initiated the discussion on realistic functions and means for the final scaffold design.

4.1.4 Preliminary Functions and Means

The brainstorming session with the client lead to the development of an initial functions and means list. The preliminary list helped the team pair the means developed from the brainstorming session with each of the functions.

List 6: Preliminary Functions and Means

- 1. Resists comparable mechanical forces to which the native dermis is subjected**
 - 1.1 Structurally mimic the dermis
 - 1.1.1 Modify level of crosslinking fibers using chemical agents
 - 1.1.2 Modify level of crosslinking fibers using physical agents
 - 1.1.3 Genetically modify cells to produce more of a certain matrix component
 - 1.1.4 Vary pore size
 - 1.1.4.1 Add polymer microparticles
 - 1.1.4.2 Add acrylic nanoparticles
 - 1.1.4.3 Add salt
 - 1.1.4.4 Use decellularization methods that do not affect the structure

- 1.1.5 Vary cell type to vary ECM composition (strength contributing fibers)
 - 1.2 Mechanically stimulate cell in bioreactor
 - 1.2.1 Tensile forces
 - 1.2.2 Shear forces
 - 1.2.3 Compressive forces
 - 1.2.4 Cyclic forces (fatigue)
 - 1.3 Vary components in cell culture media
 - 1.3.1 Ascorbic acid
 - 1.3.2 Protease inhibitors that prevent collagen breakdown
 - 1.3.3 Growth factors
- 2. Actively inhibits microbial infection**
 - 2.1 Antimicrobial peptides
 - 2.1.1 Genetically modified cells produce AMP in ECM
 - 2.1.2 Exogenously add AMPs to ECM
 - 2.1.3 Exogenously add inducer of AMP
 - 2.2 Antibiotic
 - 2.2.1 Conjugate drug to ECM
 - 2.3 Metals (silver, copper, zinc)
 - 2.3.1 Exogenously add metallic beads
 - 2.3.2 Exogenously add Beta-glucan silver-silver chloride nanospheres
 - 2.4 Chemicals
 - 2.4.1 Exogenously add terpenes
- 3. Actively establishes new blood vessel formation**
 - 3.1 Angiogenic promoting proteins
 - 3.1.1 Genetically modified cells to produce angiogenic protein
 - 3.1.2 Exogenous addition of angiogenic protein
 - 3.1.3 Induce cellular production of angiogenic protein
 - 3.1.3.1 Mechanical condition
 - 3.1.3.2 Hypoxic culture
 - 3.2 Prevascular network
 - 3.2.1 Endothelial cells during culture of ECM
 - 3.2.2 Grown in an animal model
- 4. Discourages foreign body response**
 - 4.1 Decellularization of the tissue
 - 4.2 Exogenously add immunosuppressant
 - 4.3 Complete removal of substrate material
 - 4.4 Complete removal of decellularization chemicals (if applicable)
- 5. Actively promotes cellular migration**
 - 5.1 Presentation of binding domains
 - 5.1.1 Over-express fibronectin
 - 5.1.2 Over-express RGD peptides
 - 5.2 Topography that promotes cell migration
 - 5.2.1 Modify internal structure by altering pore size
 - 5.2.1.1 Vary cell type to vary ECM composition
 - 5.2.1.2 Crosslinking of fibers
 - 5.2.1.3 Decellularization method that does not disrupt structure
 - 5.2.1.4 Add microparticles
 - 5.2.2 Modify surface topography
 - 5.2.2.1 Substrate material
 - 5.2.2.1.1 Hydrogel

- 5.2.2.1.2 PDMS
- 5.2.2.2 Substrate topography
 - 5.2.2.2.1 Nanogrooves
- 5.3 Genetically modify cells to produce chemo-attractants
- 5.4 Vary cell culture conditions
 - 5.4.1 Addition of growth factors
 - 5.4.2 Physical stimulation to produce specific factors

The first function is “resists comparable mechanical forces to which the native dermis is subjected” (see List 6). From our brainstorming discussion, the design team grouped together means into three groups to accomplish this function. The first idea is that the scaffold will have similar mechanical properties to the dermis if it is also structurally similar. To do this the design team came up with five means, including modifying the level of crosslinking fibers using chemical or physical agents, genetically modifying the cells to produce more of a certain matrix component, varying the pore size of the scaffold by the addition of porogens, such as polymer microparticles, acrylic nanoparticles, or salt, or varying the cell type to vary the composition of the deposited ECM. The porogens would be added during culture so that the cells would deposit ECM around them. The design team also noted that a decellularization method should be chosen that does not damage the structure of the matrix. Our second method for the scaffold to obtain comparable mechanical strength to dermis is to mechanically stimulate the cells in a bioreactor. The bioreactor can exert one of the following forces: tensile, shear, compressive, or cyclic. The third method is to vary components in the cell culture medium. This includes adding ascorbic acid, adding protease inhibitors that prevent collagen breakdown, or adding growth factors that increase matrix production.

The second function is “actively inhibits microbial infection.” We identified four different methods for addressing this function, including antimicrobial peptides, antibiotics, metals, and chemicals. Means for adding antimicrobial peptides (AMPs) to the CDM scaffold include genetically modifying the cells to produce AMPs, exogenously adding the AMPs to the ECM, or exogenously adding an inducer that will catalyze cell production of the AMP. The team also

considered adding antibiotics to the scaffold to make it resist microbial infection. To do this, the team would conjugate the drug to the ECM. A third method is to add metals, such as silver, copper, and zinc, to the scaffold that have been shown to inhibit microbial infection. Metals could be added exogenously as beads, or beta-glucan silver-silver chloride nanospheres could be exogenously added to the scaffold. The last mean was to exogenously add a chemical, such as terpenes, to the scaffold.

The third function is “actively establishes new blood vessel formation.” One method is to present angiogenic promoting proteins, such as vascular endothelial growth factor (VEGF), in the scaffold so that the scaffold enhances angiogenesis once implanted. Means to add these proteins include genetically modifying cells to produce and conjugate the protein to the matrix, exogenously adding the angiogenic protein to the scaffold, or inducing cellular production of the angiogenic protein, such as through mechanical or hypoxic conditioning. Another method is to create a vascular network in the tissue before decellularization, so that the resulting tubular constructs will enhance endothelial in-growth once implanted. Means to do this include using endothelial cells during the culture of the ECM, as well as growing the tissue in an animal model.

The fourth function is “discourages foreign body response.” One mean to address this function is decellularization of the tissue. This will rid the scaffold of any genetic material that can potentially cause an immune response or host rejection. Another mean is to exogenously add an immunosuppressant to the scaffold. The team also noted that it will be necessary to completely remove any substrate material from the scaffold, such as if the tissue is grown in a hydrogel, as well as any of the chemicals that are used during the decellularization method.

The fifth function is “actively promotes cellular migration.” One method is to ensure the presentation of binding domains to assist or enhance cellular migration into the scaffold. To do this, adhesion proteins or binding domains, such as fibronectin or RGD peptides, could be over-expressed in the scaffold. Another method is to enhance the topography of the scaffold to

promote cell migration. One approach is to modify the internal structure by altering pore size that is conducive to cellular migration. As mentioned before, pore size can be retained in the matrix by adding porogens, such as gelatin microspheres, during tissue culture. Pore size can also be altered by the type of cell used to form the tissue, by the structure disturbance caused by the decellularization method, or by crosslinking the fibers. Another approach is to modify the surface topography of the scaffold. This can be done by altering substrate material, such as hydrogels or PDMS, as well as the topography of these substrates, such as the addition of micropatterns (Bush, 2009). A third method to promote cellular migration is to genetically modify cells to produce chemo-attractants. A fourth method includes varying cell culture conditions that enhance growth factor expression in the CDM scaffold. These means include the exogenous addition of growth factors to the matrix, as well as physical stimulation of the tissue to induce the cells to produce specific growth factors.

4.2 Evaluation of Alternative Designs

From the brainstorming session, the team compiled a number of alternative designs, or means, to address each function. Each alternative design was rated against each other using a set of metrics and prioritized objectives in an evaluation matrix. The top-rated alternative design for each function was compiled into a final design.

4.2.1 Generation of final functions and means

The design team reevaluated the initial functions and means list to focus the attributes of the scaffold on the ranked objectives. Specifically, “discourages foreign body response” and “actively promotes cellular migration” were eliminated from the list. The design team felt that discouraging foreign body response was more of a constraint for the scaffold. The scaffold will not be successful if it is rejected in any way by the body. The design team also felt that the main function of the scaffold was not to enhance cellular migration. The clients clearly communicated the need for a mechanically strong scaffold above all other attributes, with antimicrobial and

angiogenic properties as secondary objectives. Therefore, enhancing cellular migration is outside of the scope of the client statement, and was eliminated from the list.

List 7: Final Functions & Means

1. Withstands mechanical forces similar to native dermis

- 1.1 Modify matrix
 - 1.1.1 Crosslinking
 - 1.1.1.1 Chemically (formaldehyde, hexamethylene-diisocyanate, glutaraldehyde, poly-epoxy compounds)
 - 1.1.1.2 Physically (UV, gamma, heat)
 - 1.1.1.3 Biologically (Lysyl-oxidase, tissue transglutaminase)
 - 1.1.2 Improve/add matrix components
 - 1.1.2.1 Add proteoglycans
 - 1.1.3 Grow cells on a substrate
- 1.2 Modifying cells that produce matrix
 - 1.2.1 Improve/add matrix components
 - 1.2.1.1 Increase collagen production
 - 1.2.1.1.1 Stimulation in bioreactor
 - 1.2.1.1.2 Ascorbic acid in media
 - 1.2.1.2 Maximize extracellular matrix retention
 - 1.2.1.2.1 Protease inhibitors

2. Actively inhibits microbial infection

- 2.1 Modify cells
 - 2.1.1 Genetically modified cells produce AMP in ECM
 - 2.1.2 Exogenous addition of inducer of AMP
- 2.2 Modify matrix
 - 2.2.1 Conjugate antibiotic to ECM
 - 2.2.2 Exogenous addition of metallic beads (silver, copper, zinc)
 - 2.2.3 Exogenously add terpenes
 - 2.2.4 Exogenous addition of AMPs to ECM

3. Actively establishes new blood vessel formation

- 3.1 Modify cells
 - 3.1.1 Genetically modified cells to produce angiogenic protein
 - 3.1.2 Induce cellular production of angiogenic protein
 - 3.1.3 Induce prevascular network
 - 3.1.3.1 Endothelial cells during culture of ECM
 - 3.1.3.2 Grown in animal model
- 3.2 Modify matrix
 - 3.2.1 Exogenous addition of angiogenic protein

Pruning the initial list generated a final functions and means list with three functions, as seen above. These functions better suit the client's deliverables by providing means that allow the scaffold to be mechanically strong and exhibit antimicrobial and angiogenic properties. The

means were reorganized for each function into two different groups: means that directly modify the matrix and means that modify the cells that produce the matrix. All of the lowest level means were evaluated against each other in an evaluation matrix, as discussed in section 4.2.2.

4.2.2 Description of Alternative Designs

After pruning the functions, a final list of means were developed. Each mean can be considered as an alternative design that can achieve its appropriate function.

To satisfy the function “withstand mechanical forces similar to native dermis,” means to modify the matrix or modify the cells were developed. To modify the matrix to make it mechanically strong, the matrix can be crosslinked using chemicals, such as formaldehyde, hexamethylene-diisocyanate, glutaraldehyde, or poly-epoxy compounds. Additionally, physical methods, such as UV, gamma, or heat exposure, and biological methods, such as lysyl-oxidase and tissue transglutaminase, can also be used to crosslink the matrix. Another mean is to improve the matrix by adding proteoglycans. A fifth mean to modify the matrix is to grow the cells on a substrate to achieve optimum matrix alignment. Means that modify the cells to produce matrix include stimulating in a bioreactor or adding ascorbic acid to the media to increase collagen production. Protease inhibitors can also be added to maximize extracellular matrix retention.

To satisfy the function “actively inhibits microbial infection,” the team identified six alternative designs. Modifying the matrix can be achieved by conjugating an antibiotic to the CDM or exogenously adding metallic beads, terpenes, or antimicrobial peptides to the matrix.

To satisfy the function “actively establishes new blood vessel formation,” the team identified five alternative designs. One mean is to modify the matrix by exogenously adding an angiogenic protein. The other means modify the cells used to derive the matrix. In one alternative design, the cells are genetically modified to produce an angiogenic protein that will be retained in the matrix. Another design is to induce the cells to produce an angiogenic protein

by culturing them in hypoxic conditions. The last two alternative designs relate to inducing a prevascular network in the scaffold. One mean is to use endothelial cells during the culture of the CDM, and the other mean is to grow the scaffold up in an animal model. The final functions and means can be visualized in the tree below (see Figure 9).



Figure 9: Final Functions/Means Tree

4.2.3 Decision Matrix

Following the design of metrics, the team developed a set of decision or evaluation matrices (see Appendix B: Metrics) to numerically quantify the means. When completed, the matrices established a quantitatively ordered ranking of means for each objective evaluated on

the matrix (see Appendix C: Decision Matrices). Each function had a corresponding design matrix, and each means (or “alternative design”) was scored according to the priority of the main objective, as well as the priority of each sub objective. The evaluation matrix was a key component in selecting design components that abided by the objectives and constraints of the project, helping the team to build a design that would fulfill the goals of the clients and team.

4.2.3.1 Generation of the Matrices

Each decision matrix for each function was set up and completed in the same manner. Each row of the decision matrix contained either an objective or constraint and each column contained one of the alternative designs or means. The constraints applied were those listed in Section 3.6 (budget (\$368 USD), time (21 weeks), cell-derived tissue, acellular, biodegradable, biocompatible, does not harm scaffold). The objectives in blue are the main or top level objectives of the project—structurally and mechanically similar to native dermis, bioactive, ease of laboratory processing, clinical ease of use, and ease of production. Each main objective was given a weight % value according to its priority level for the project. Each main objective was ranked 1-5, with 5 being the most important objective, according to the priority level of the objective established in the overall PCC. These values are noted on the metrics (see Appendix B: Metrics). The value of the objective was then divided over the sum of the value for all main objectives to determine the overall weighting. For example, “structurally and mechanically similar to native dermis” (Function 1) is the most important objective according to the overall PCC of the project; therefore, it receives a score of 5. The sum of all values for this objective would be 15. This number is derived from 5 for “structurally and mechanically similar”, 4 for “bioactive”, 3 for “ease of laboratory processing”, 2 for “clinical ease of use”, and 1 for “ease of production” ($5+4+3+2+1=15$). Therefore, the overall weighting of structurally and mechanically similar to native dermis is $15/3=0.333$. This process was repeated for each of the top level objectives.

This process was repeated for lower level objectives as well. However, not all sub-objectives were included. Because the “suture pullout strength” and “adhesion to wound bed” objectives were the lowest priorities of “structurally and mechanically similar” (see Table 13), these two objectives will not be used to rank the designs. Also, the team decided not to include “improved wound healing” because this objective will theoretically be met through the overall final design. Furthermore, the sub-objectives for “clinical ease of use” and “ease of production” were not scored because these two sub-objectives are ranked the lowest and should not have extensive bearing over the design of the project. Lastly, “minimize the difficulty of steps” was not listed under ease of laboratory processing. The team decided that this sub-objective was not worthy of being a factor for determining the means used to achieve each function. The sub-objectives were weighted in the same manner as the main objectives. The priority level of each sub-objective was established in the respective PCC for each main-objective and is indicated on the metrics. The overall weighting for these values is listed in parenthesis.

4.2.3.2 Completion of the Matrices

Each alternative design was first evaluated against the constraints. The design was designated with either a “Y” if the means satisfied the constraint or an “N” if the means did not satisfy the constraint. If at least one of the constraints was not met, the alternative design was highlighted a light red no further evaluated as an alternative design. Next, each alternative design was evaluated against each objective according to the developed set of metrics. For example, when looking at the alternative designs for “inhibits microbial infections,” each means can either receive a 1 or a 2, according to the metrics. The scores given were reflections of judgment and literature. If the top-level objective had no relation to the alternative designs being evaluated, the top-level and sub-objectives were grayed out. For example, alternative designs for inducing antimicrobial properties were not evaluated against the objective “structurally and mechanically similar to native dermal tissue.” If only a sub-objective was irrelevant and not the

top-level objective, then an “X” was placed in the each box for each means for that one sub-objective (e.g. inhibits microbial infection for establishing tubular construct formation).

4.2.3.3 *Calculating the Ranking of Alternative Designs*

In order for an ordered ranking of alternative designs to be produced from the matrix, the scores of each objective and sub-objective had to be calculated. This was completed by first normalizing the values. The value for each sub-objective was divided by the total number of scoring options available in the metrics for that sub-objective. For example, “conjugate antibiotic to ECM” received a score of 2 for “inhibits microbial infections.” On the metrics, there are two options for a score, either a 1 or a 2. Therefore, the normalized value for this sub-objective was $2/2=1.0$. The total normalized values for each sub-objective were then added up and divided by the total number of sub-objectives that received a score and placed in the top-level objective box. This value appears blue on the matrix. Next, the normalized value of the top-level objective was multiplied by its overall weighting to determine the weighted sum for that top-level objective. Then, the normalized value for each sub-objective was multiplied by its own overall weighting. This value was then placed in parenthesis in the weighted sum box for that sub-objective. Then, the weighted sum values for all the sub-objectives were multiplied by the overall weighting of the top-level objective. This number was also placed in parenthesis in the weighted sum box for the top-level objective. Finally, all the regular top-level objective values for each alternative design were summed and placed in a total box at the bottom of the matrix. The same was completed for the values in parenthesis. These latter values indicate how closely each means fits the prioritized sub-objectives of the project. If only the first approach is used, then the ranked means only reflect how well each alternative design fits the overall top-level objective, and not how each alternative designs fits each individual objective within each top-level.

4.2.4 Results of Decision Matrix

The team was able to rank the alternative designs according to the total values listed on each matrix, with larger values equaling a more appropriate or better means. The results for each function are listed in the tables below (see Table 14-Table 16). The values on the left refer to the scores calculated against only the overall weighting, and the values on the right refer to the scores calculated against the overall weighting *and* the prioritized sub-objectives. The actual score received by each alternative design have no importance. The scores are merely a means for comparing the different alternatives in a manner that is consistent and relates the effectiveness of the means compared to each other. The system does not necessary state how good a design is, but rather how it compares to others.

4.2.4.1 Withstands Mechanical Forces Similar to Native Dermis

Table 14: Decision Matrix Results for “Withstands Mechanical Forces Similar to Native Dermis”

Design	Overall Weighting Score	Design	Prioritized Overall Weighting Score
Ascorbic Acid	.733	Ascorbic Acid	.609
Bioreactor	.617	Biologically crosslink	.556
Biologically crosslink	.616	Bioreactor	.520
Protease Inhibitors	.608	Protease Inhibitors	.512
Culture on substrate	.567	Culture on substrate	.470

The first design alternatives included means for achieving the function “withstands mechanical forces similar to native dermis” (see Table 14). Ascorbic acid ranked the highest for both scores, but there was variation in the second ranked means between the two systems. It is anticipated that using a bioreactor would be better at achieving the overall goal than biologically crosslinking the scaffold; however, biologically crosslinking the scaffold may fit the sub-

objectives of tensile strength, stiffness, shear resistance, permeability/diffusivity, and thickness better.

4.2.4.2 *Actively Inhibits Microbial Infection*

Table 15: Decision Matrix Results for “Actively Inhibits Microbial Infection”

Design	Overall Weighting Score	Design	Prioritized Overall Weighting Score
Genetically Modify Cells	.593	Genetically Modify Cells	.609
Exogenously Add AMPs	.589	Exogenously Add AMPs	.556
Conjugate Antibiotic to ECM	.542	Conjugate Antibiotic to ECM	.498
Exogenously Add Terpenes	.542	Exogenously Add Terpenes	.498

The second set of matrices includes the design alternatives for inhibiting microbial infection (see Table 15). There was no variation in the ranking between the two scoring systems and using genetically engineered cells ranked first. Exogenously adding AMPs came in second because of the cost associated with AMPs. Instead, the team has the resources to genetically modify the cells, with the production of AMPs as a possibility. Antibiotics were ranked lower because they are also costly and terpenes would require extra labor because a conjugation method would need to be devised for effective antimicrobial properties.

4.2.4.3 *Actively Establishes Tubular Constructs for Enhanced in vivo Vascularization*

Table 16: Decision Matrix Results for “Actively Inhibits Microbial Infection”

Design	Overall Weighting Score	Design	Prioritized Overall Weighting Score
Endothelial Cell Co-Culture	.584	Hypoxia Stress	.432
Hypoxia Stress	.534	Hypertonic Stress	.398
Hypertonic Stress	.509	Endothelial Cell Co-Culture	.383

The final matrices correspond to establishing tubular constructs for enhanced in vivo vascularization. Overall, the addition of endothelial cells ranked the highest for establishing

tubular constructs. When looking at the prioritized values, however, hypoxia stress induced angiogenesis ranks first.

4.3 Final Conceptual Design

The highest ranking means from the evaluation matrix for each function were compiled into a final design. These means satisfy the client's and design team's desired objectives, as well as the two top functions specified for the scaffold: withstands mechanical forces similar to those that the native dermis are subjected and actively inhibits microbial infection. The function "establishes new blood vessel formation" was eliminated to focus the scope of the design. The final design consists of the addition of ascorbic acid to increase mechanical collagen production and matrix strength as well as genetically modified cells to produce antimicrobial peptides. A schematic of the final design is shown below (see Figure 10).

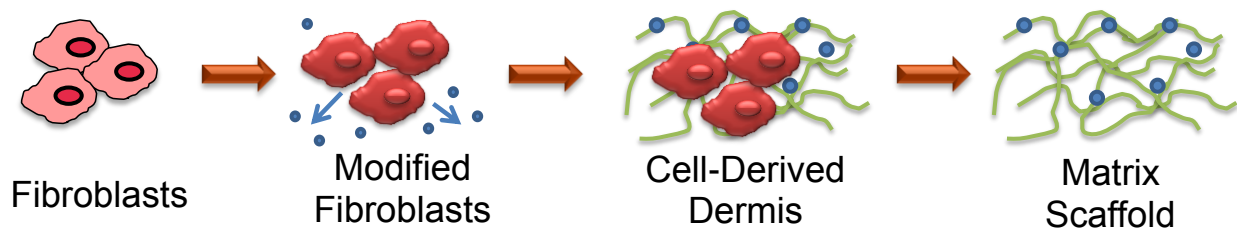


Figure 10: Schematic of Final Design

Fibroblasts will be genetically modified to produce an antimicrobial peptide. The peptide will include a matrix binding domain so as to improve retention in the scaffold after decellularization.

L-ascorbic acid phosphate magnesium salt n-hydrate is added to the medium at a concentration of 50 $\mu\text{g}/\text{mL}$ (Hu, 2010), has been reported to increase collagen production of human dermal fibroblasts. The ascorbic acid is added to standard medium components for fibroblasts, which include 1X Iscove's Modified Dulbecco's Medium (IMDM) (Mediatech, Inc), 10% fetal bovine serum (FBS) (PAA) and 1% penicillin/streptomycin (Invitrogen).

4.3.1 Design Fabrication

Some components of the design, such as cell type, were required for product fabrication, but were inappropriate to rank against means for achieving our objectives. Such components relate more to how the scaffold will be made as opposed to attributes of the scaffold that will allow it to achieve the desired functions.

4.3.1.1 Cell Type

A list of cell types to consider for the formation of the tissue were initially collected according to the literature review. Cell types found in the natural dermis were considered. These include fibroblasts, endothelial cells, and keratinocytes. Mesenchymal stem cells have also been shown to contribute to collagen deposition and wound repair and were also considered (Fathke et al., 2004). The following decision matrix lists the pros and cons for each cell type (see Table 17).

Table 17: Cell Type Decision Chart

Cell Type	Pro	Con
Neonatal Fibroblasts	<ul style="list-style-type: none"> • Main cells responsible for production and deposition of new ECM • Synthesizes most ECM molecules and produce proteases required for remodeling • Secretes growth factors and cytokines conducive to wound healing: PDGF-α, TGF-α, IL-6, IL-8, bFGF • Addition of ascorbic acid stimulates collagen I and III production • Mechanical stimulation enhances tenascin C, which improves mechanical strength • Easy to acquire and maintain <ul style="list-style-type: none"> ○ Isolation of neonatal fibroblasts from foreskins ○ Available to purchase from the WPI Pins Lab • Media available to purchase from WPI Rolle Lab 	
Mesenchymal Stem Cells	<ul style="list-style-type: none"> • Actively participates in skin wound healing • Can function as perivascular cells when combined with endothelial cells • Secrete bioactive factors • Can be mechanically stimulated to increase collagen production • Produces collagen I and III 	<ul style="list-style-type: none"> • Inconsistency in reports of growth characteristics and differentiation • Hard for design team to acquire and maintain
Endothelial Cells	<ul style="list-style-type: none"> • Can create a prevascular network when co-cultured with fibroblasts <ul style="list-style-type: none"> ○ Promotes host vasculature within 4 days • Produce VEGF • Available to purchase from WPI Rolle Lab • Media available to purchase from WPI Rolle Lab 	<ul style="list-style-type: none"> • Deposits minimal to no matrix • Only beneficial in a co-culture system
Keratinocytes	<ul style="list-style-type: none"> • Main cell type of epidermis • Deposit growth factors and integrins into the acellular scaffold that will increase subsequent keratinocyte migration • Produces bFGF, which is angiogenic and a fibroblast growth factor • Available to purchase from WPI Pins Lab 	<ul style="list-style-type: none"> • Deposits minimal to no matrix • Only beneficial in a co-culture system • Extremely expensive media

Characteristics of each cell type were evaluated as well as laboratory feasibility, including whether or not the design team would have immediate access the cells and their respective culture media. Decisions were also based on the design of a single culture system for the simplicity of scaffold fabrication and cost restraints. Ultimately, the final cell type choice

was based on which cell would provide the team with the most desired scaffold attributes with the smallest amount of external conditioning.

Human dermal fibroblasts were chosen as the cell type for the final design. Fibroblasts are responsible for production and deposition of new ECM, and secrete growth factors that are conducive to wound healing. These growth factors, if retained in the acellular scaffold, will increase the healing potential of the scaffold. Neonatal fibroblasts were chosen because they are more robust than adult fibroblasts. Fibroblasts are also advantageous as can be subjected to relatively straightforward methods to enhance their matrix production. The addition of ascorbic acid, which is one of the means in our final design, has been shown to stimulate fibroblast production of collagen I and III. Mechanical stimulation can be used to increase the mechanical strength; this is our second highest ranked mean for its category and will be used as our next approach if ascorbic acid does not significantly increase the strength of the scaffold. Furthermore, fibroblasts are relatively easy to acquire from the Pins Laboratory and maintain.

4.3.1.2 Decellularization Method

A variety of decellularization methods have been developed to remove cellular components from a tissue. These include physical methods, hypotonic and hypertonic solutions, non-ionic detergents, ionic detergents, zwitterionic detergents, enzymes and chelating agents, and acids and bases (Gilbert et al., 2006). The design team narrowed down three possible methods to examine in the laboratory. These methods were chosen based on their projected success in minimal matrix disruption and maximum retention of matrix components (Badylak, 2007; Crapo, Gilbert, & Badylak, 2011). The methods were also chosen based on the feasibility of the completion relating to the difficulty of the process and necessary resources.

Non-ionic and detergents and zwitterionic were not chosen because of their destruction of the scaffold ultrastructure and removal of GAGs. Enzyme and chelating agents are not effective alone, and would be detrimental if remnants remained in the scaffold. Acids and bases

were not chosen because of their damaging effects to collagen, GAGs, and growth factors (Gilbert et al., 2006).

The remaining three methods were chosen to experimentally test in the laboratory: freeze-thaw cycles (Ngangan & McDevitt, 2009) , ionic detergents (Elder, Eleswarapu, & Athanasiou, 2009), and hypotonic and hypertonic solutions (Meyer et al., 2006). These methods are feasible for the design team to test in the laboratory and have been successfully used in previous literature. There are still obvious limitations with these techniques, and laboratory testing for scaffold mechanical strength and retention of structure will allow the design team to choose the most appropriate method.

4.4 Conclusion

Following the design process, the team developed a final design for the client's acellular scaffold. The team started this process by brainstorming initial functions and specifications as a team, and then conducted a brainstorming session with the client to develop conceptual designs. The team used this session to develop a list of preliminary functions and means. This list was then revised to better fit the scope of the client's objectives. Using evaluation matrices, the team ranked the alternative designs, and compiled the top ranking means into a final design. C-term experiments are listed in Appendix E: C-Term Gantt Chart.

5 Design Verification

The conceptual design can be broken down into a four-step process. The first is genetic engineering of the fibroblasts to achieve antimicrobial properties within the scaffold. The second and third are simultaneous steps that include cell-derived sheet fabrication and the use of ascorbic acid to produce a robust cell-derived sheet. The final step is decellularization of the fabricated cell sheet, resulting in an extracellular matrix scaffold. Initial experiments were conducted to verify and optimize these aspects of the design. A materials list and cost estimate for these experiments can be found in Appendix F: Materials List.

5.1 Developing Recombinant Cathelicidin

Human cathelicidin is naturally synthesized as a preproprotein, hCAP-18, from the CAMP gene located on chromosome 3 (Sorensen et al., 2001). It is 170 amino acids long and contains an N-terminus signal sequence (30aa), a conserved cathelin-like domain, and a C-terminus 37-amino acid antimicrobial peptide domain (LL-37). Figure 11 shows the sequence

```
MKTQRDGHSLGRWSLVLLLLGLVMPLAIIAQVLS  
YKEAVLRAIDGINQRSSDANLYRLLDLDPRPTMD  
GPDTPKPVSTFKETVCPRTTQQSPEDCDFKKD  
GLVKRCMGTVTLNQARGSFDISCDKDNKRFBLLG  
DFFRKSKEKIGKEFKRIVQRIKDFLRNLPRTES
```

Figure 11: Amino acid sequence of human cathelicidin, hCAP-18. The signal sequence is red, cathelin-like domain is blue, and the LL-37 antimicrobial peptide is blue.

and domains of hCAP-18.

5.1.1 Gene Design

A recombinant form of cathelicidin was produced to include certain features that would allow its incorporation into a cell-derived matrix scaffold. A collagen binding domain (CBD) was added to the C-terminus of LL-37 in order to tether the peptide to the synthesized matrix. Two CBDs were chosen, corresponding to the natural collagen-binding sites of fibronectin and

collagenase. The fibronectin-derived domain, CQDSETGTFY, was chosen because it is a relatively short peptide and has shown good affinity for collagen types I and III (Sistiabudi & Ivanisevic, 2008). Its ability to act as a biomolecular anchor was experimentally observed by Sistiabudi et al. (Sistiabudi & Ivanisevic, 2008). The collagenase-derived domain, TKKTLRT, has also shown similar specificity for binding collagen type I. Its functionality as a fusion domain has also been determined by a study on recombinant collagen binding VEGF (vascular endothelial growth factor) (Zhang et al., 2009). Two recombinant forms of cathelicidin were designed to include either the fibronectin collagen anchor (Fib-CBD) or the collagenase collagen anchor (Col-CBD). Each collagen binding site was incorporated with a FLAG-tag octapeptide, DYKDDDDK, so as to allow flexible anchorage of the antimicrobial peptide LL-37. This feature is important for both visualizing the protein's expression as well as providing a buffer between the collagen bound amino acids and the dynamic activity of the AMP. A schematic of the recombinant cathelicidin and its added features is shown in Figure 12. The designed DNA and protein sequences of both recombinant forms are also included in the proceeding sections.

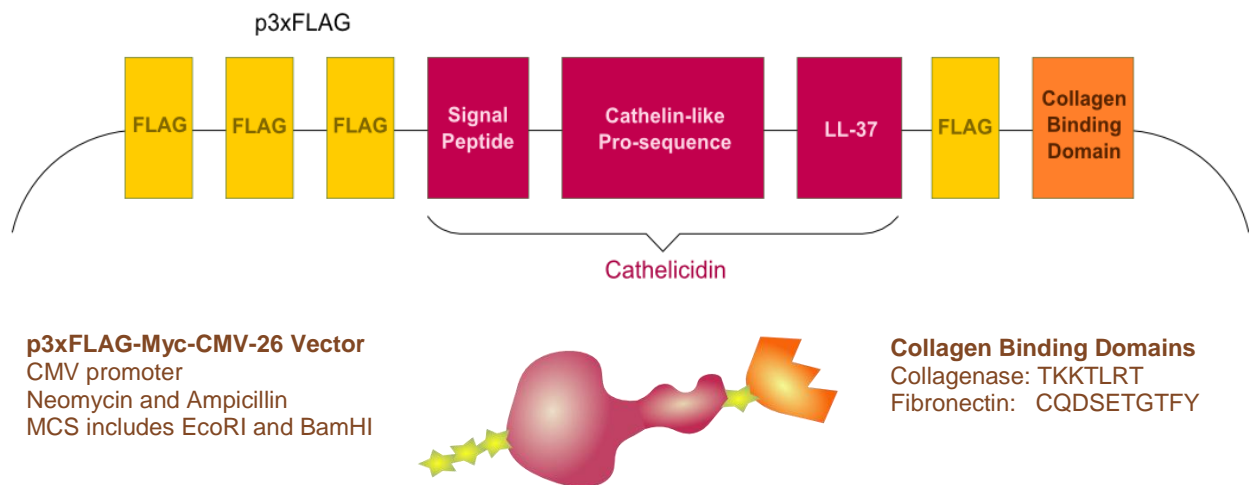


Figure 12: Proposed Gene Design of Recombinant Collagen-binding Cathelicidin Insert

5.1.1.1 Col-CBD-Cathelicidin DNA Sequence

5'-CGG-AAT-TC^A-ATG-AAG-ACC-CAA-AGG-GAT-GGC-CAC-TCC-CTG-GGG-CGG-TGG-TCA-CTG-GTG-CTC-CTG-CTG-CTG-GGC-CTG-GTG-ATG-CCT-CTG-GCC-ATC-ATT-GCC-CAG-GTC-CTC-AGC-TAC-AAG-GAA-GCT-GTG-CTT-CGT-GCT-ATA-GAT-GGC-ATC-AAC-CAG-CGG-TCC-TCG-GAT-GCT-AAC-CTC-TAC-CGC-CTC-CTG-GAC-CTG-GAC-CCC-AGG-CCC-ACG-ATG-GAT-GGG-GAC-CCA-GAC-ACG-CCA-AAG-CCT-GTG-AGC-TTC-ACA-GTG-AAG-GAG-ACA-GTG-TGC-CCC-AGG-ACG-ACA-CAG-CAG-TCA-CCA-GAG-GAT-TGT-GAC-TTC-AAG-AAG-GAC-GGG-CTG-GTG-AAG-CGG-TGT-ATG-GGG-ACA-GTG-ACC-CTC-AAC-CAG-GCC-AGG-GGC-TCC-TTT-GAC-ATC-AGT-TGT-GAT-AAG-GAT-AAC-AAG-AGA-TTT-GCC→CTG-CTG-GGT-GAT-TTC-TTC-CGG-AAA-TCT-AAA-GAG-AAG-ATT-GGC-AAA-GAG-TTT-AAA-AGA-ATT-GTC-CAG-AGA-ATC-AAG-GAT-TTT-TTG-CGG-AAT-CTT-GTA-CCC-AGG-ACA-GAG-TCC-GAC-TAC-AAA-

RNSMKTQRDGHSLGRWSLVLLLLGLVMPLAIIAQVLSYKEAVLRAIDGINQRSSDANLYRLLDLDRPPTMDGDPDTPKPVSTFKETVCPRTTQQSPEDCDFKKGDLVKRCMGTVTLNQARGSFDISCDKDNKRFALLGDFFRKSKEKIGKEFKRIVQRIKDFLRNLVPRTESDYKDDDDKTKKTLRT*GS

5.1.1.3 Fib-CBD-Cathelicidin DNA Sequence

5'-CGG-AAT-TC^A-ATG-AAG-ACC-CAA-AGG-GAT-GGC-CAC-TCC-CTG-GGG-CGG-TGG-TCA-CTG-GTG-CTC-CTG-CTG-CTG-GGC-CTG-GTG-ATG-CCT-CTG-GCC-ATC-ATT-GCC-CAG-GTC-CTC-AGC-TAC-AAG-GAA-GCT-GTG-CTT-CGT-GCT-ATA-GAT-GGC-ATC-AAC-CAG-CGG-TCC-TCG-GAT-GCT-AAC-CTC-TAC-CGC-CTC-CTG-GAC-CTG-GAC-CCC-AGG-CCC-ACG-ATG-GAT-GGG-GAC-CCA-GAC-ACG-CCA-AAG-CCT-GTG-AGC-TTC-ACA-GTG-AAG-GAG-ACA-GTG-TGC-CCC-AGG-ACG-ACA-CAG-CAG-TCA-CCA-GAG-GAT-TGT-GAC-TTC-AAG-AAG-GAC-GGG-CTG-GTG-AAG-CGG-TGT-ATG-GGG-ACA-GTG-ACC-CTC-AAC-CAG-GCC-AGG-GGC-TCC-TTT-GAC-ATC-AGT-TGT-GAT-AAG-GAT-AAC-AAG-AGA-TTT-GCC→CTG-CTG-GGT-GAT-TTC-TTC-CGG-AAA-TCT-AAA-GAG-AAG-ATT-GGC-AAA-GAG-TTT-AAA-AGA-ATT-GTC-CAG-AGA-ATC-AAG-GAT-TTT-TTG-CGG-AAT-CTT-GTA-CCC-AGG-ACA-GAG-TCC-GAC-TAC-AAA-GAC-GAT-GAC-GAC-AAG-TGC-CAG-GAT-TCA-GAG-ACT-GGG-ACG-TTT-TAT-TGA-GGA-TCC-CG-3'

5.1.1.4 Fib-CBD-Cathelicidin Protein Sequence

RNSMKTQRDGHSLGRWSLVLLLLGLVMPLAIIAQVLSYKEAVLRAIDGINQRSSDANLYRLLDLDRPTMDGDPDTPKPVSTFKETVCPRTTQQSPEDCDFKKGDLVKRCMGTVTLNQARGSFDISCDKDNKR FALLGDFFRKSKEKIGKEFKRIVQRIKDFLRNLVPRTESDYKDDDDKCQDSETGTFY*GS

Red: Cathelin-like domain
Pink: LL-37
Green: FLAG-Tag linker
Orange: Collagen Binding Domain (CBD)
Purple: Restriction sites (EcoRI and BamHI)
Blue: Stop Codon

5.1.2 Cathelicidin Isolation

The 510bp cathelicidin insert was isolated and amplified from pANT7 cGST (DNASU Plasmid Repository, Clone ID HsCD00357894, GenBank Acc. No.570277) using PCR. Primers were designed to include and incorporate the recombinant features onto the cathelicidin insert. One forward and two reverse primers (corresponding to each CBD) were ordered from Integrated DNA Technologies (IDT). The sequences of the three primers are shown in Figure 13.

Forward primer:

5'-CGG-AAT-TCA-ATG-AAG-ACC-CAA-AGG-GAT-GGC-3'

Reverse primers:

5'-CG-GGA-TCC-TCA-ATA-AAA-CGT-CCC-AGT-CTC-TGA-ATC-CTG-GCA-CTT-GTC-GTC-ATC-GTC-TTT-GTA-GTC-GGA-CTC-TGT-CCT-GGG-TAC-AAG-3' with fibronectin derived anchor

5'-CG-GGA-TCC-TCA-GGT-CCT-CAG-GGT-CTT-CTT-GGT-CTT-GTC-GTC-ATC-GTC-TTT-GTA-GTC-GGA-CTC-TGT-CCT-GGG-TAC-AAG-3' with collagenase derived anchor

Red: Cathelin-like domain

Pink: LL-37

Green: FLAG-Tag linker

Orange: Collagen Binding Domain (CBD)

Purple: Restriction sites (EcoRI and BamHI)

Blue: Stop Codon

Figure 13: Design of Forward and Reverse PCR Primers

For PCR, the samples were prepared by combining 10µL of Promega's GoTaq Green Mastermix, 1 µL of the template (pANT7-cGST), 1 µL forward primer, 1 µL reverse primer, and ddH₂O to 20 µL. PCR controls included a sample with no primers, and two with primers and no template (the two corresponding to each of the reverse primers). The PCR thermocycler (Bio-Rad, MyCycler) was set to 4minutes at 90°C (30s at 95°C, 30s at 55°C, 1 minute at 72°C)_{x30}, 4 minutes at 72°C, and ∞ at 10°C. Agarose gel electrophoresis, pre-stained with Sybr green was used to verify the recombinant amplified cathelicidin fragments (Figure 14). The isolated fragments were subsequently purified with Promega's Wizard SV Gel and PCR Clean-up System (Cat. No. A9281).

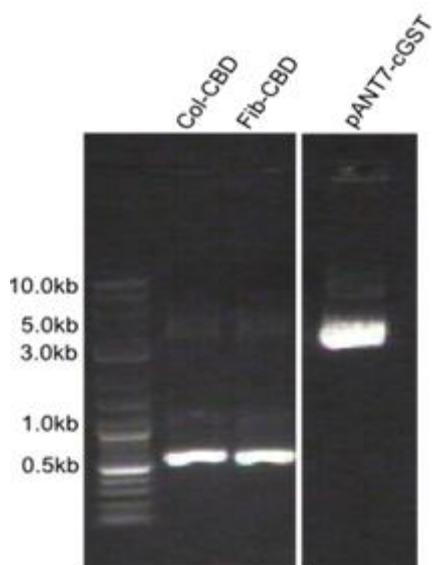


Figure 14 : Purified PCR Fragments of Recombinant Cathelicidin

Gel electrophoresis of the PCR fragments (see Figure 14) as well as the original vector confirms the isolation and construction of both recombinant forms of cathelicidin. The first lane is the DNA ladder, the second lane represents cathelicidin with the collagenase CBD (Col-CBD), while the third lane represents cathelicidin with the fibronectin CBD (Fib-CBD). The last lane is a sample of the pANT7 cGST vector. From the gel, it can be estimated that the size of the recombinant fragments is approximately 600bp, and the original vector is ~5000bp. To

compare, the expected sizes of the Col-CBD and Fib-CBD fragments were 575bp and 584bp. The expected size of the vector was ~5700bp.

5.1.3 Ligation into pGEM Vector

The purified PCR fragments were ligated into pGEM using Promega's T-vector system. The ligation reactions were set up to include 5 µL Ligation Buffer, 1 µL pGEM, 2 µL PCR fragment, 1 µL T4 DNA ligase, and filled to 10 µL with ddH₂O. A positive control was prepared with control DNA, instead of the PCR fragments, and a negative control was prepared without DNA. The ligation reaction was run overnight at 4°C.

5.1.4 *E. Coli* Transformation, Screening, and pGEM Isolation

The pGEM vectors from the ligation reactions were used to transform chemically competent JM109 (Promega >10⁸cfu/µg, Cat.No. L2001) *E. coli* cells. For each transformation, 50 µL of *E. coli* were transferred into a cold Eppendorf tube containing 2µL of the ligation reaction. The mixture was mixed by tapping the tube on the benchtop. It was allowed to incubate on ice for 20 minutes, then heat shocked in a 42°C waterbath for 60 seconds, before it was returned to ice for another 2 minutes. The *E. coli* then received 450 µL of prewarmed LB media and incubated at 37°C under moderate shaking for 1 hour. Prewarmed LB agar ampicillin plates were prepared with 20 µL of 50 mM X-Gal and 40 µL of 100mM IPTG, spread on the surface of the agar. Sample plates were prepared in duplicate with 150 µL of transformed *E. coli* added to each. A plate of each of the negative ligation and the positive ligation were prepared as controls. All of the plates were cultured overnight at 37°C and then incubated at 4°C for 6 hours.

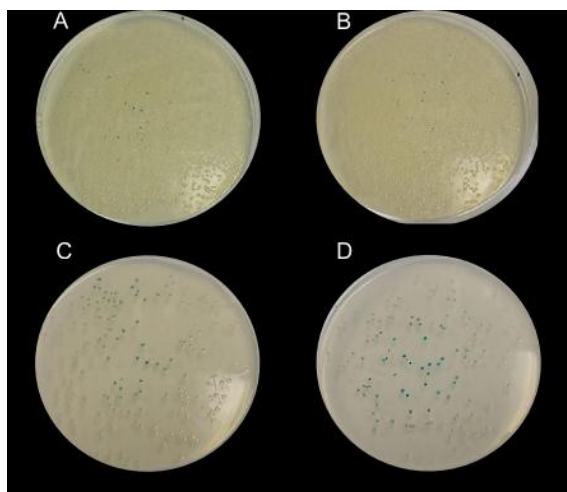


Figure 15: pGEM Transformations in JM109 *E. Coli*. (A) Cathelicidin-col-pGEM, (B) Cathelicidin-fib-pGEM, (C) Positive control, (D) Negative control

Blue –white colony screening (Figure 15) was used to isolate positive (white) colonies and test for fragment incorporation into the vector. The pGEM vector includes the LacZ gene for β -galactosidase (β -gal) with the multiple cloning site (MCS) positioned in the middle of the gene. The expression of β -gal and the presence of X-gal, results in a blue bacterial phenotype. When the LacZ gene is interrupted by the insertion of a gene of interest, in this case cathelicidin, the β -gal is not expressed, and thus the colony phenotype is white.

Both plates transformed with pGEM containing cathelicidin showed very few blue colonies. The positive and negative controls, containing pGEM ligated with a test fragment or no fragment respectively, showed mostly blue colonies, which means that they did not contain a gene insert or were inefficiently ligated. Individual colonies were screened by a miniprep protocol which included inoculating 3 mL of LB 1x AMP media and incubating it overnight at 37°C. Half of the culture was used to isolate the plasmid. The cells were pelleted by centrifugation at 12,000 rcf for 30 seconds, and the supernatant was aspirated. A resuspension solution was prepared with 50mM Glucose, 25mM TRIS-HCL and 10mM EDTA at pH 8.0, autoclaved and vacuum sterile filtered. Then 100 μ L of ice-cold resuspension solution (~4°C) was added to the pelleted cells. The cells were vortexed until fully resuspended. A cell lysis

solution was freshly prepared with 100 μ L NaOH (10N), 500 μ L 10% SDS, and 4.4 mL of water and stored at room temperature until 200 μ L was added to the resuspended cells, and each tube was inverted ten times and incubated on ice for 3 minutes. A third solution was prepared to precipitate the cellular debris (60 mL 5M potassium acetate, 11.5 mL glacial acetic acid, and 28.5 mL H₂O, and stored at 4°C) and 150 μ L was added to the lysed cells. They were then vortexed in an inverted position at low speed for 10 seconds. The mixture was incubated on ice for 10min, and then centrifuged at 12,000rcf for 5 minutes. The 450 μ L of supernatant was transferred to a fresh vial, and two volumes of 100% cold ethanol were added, mixed by vortex, and left to incubate on ice for 2 minutes. The DNA was pelleted by centrifugation at 12,000 rcf for 5 minutes, and the supernatant ethanol was removed by pipette. The pellet was then rinsed with 1 mL of 70% ethanol and left to dry for 10 minutes at room temperature. After completely dry, the pellet was resuspended in 50 μ L of 1xTE (10mM Tris, 1mM EDTA, pH 7.5).

5.1.5 Restriction Digest and Fragment Purification

Restriction digests were performed to isolate the recombinant cathelicidin inserts from the pGEM vector. Once a colony proved positive for the vector and insert, the DNA was isolated with a large scale plasmid isolation, using Promega's Midiprep Plasmid Isolation kit (Cat. No. A2492). The restriction reactions of the Midiprep DNA were conducted using 3 μ L ligated DNA, 2 μ L 10x Buffer E (Promega), 1 μ L BamHI, 1 μ LEcoRI, 1 μ L RNase A, and to 20 μ L total with ddH₂O. Controls were also run; one without BamHI, one without EcoRI, and one with neither restriction nuclease. Gel electrophoresis was performed to verify the restrictions. One positive restriction of each recombinant form of the cathelicidin insert (fib and col) was run again in triplicate. The gel is shown in Figure 16. The isolated cathelicidin inserts were purified by Promega's SV Gel Clean-up kit and protocol.

The gel image of the restriction digest shows an unrestricted pGEM vector in the second lane, one digested with EcoRI alone [BamHI (-)] in the second lane, one restricted with BamHI

alone [EcoRI(-)] in the third lane, then the Col-CBD digestion in lanes 4-6 run triplicate, and the Fib-CBD digestion in lanes 7-10 also run in triplicate. Unrestricted pGEM ran at ~2500bp, but was expected to be 3000bp. All of the recombinant cathelicidin fragments ran at the expected size range of 500-600bp (see Figure 16).

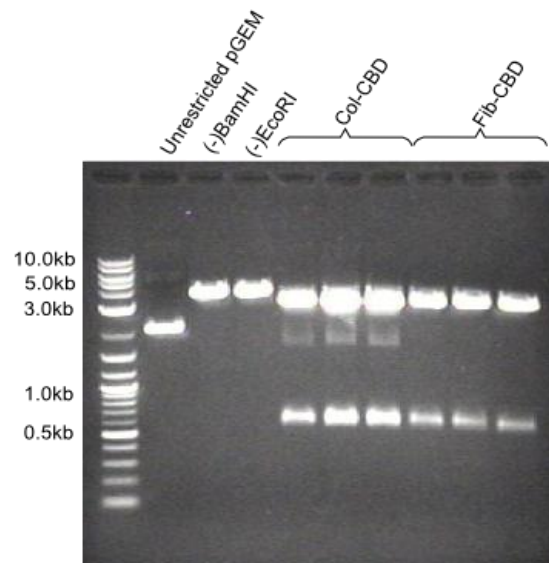


Figure 16: Restriction Analysis of pGEM Containing Recombinant Cathelicidin inserts.

5.1.6 Sequence Analysis

DNA Sanger sequencing followed by analysis with CLC Gene Viewer 6 confirmed 100% consensus between designed inserts and the isolated DNA. Sequencing results for both cathelicidin inserts are shown in Figure 17 and Figure 18 below.

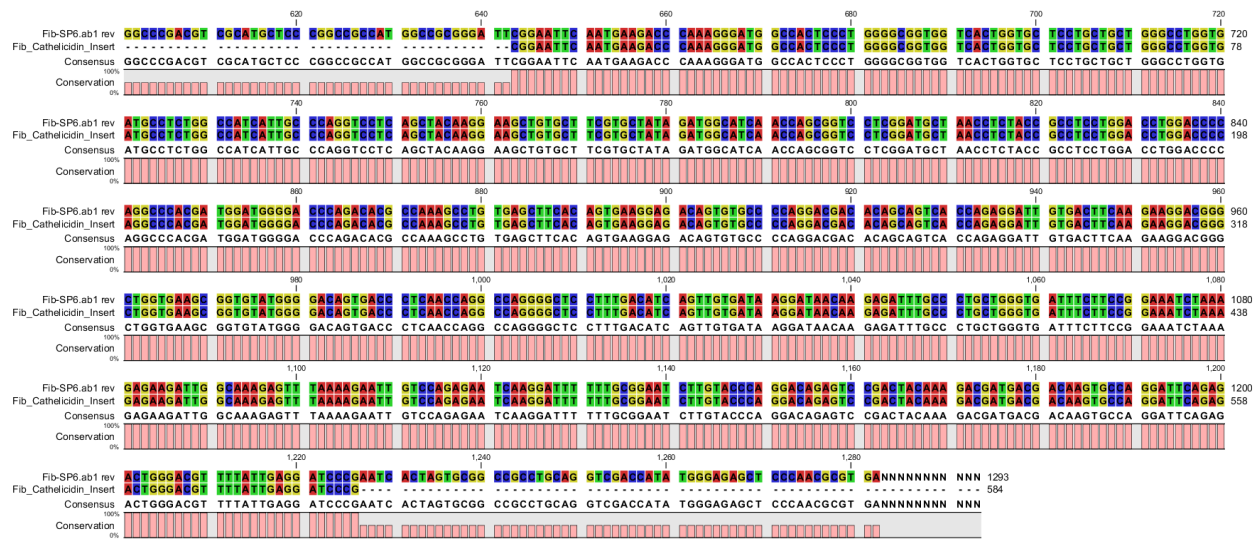


Figure 17: Alignment of Theoretical and Isolated Fib-CBD

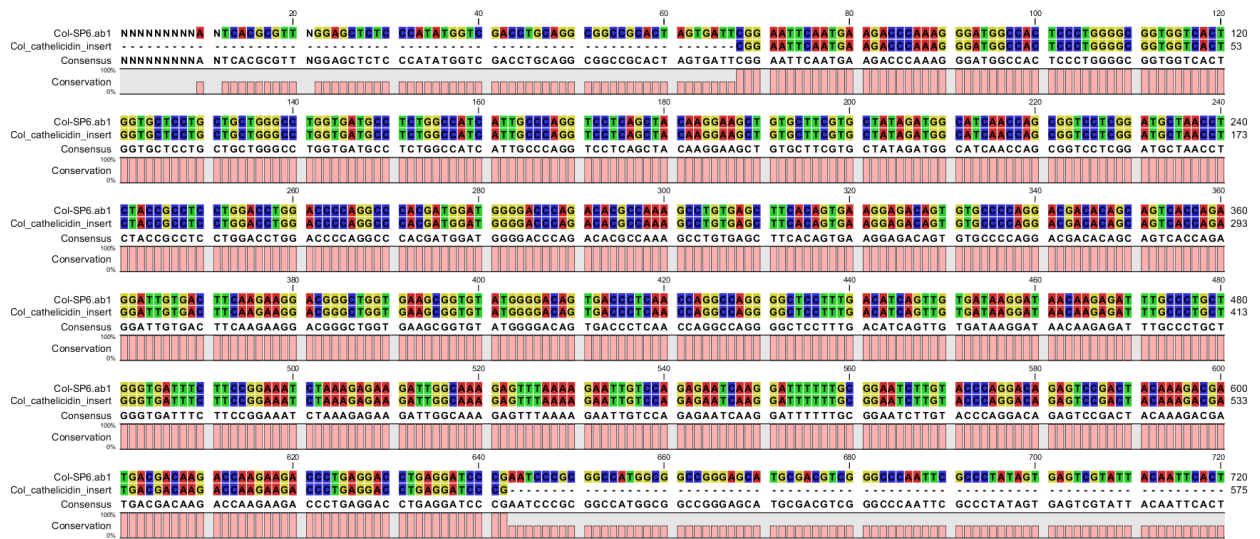


Figure 18: Alignment of Theoretical and Sequenced Col-CBD

5.1.7 p3xFLAG Ligation, Transformation, and Verification

The two recombinant cathelicidin inserts were ligated to form the final construct in p3xFLAG-Myc-CMV-26 vector (Sigma Aldrich, Cat. No. E7283), as shown in Figure 19. The ligation reaction was prepared with 5 μ L 10x T4 ligase buffer, 2 μ L p3xFLAG, 3 μ L purified DNA inserts, 1 μ L T4 ligase, to a total of 10 μ L with ddH₂O. A negative control was prepared with no insert DNA. The ligations were incubated overnight at 4°C.

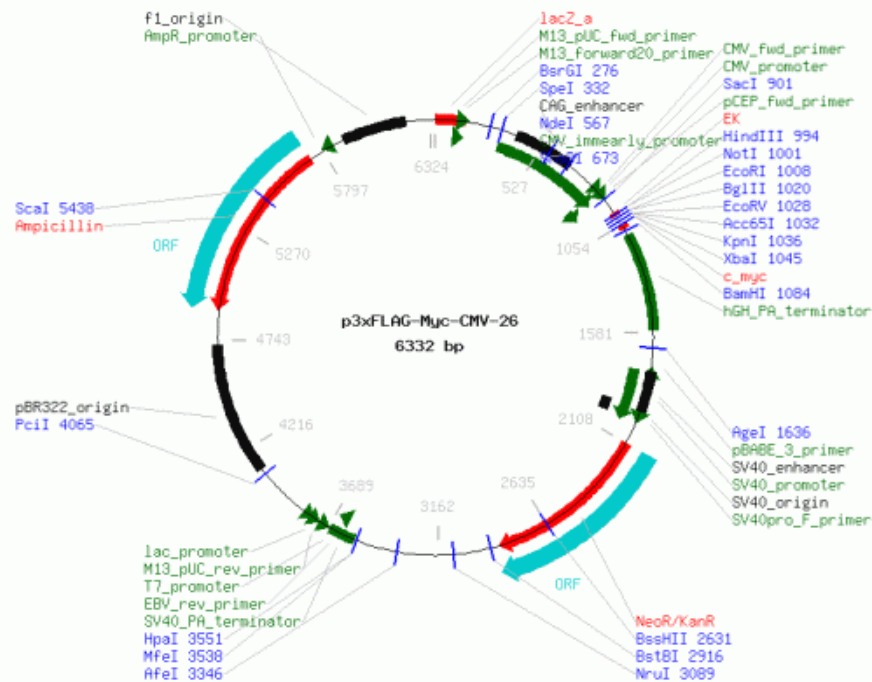


Figure 19: Map of p3xFLAG-Myc-CMV-26 vector

Transformations into JM109 *E. coli* were performed following the same protocol as for the pGEM transformations (see Figure 20). Cells were plated on LB-AMP agar plates, and cultured overnight at 37°C. The transformation results are shown in Figure 20. The colonies transformed with ligated p3xFLAG vector were selected by ampicillin resistance. The negative control, containing p3xFLAG with no insert, showed very few colonies, due to the improper ligation of the vector, resulting from the mismatching restricted ends (EcoRI and BamHI).

The colonies were screened for properly ligated p3xFLAG and insert using the miniprep protocol, followed by restriction analysis. Positive colonies were then cultured and their DNA was isolated using Promega's Midiprep kit. A restriction analysis of the final construct was done to verify the insertion of the recombinant cathelicidin inserts (see Figure 21). In the gel image, lane 2 represents unrestricted p3xFLAG, lanes 3 and 4 are each ligated with only one restriction

enzyme (EcoRI or BamHI, respectively), and lanes 5 and 6 are the digested inserts of Col-CBD and Fib-CBD, respectively. Unrestricted p3xFLAG ran at 6000bp, similar to its expected size of 6332bp. Both recombinant fragments ran at approximately 600bp, close to their expected size, thus confirming the successful incorporation of the inserts into the p3xFLAG vector.

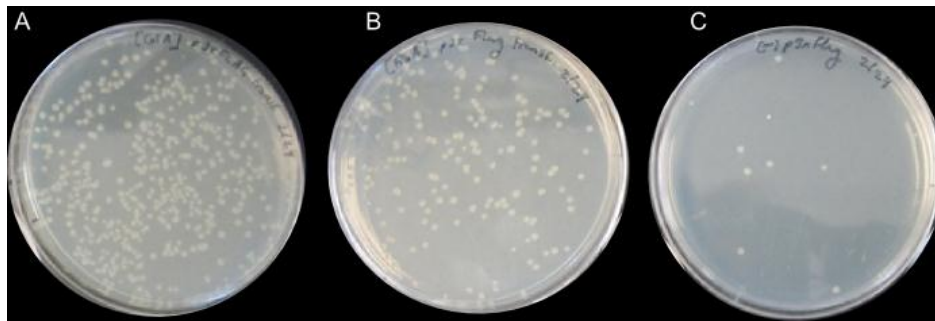


Figure 20: *E. coli* Transformation of p3xFLAG Final Constructs. (A) Col-CBD transformation, (B) Fib-CBD transformation, (C) Negative control

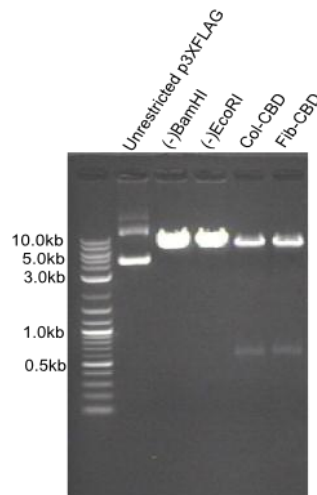


Figure 21: Restriction Digest of p3xFLAG with Ligated Recombinant Cathelicidin Inserts

5.1.8 H1299 Transfection

Because of the low transfection efficiency of primary dermal fibroblasts, human lung carcinoma (H1299) cells were used as a model cell type to verify the design of the construct and its mammalian expression. The cells were seeded to attain 80% confluence after 24 hours of culture. They were maintained with standard DMEM with 10% FBS on 6-well tissue culture plates (CellTreat, Cat. No. 229106) and incubated at 37°C. The cells were transfected with the two cathelicidin p3xFlag constructs using Qiagen's Effectene lipofection kit (Cat. No. 301425)

and protocol. A GFP-Flag-Apoptin control vector was used to verify the success of the transfection (Heilman, Teodoro, & Green, 2006). Each construct was transfected in duplicate.

5.1.9 Western Blot

Expression of the control GFP vector was assessed 24hrs after transfection by examining the cells using a Zeiss Axiovert 40CFL inverted fluorescence microscope at 200x. The fluorescence image (Figure 22A) shows that GFP was expressed, which confirmed the success of the transfection.

To prepare cell lysates for Western blot analysis, each well was scraped after 2 washes with 1x PBS. The cell solution from each well (in 400 μ l PBS) was centrifuged at 1500rpm for 10 minutes. The supernatant was removed and the cell pellet was resuspended in 200 μ l RIPA lysis buffer (50mM Tris pH 7.6, 200mM NaCl, 1%NP-40, 0.1%SDS, and 2mM PMSF) and incubated on ice for 20 minutes. The suspension was then centrifuged at 5000rcf for 10 minutes, and the clarified lysate was transferred to a fresh vial. Lysates were stored at -20°C until ready for Western analysis.

For the Western blot, a 16% SDS-polyacrylamide resolving gel was prepared with 5.3 mL 30% Acrylamide/0.8% Bis, 2.5 mL resolving buffer (1.5M Tris-HCL pH8.8), 0.1mM 10% SDS, and 2.1 mL ddH₂O. The polymerization was catalyzed with 50 μ L 10% ammonium persulfate (APS) and 7 μ L TEMED. The gel was poured using a Bio-rad mini apparatus. The stacking gel consisted of 0.65 mL 30% Acrylamide/0.8%Bis, 1.25 mL stacking gel buffer (0.5M Tris-HCL pH 6.8), 50 μ L 10% SDS, and 3.05 mL ddH₂O. The gel was polymerized with 25 μ L 10% APS and 5 μ L TEMED.

The Western samples were prepared with 20 μ L of lysate and 5 μ L of protein loading dye. The samples were denatured on a heating block at 95°C for 5 minutes before loading them onto the gel. Invitrogen's Novex Sharp prestained ladder (Cat. No. LC5800) was used as the

standard. The gel was run in a 1x Tris-Glycine pH 8.3 running buffer (0.3% tris, 1.44% glycine, 0.1% SDS), at 35mAmps for 2 hours at a constant current.

The gel was transferred onto a nitrocellulose membrane, and run in a 1x Tris-Glycine (without SDS) transfer buffer containing 20% methanol, for 1 hour at 200mAmps constant current. Immediately after the transfer, the membrane was blocked on a shaker at 4°C overnight with 5% powdered milk in 1x Tris Buffered Saline Tween-20, pH 7.3 (TBS-T) (25mM Tris-HCL, 137mM NaCl, 2.7μM KCl, to 1000 mL with ddH₂O, and 0.5% tween-20).

The blocked membrane was washed 5 times for 5 minutes each time in TBS-T, then incubated in α-FLAG mAb M2 1/5000 (Sigma, Cat. No. F3165-.2MG) in TBS-T for 5 hours at 4°C and 1 hour at room temperature on an agitator. After the primary incubation, the membrane was washed five times for 5 minutes each in TBS-T. It was then incubated in goat α-mouse 1/10000 antibody (Sigma, Cat. No. A4416-.5ML) for 1 hour on an agitator at room temperature. It was then washed five times for 5 minutes each in TBS-T and then washed two times for 5 minutes in TBS (without Tween-20).

Promega's horseradish peroxidase chemiluminescence ECL reagents (Cat. No. W1001) was used for the detection of the secondary antibody on the membrane. The two bands on the Western blot confirm the expression of both Col-CBD and Fib-CBD in H1299 cells. No bands are seen in the lower molecular weight range (see Figure 22B).

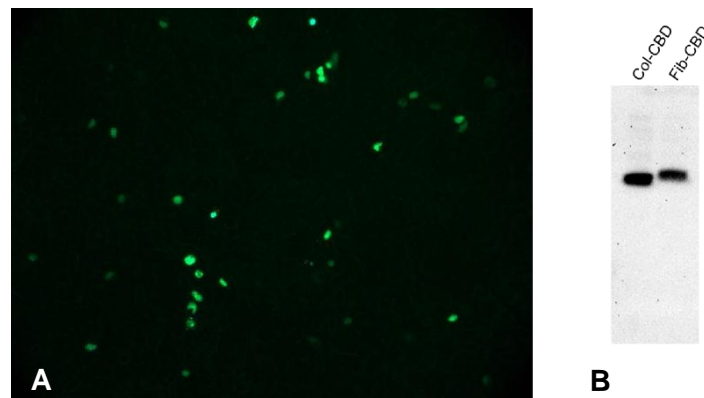


Figure 22: H1299 Transfection. (A) Transfection efficiency monitored by GFP expression, (B) Western blot confirming expression of cathelicidin constructs by H1299 cells

5.2 Cell-Derived Sheet Culture

The design team conducted various experiments to determine a method for fabricating fibroblast cell-derived sheets (CDSs). In most experiments, the team used human neonatal fibroblasts (NHF) to produce the cell sheets. However, due to the fibroblasts' slow proliferation rate, the design team decided to use a model cell type for additional proof-of-concept experiments. Rat aortic smooth muscle cells (RASMCs) were chosen based on their fast proliferation rate. These cells were used only to investigate the effectiveness of anchors to hold down the CDS; the design team recognized that characteristics of the RASMCs other than the physical production of a sheet were not translatable to fibroblasts.

In the following experiments, medium will be referred to as complete or unsupplemented. Two types of media were used, 1X Dulbecco's Modified Eagle Medium (DMEM) (Mediatech, Inc.) and Iscove's Modification of DMEM (IMDM) (Mediatech, Inc.). Complete DMEM consisted of 10% fetal bovine serum (FBS) and 1% nonessential amino acids (including alanine, asparagine, aspartic acid, glycine, glutamic acid, proline, and serine), penicillin/streptomycin, sodium pyruvate, and L-glutamine. Complete IMDM consisted of 10% FBS, 1% penicillin/streptomycin, L-glutamine, and 25 mM HEPES. For fabricating cell sheets, the FBS content of the complete media was reduced to 5% in order to moderate proliferation and encourage matrix production. Unsupplemented media refers to DMEM or IMDM without any added supplements.

For cell sheets treated with 50 µg/mL of ascorbic acid, the media was prepared fresh before use. First, a 100X stock was made with 5mL of unsupplemented IMDM and 25mg of L-ascorbic acid (Wake Pure Chemical Industries, Ltd). The stock was sterile filtered using a 0.2 µm cellulose acetate sterile syringe filter. Next, 100µL of the 100X stock was added to 10mL of complete IMDM, of which 1mL was added to each well.

Cell sheets were characterized using histology and uniaxial tensile testing. The mechanical testing protocol for cell sheets can be found in Section 5.4. To obtain histological sections, the cell sheets were processed and stained with Hoechst, H&E, or Picrosirius Red/Fast Green. Hoechst stains for nuclei (blue), H&E differentiates nuclei (blue), cytoplasm (pink), and red blood cells (red), and Picrosirius Red/Fast Green stains collagen red and non-collagenous fibers green. To process the samples, the cell sheets were housed in cassettes and fixed in formalin for 1 hour. Next, the tissues were submerged in an alcohol and xylene series, after which they were embedded in paraffin. A processing protocol is detailed in Appendix G. The paraffin blocks containing the cell sheet samples were cut into 6 μ m sections using a microtome. To stain the samples, slides containing the cell sheet sections were dehydrated through a series of xylene and alcohol and then stained with the appropriate stain. Afterwards the tissues were rehydrated using the appropriate protocol, and cover-slipped. Detailed protocols for Hoechst, H&E, and Picrosirius Red/Fast Green stains can be found in Appendix H: Staining Protocols for Paraffin Sections.

5.2.1 Experiment 1: Fibroblast Sheets on UpCell™ Plate

The design team explored the use of NUNC UpCell™ 24-well plates (Thermo Fisher Scientific, Inc.). These plates contain temperature-responsive NIPAAM (poly(N-isopropylacrylamide)) surfaces that allow for easy harvesting of cell sheets. When the temperature of the culture decreases, the NIPAAM surfaces release the adherent cells with their structural proteins intact (Thermo Fisher Scientific, 2010). From this experiment, the team wanted to develop a method for growing the cells into a sheet and harvesting these sheets.

Human neonatal fibroblasts were grown to 80% confluence in complete DMEM at 5% CO₂. Due to a low supply of fibroblasts only 7 wells were seeded. Fibroblasts at p10 were seeded in three wells at 2x10⁶ cells/cm² and one well at 1x10⁶ cells/cm². Fibroblasts at p7 were seeded in three wells at 2x10⁶ cells/cm². The experimental set up is shown in Table 18.

Table 18: Experimental Setup of Fibroblast Sheets

UpCell™	1	2	3	4	5	6
NHF p7	2x10 ⁶	2x10 ⁶	2x10 ⁶	1x10 ⁶		
NHF p10	2x10 ⁶	2x10 ⁶	2x10 ⁶			

After 24 hours, the team observed the formation of cell sheets in all of the wells (see Figure 23). These sheets were dislodged from the bottom and sides of the plate and were beginning to form into balls. As seen in Figure 23, the media in wells 1-3, containing p7 fibroblasts seeded at 2x10⁶ cells/cm², were very yellow, while the media in wells 5-7, containing p7 fibroblasts at the same concentration, remained pink. Because these six wells should have contained the same amount of cells, the media should have looked the same color after 24 hours. Therefore, it is likely that since the media in wells 1-3 were yellow, more cells were delivered to those wells. Because the p10 and p7 fibroblasts were counted at different times, it is likely that an error occurred in the cell count. Despite this discrepancy, the design team reasoned that the sheets might have dislodged for three reasons: 1) both the 2x10⁶ cells/cm² and 1x10⁶ cells/cm² seeding densities were too high for the cells to form proper sheets, 2) the cells were nutrient deprived, 3) the UpCell™ surfaces were compromised due to a long storage period.

The design team noticed that in wells 1-4, all of the fibroblasts were incorporated into the formation of the detached cell sheet. However, in wells 5-7, some fibroblasts remained attached to the bottom of the plate and had not been incorporated into the cell sheet. These sheets were further cultured as described in Experiment 1A.

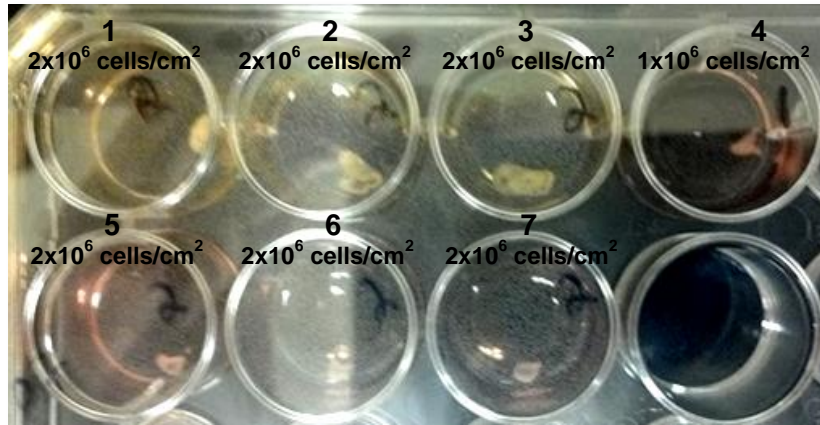


Figure 23: Fibroblast CDSs after 24 Hours on UpCell Plate

One floating cell sheet at each density (wells 1 and 5) were processed and stained with Hoechst, Hematoxylin and Eosin (H&E), and Picrosirius Red/Fast Green (see Appendix H: Staining Protocols for Paraffin Sections).

Figure 24 shows the histology of the cell sheet with p10 fibroblasts (images A-C) and the cell sheet with p7 fibroblasts (images D-F). The images show that the fibroblasts aggregated into a sheet overnight. However, the Picrosirius Red/Fast Green stains (C and F) show that no collagen was formed in the cell sheet because no red-stained fibers are observed. This suggests that the cells had not been in culture long enough to produce collagen.

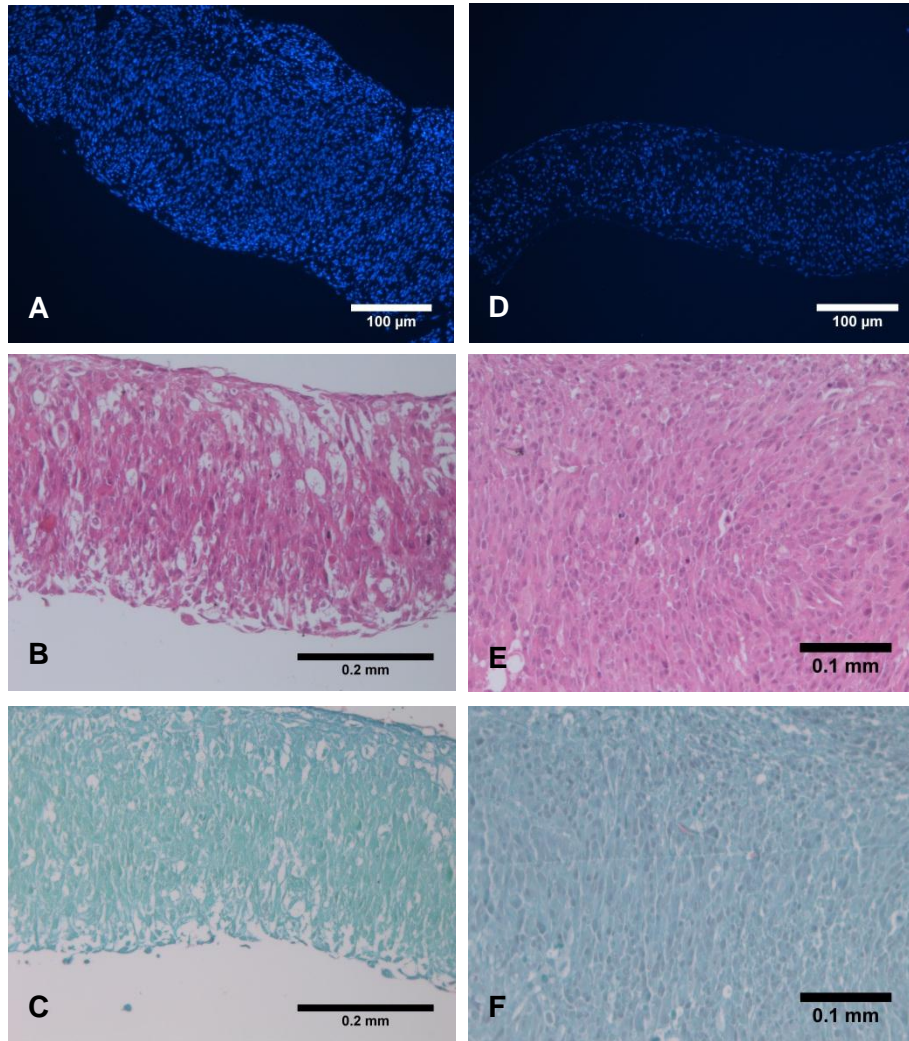


Figure 24: Histology of fibroblast CDSs after 24 hours on UpCell plate. Figures A and D are stained with Hoechst; B and E with H&E; and C and F with Picrosirius Red.

5.2.2 Experiment 1A: Fibroblast Sheets on UpCell Plate

Although the concentration of cells was unknown, the fibroblasts that remained on the bottom of the UpCell™ plate in three wells from Experiment 1 were kept in culture. These cells were maintained in IMDM with 5% FBS. Ascorbic acid was added at 50 μg/mL when the cells were fed. The media was changed (1mL) every 48 hours. While in culture, cell sheets visually formed on the bottom of the wells. Figure 25 shows the cell sheet after 12 days in culture.

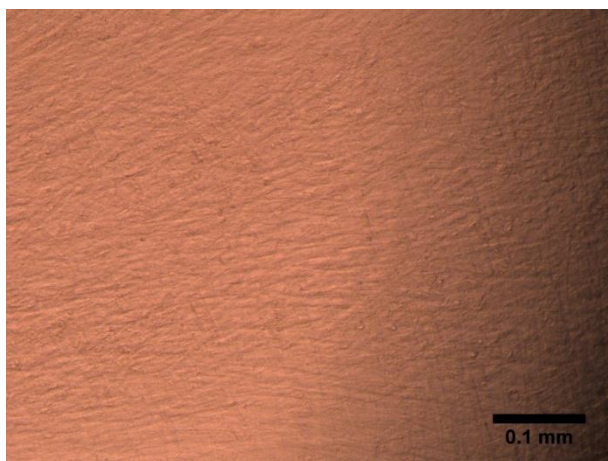


Figure 25: Fibroblast CDS after 12 Days on UpCell Plate

After 17 days, parts of the cell sheet had begun to detach from the sides of the well. That same day, the sheets were harvested by placing the UpCell™ plate at 25°C for 60 minutes. Tweezers were used to pull the tissue off the plate. The sheets came off the plates easily and were placed in PBS. One CDS was removed for processing (see Appendix G).

Figure 26 shows the histology of the CDS. Although the sheet does not look as thick and cohesive as the CDS from Experiment 2, the Picrosirius Red stain clearly shows that the production of collagen (red) was greater in these cell sheets (Figure 26C).

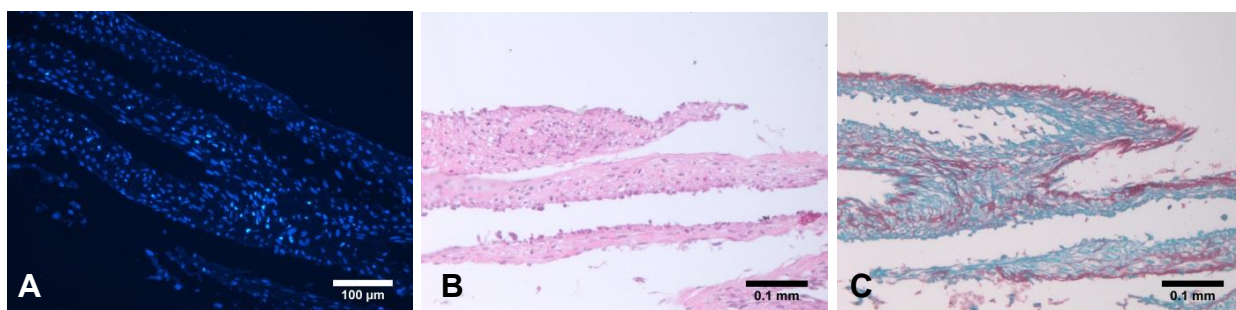


Figure 26: Histology of Fibroblast CDSs after 17 Days on UpCell Plate. Figure A is stained with Hoechst; B with H&E; and C with Picrosirius Red/Fast Green.

5.2.3 Experiment 2: Anchors on RASMC Sheets

Because the higher density tissues dislodged from the plate overnight, the design team wanted to be sure that tissues with an initial lower density would not dislodge over time in culture. The team decided to use an anchor to restrain the cell sheets from contracting into a

ball. The anchor consisted of a porous polyethylene ring cut to the dimensions of the 2 cm diameter well. By using a polyethylene mesh, the cell sheet could integrate into the mesh and be harvested as a flat sheet. Since the polyethylene floats in media, a stainless steel washer was placed over the ring to secure it against the bottom. The following diagram shows the setup of the ring and washer in the well (see Figure 27).

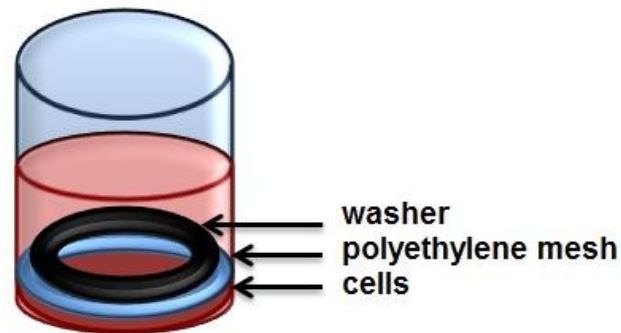


Figure 27: Anchor System

Because fibroblast supply was insufficient for seeding, the team used rat aortic smooth muscle cells (RASMCs) this experiment. To test the effectiveness of the anchors, the team seeded the RASMCs at higher densities that would form tissues overnight according to Experiment 1. If the anchors were able to hold down these CDSs of higher densities, then the anchors would be an effective method to control the cell sheets. The team also seeded at lower densities to observe the effects of the anchors when the CDS formed from a subconfluent density. The cells were seeded in 6 wells each of 500,000 cm^2/mL , 250,000 cm^2/mL , 100,000 cm^2/mL , and 50,000 cm^2/mL . Each density was plated with and without an anchor. The following chart shows the experimental setup of the plate (see Table 19).

Table 19: Experimental Setup using Anchors on RASMCs

TCPS	1	2	3	4	5	6
- anchor	50,000	50,000	50,000	100,000	100,000	100,000
+ anchor	50,000	50,000	50,000	100,000	100,000	100,000
- anchor	250,000	250,000	250,000	500,000	500,000	500,000
+ anchor	250,000	250,000	250,000	500,000	500,000	500,000

The cells were plated in 1mL of IMDM on standard tissue culture polystyrene plates and were observed after 24 hours. Figure 28 shows the plate after 1 day in culture. Visible cell sheets formed in all of the wells that had been seeded at 500,000 cells/cm² or 250,000 cells/cm² (Figure 28). Regardless of the anchor, these sheets had all dislodged from the bottom of the plate and contracted. Figure 29 shows the cell sheets that dislodged. Figure 30 shows that the RASMCs seeded at lower densities with and without anchors formed sheets that remained attached to the bottom of the well.

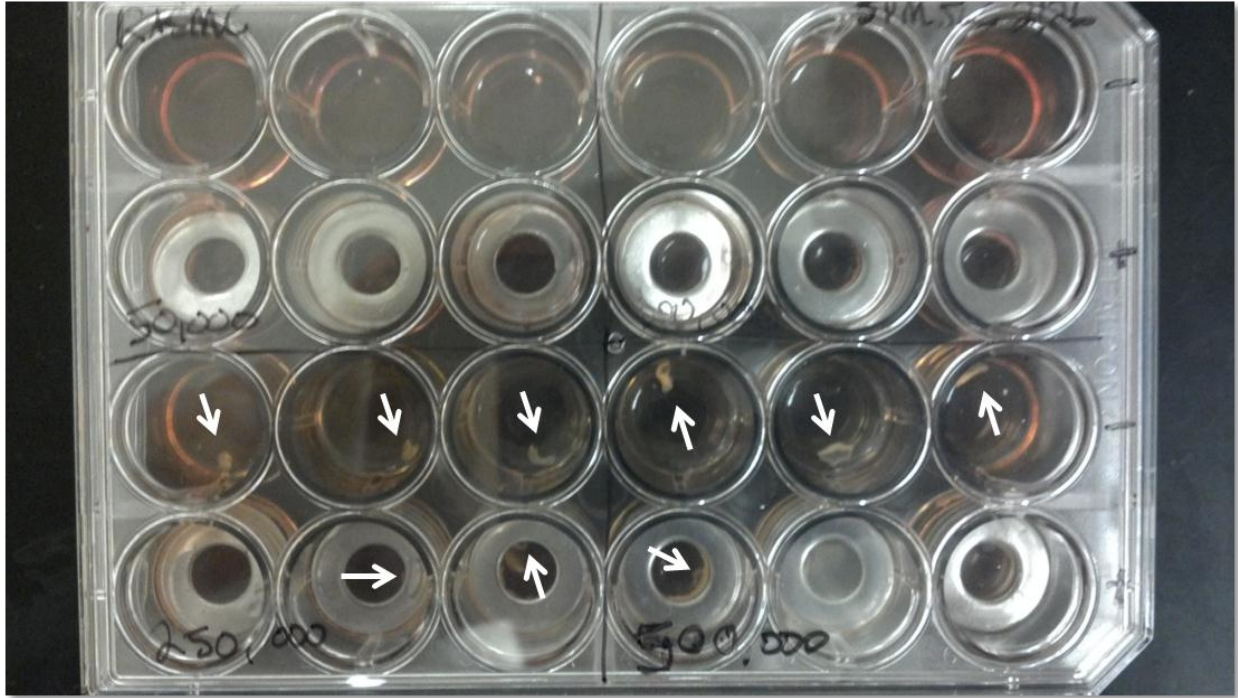


Figure 28: RASMC CDSs with Anchors after 24 Hours on TCPS

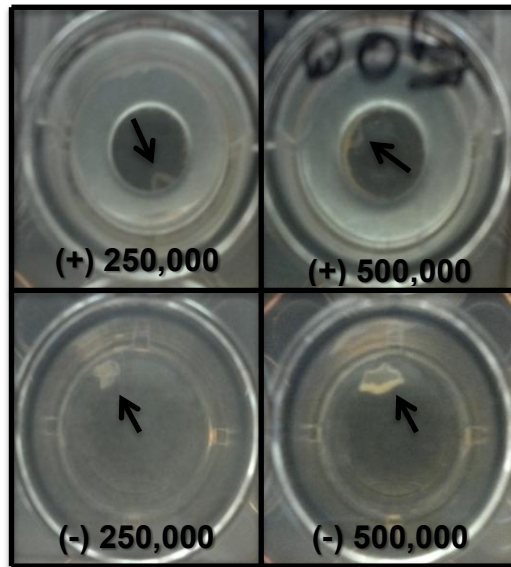


Figure 29: Setup for Anchor Experiment

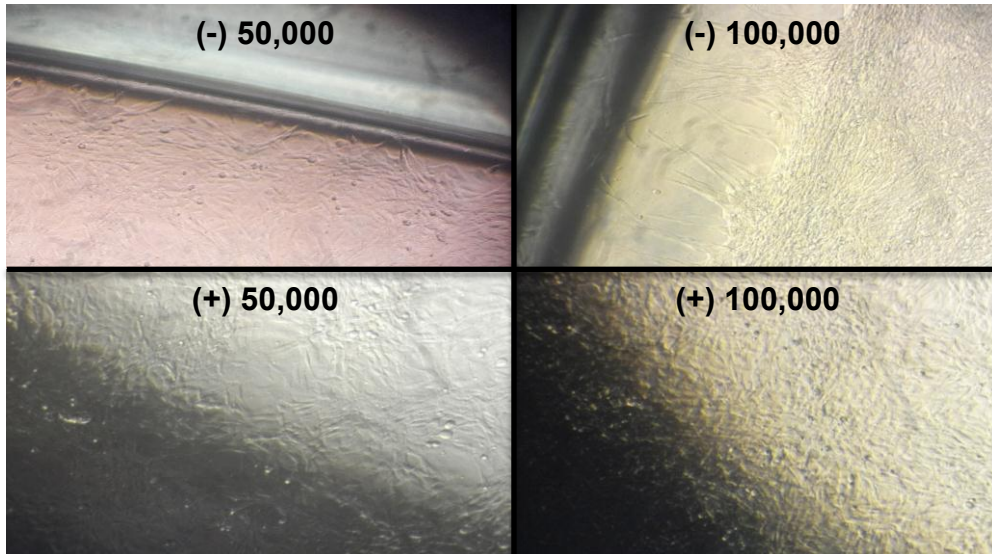


Figure 30: RASMC CDSs at 50,000 and 100,000 cells/cm² with and without anchors

Because the anchors were not able to hold down the cell sheets that formed in the higher density wells, the team believed that the anchors would not be useful for the lower density wells in a longer culture. Furthermore, the cell sheets on the UpCell™ plate with unknown density of fibroblasts were very easy to detach from the plate without the use of an anchor and had remained adhered to the well bottom for 17 days (Experiment 1A). Therefore, the team decided that anchors were unnecessary, and the most important aspect was growing these cell sheets for two weeks following a seeding at a sub-confluent density of 100,000 cells/cm².

5.2.4 Experiment 3: Lower Density Fibroblast CDSs on UpCell™ Plates

Using the results from the proof-of-concept experiments, the team decided that the fibroblast cell sheets should be cultured on UpCell™ plates at densities lower than 250,000 cells/cm². Because Experiment 2 with RASMCs could not be completely translatable, a variety of densities were chosen to explore, including 100,000 cells/cm², 50,000 cells/cm², 25,000 cells/cm², and 12,500 cells/cm².

Fibroblasts were grown in complete IMDM until passage 11. The fibroblasts were seeded on one plate at 100,000 cells/cm² and 50,000 cells/cm². To be able to observe the effects of ascorbic acid on the mechanical strength of the tissue, columns 1-3 were fed with 50 µg/mL of ascorbic acid and columns 4-6 were not treated with ascorbic acid. Accordingly, a total of 6 samples for each density received the ascorbic acid treatment. Table 21 shows the experimental setup, with the cell densities shown and (+aa) corresponding to the ascorbic acid treatment.

Table 20: Experimental Setup of Fibroblasts on UpCell™ Plate 1

UpCell™ Plate 1	1 (+aa)	2 (+aa)	3 (+aa)	4 (-aa)	5 (-aa)	6 (-aa)
[cells/cm ²]	100,000	100,000	100,000	100,000	100,000	100,000
[cells/cm ²]	100,000	100,000	100,000	100,000	100,000	100,000
[cells/cm ²]	50,000	50,000	50,000	50,000	50,000	50,000
[cells/cm ²]	50,000	50,000	50,000	50,000	50,000	50,000

On a second UpCell™ plate, cells were seeded at two lower densities (25,000 cells/cm² and 12,500 cells/cm²) in the event that the seeding densities in the first UpCell™ plate were still too high, leading to the tissues dislodging during culture. Table 21 shows the experimental setup. The goal was to find the maximum number of cells that could be used to create cell sheet formation without detaching from the bottom of the well over time.

Table 21: Experimental Setup of Fibroblasts on UpCell™ Plate 2

UpCell™ Plate 2	1	2	3	4	5	6
	(+aa)	(+aa)	(+aa)	(+aa)	(+aa)	(+aa)
[cells/cm ²]	25,000	25,000	25,000	25,000	25,000	25,000
[cells/cm ²]	12,500	12,500	12,500	12,500	12,500	12,500

These cell sheets remained in culture for two weeks. Media (1mL) was changed every other day, and 50µg/mL of ascorbic acid was freshly added for sheets receiving treatment. To harvest the sheets, the UpCell™ plates were left at room temperature for 60 minutes. The sheets were then peeled away from bottom of the well. No noticeable damage occurred during harvesting, however the cell sheets contracted if not submerged in liquid. Figure 31 shows a freshly harvested fibroblast sheet at 100,000 cells/cm² pinned to a PDMS platform. As seen in Figure 31, the sheets do not remain flat without manipulation. Figure 32 shows that noticeable macroscopic differences in size and opacity of the tissues can be observed between the 100,000 cells/cm² and 50,000 cells/cm² grown with ascorbic acid. This was true for cell sheets derived from cells seeded at all initial cell seeding densities.

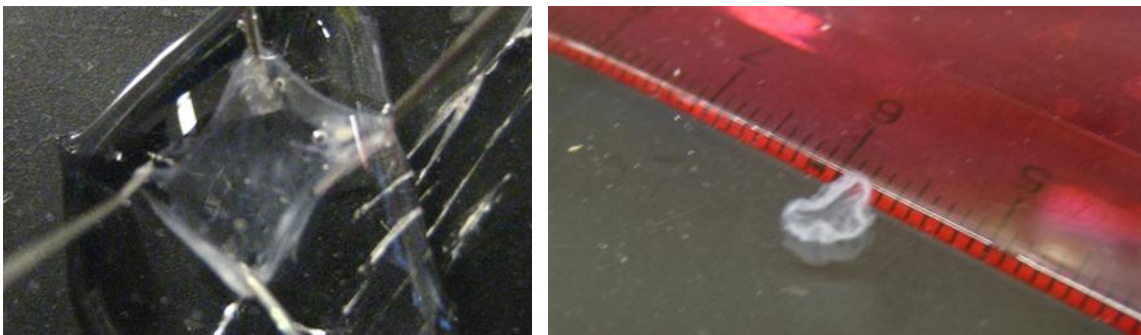


Figure 31: Freshly harvested fibroblast sheets (100,000 cells/cm²)

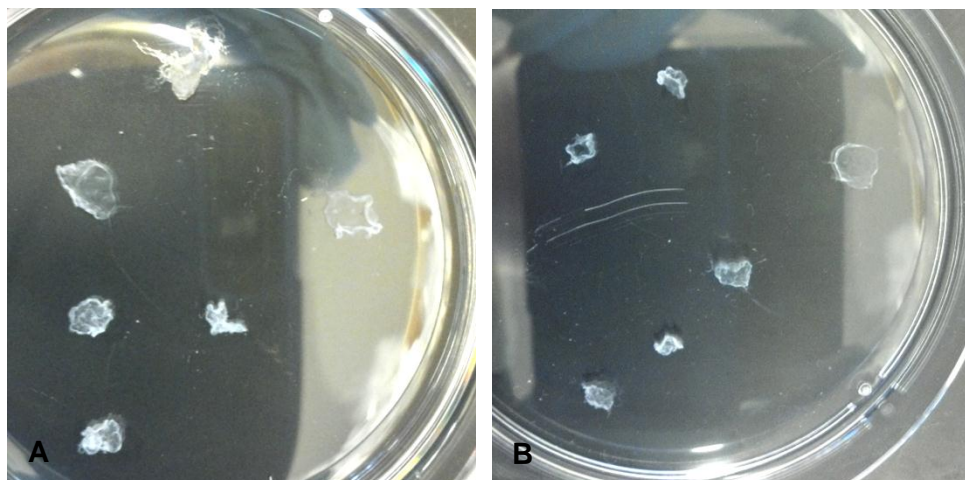


Figure 32: Fibroblast sheets with ascorbic acid. (A) 100,000 cells/cm², (B) 50,000 cells/cm²

After harvesting, the CDSs were characterized. One cell sheet at each density and with or without ascorbic acid treatment was processed immediately. One cell sheet at each density (all with ascorbic acid) was subjected to either freeze-thaw, SDS, or hypertonic/hypotonic solutions (as described in 5.3: Decellularization, pp. 116). After processing, these sheets were sectioned and stained using Hoechst, H&E, and Picrosirius Red/Fast Green. Additionally, one cell sheet with and without ascorbic acid at each density was subjected to mechanical testing (as described in 5.4: Mechanical Testing of Tissues, pp. 130).

Histology was performed to determine (1) if ascorbic acid affected collagen production and tissue structure and (2) which density was optimal for creating a cohesive cell sheet. Because the tissue samples were so small, some samples were lost during processing and embedding. The protocol was revised in future experiments to eliminate this problem.

Picrosirius Red/Fast Green staining was used to observe the contribution of collagen production from ascorbic acid. Figure 33 shows the differences in collagen production between cell sheets seeded at 100,000 cells/cm² cultured with ascorbic acid (Figure 33B) and without ascorbic acid (Figure 33A). The cell sheet in Figure 33B has visibly more collagen synthesis (red fibers); however, production was limited to only one side of the sheet. These images were representative of cell sheets grown at all densities.

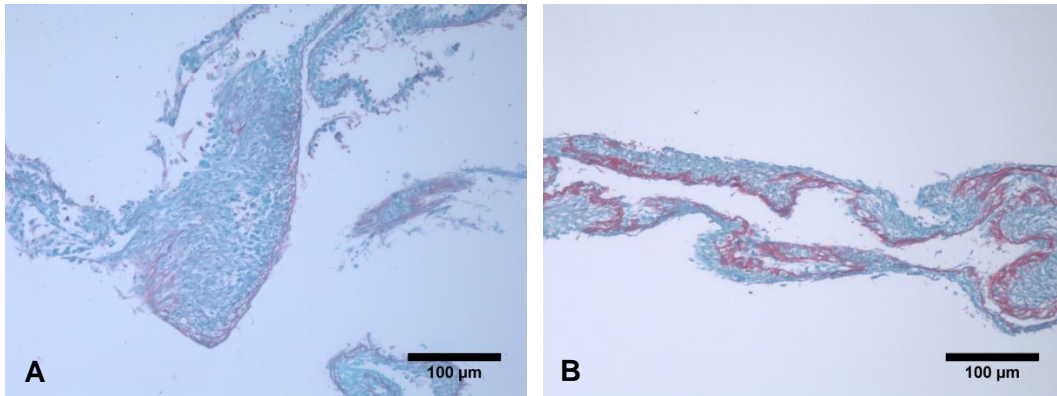


Figure 33: Picrosirius Red/Fast Green Stains of CDSs. (A) Untreated, (B) 50µg/mL Ascorbic Acid

5.2.5 Experiment 4: Final Validation of Fabricating CDSs

The goal of this experiment was to (1) validate fibroblast sheet fabrication method, (2) measure tissue thickness, (3) evaluate collagen synthesis in cell sheets treated with or without ascorbic acid, (4) assess the strength of sheets with and without ascorbic acid, (5) assess strength of tissues before and after decellularization, and (6) perform histological analysis (H&E and Hoechst staining) on decellularized tissues to assess preservation of tissue structure and nuclei, respectively.

The final fibroblast sheets were seeded at 100,000 cells/cm² on UpCell™ plates and were cultured in IMDM with 5% FBS at 5% CO₂ for 14 days. Media (1mL) was changed every other day, and 50µg/mL of ascorbic acid was freshly added for sheets receiving treatment. To utilize the amount of cells that the team could obtain, fibroblasts cultured to two different passage numbers were used (p6 and p12). Table 22 shows the experimental setup, with dark blue representing p6 fibroblasts and light blue representing p12 fibroblasts. Wells marked with a plus sign were treated with ascorbic acid, while wells with a minus sign did not receive ascorbic acid.

After two weeks of culture, the sheets were harvested. After sitting at room temperature for 60 minutes, the sheets were peeled from the UpCell™ plates. Five cell sheet samples had detached from the bottom of the plate by the end of the culture period and were not used for testing. These included two p12 with ascorbic acid, two p6 with ascorbic acid, and one p6

without ascorbic acid, and are marked with X's in Table 22. The cell sheets detaching from the plate while in culture was surprising, since this was not the case in Experiment 3 for the same cell density.

Two sheets treated with ascorbic acid and two sheets treated without ascorbic acid were fixed and processed. These sheets are marked "P" in Table 222. The processing protocol was modified so that tissue sheets were placed inside a folded piece of filter paper, which was sandwiched between two sponges and then secured in a cassette. Three sheets treated with ascorbic acid and three sheets treated without ascorbic acid were used for mechanical testing immediately after harvesting (see Section 5.3.4.2.3). These sheets are marked "M" in Table 222. Five sheets marked with "DP" or "DM" were set aside for decellularization and subsequent processing and mechanical testing, respectively; however the team was not able to complete these protocols.

Table 22: Experimental Setup for Final Fibroblast Sheets

UpCell Plate™	1	2	3	4	5	6
A	(+) P	(+) P	(+) X	(-) M	(-) M	(-) M
B	(+) M	(+) M	(+) M	(+) DP	(-) P	(-)P
C	(+) DP	(+)DM	(+) DM	(+) X	(-) X	(-) M
D	(+) X	(+) X	(+) DM	(+)	(-)	(-)

Figure 34 shows a picture of a fibroblast sheet, which was macroscopically representative of sheets grown with and without ascorbic acid. However, Figure 35 shows that the cellular orientation appeared to vary in sheets cultured with (Figure 35B) and without (Figure 35A) ascorbic acid.

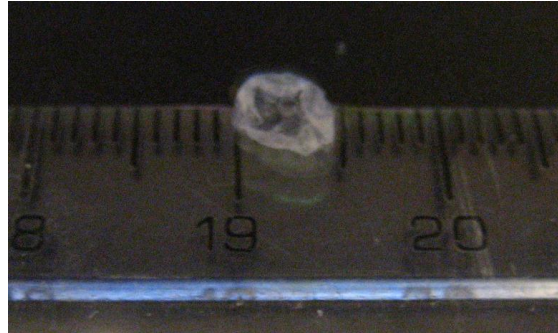


Figure 34: Freshly Harvested Fibroblast Sheet for Mechanical Testing

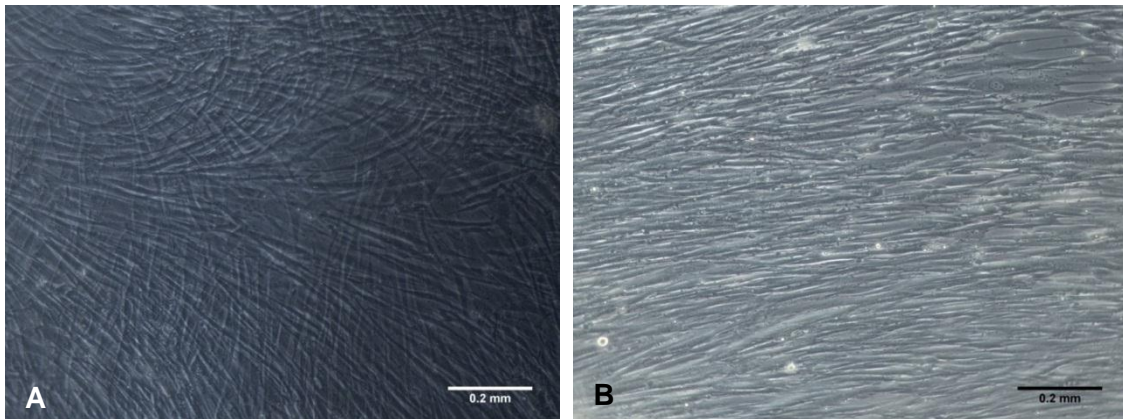


Figure 35: Cellular Alignment of Fibroblast Sheets. (A) Untreated Ascorbic Acid, (B) 50µg/mL Ascorbic Acid

Before harvesting, tissue thickness was determined using a Mitutoyo absolute digital caliper in conjunction with an Olympus CK2 confocal microscope. The microscope was focused on the bottom of a blank well to determine the starting distance. The change in distance was recorded as the position of the objective moved to where the top layer of the cell sheet became just out of focus, which equated to the thickness of the cell sheet. The thicknesses of the sheets are recorded in Table 23. T-test was used to compare the thicknesses of the two groups, and showed that there was a significant difference ($p=0.047 < p=0.05$) between the cell sheets grown with and without ascorbic acid.

Table 23: Cell Sheet Thickness

	(-aa)	(+aa)
	0.365	0.446
	0.337	0.283
	0.25	0.447
	0.405	0.456
	0.302	0.359
	0.296	0.423
	0.355	0.457
	0.215	0.339
		0.281
Average	0.315625	0.387889
Std Dev	0.058562	0.069259

Picrosirius Red/Fast Green stain was used to identify collagen production in the fibroblast cell sheets. This stain identifies collagen fibers in red and non-collagenous fibers in green. Figure 36 shows representative images of fibroblast sheets with and without ascorbic acid. Sheets cultured in the presence of ascorbic acid visibly had more collagen (red) throughout the tissue. The boxes in Figure 36 represent the areas imaged at higher magnification (Figure 37). Figure 37 better identifies the difference in collagen production between the two cell sheets. No collagen is observed in the sheets grown without ascorbic acid.

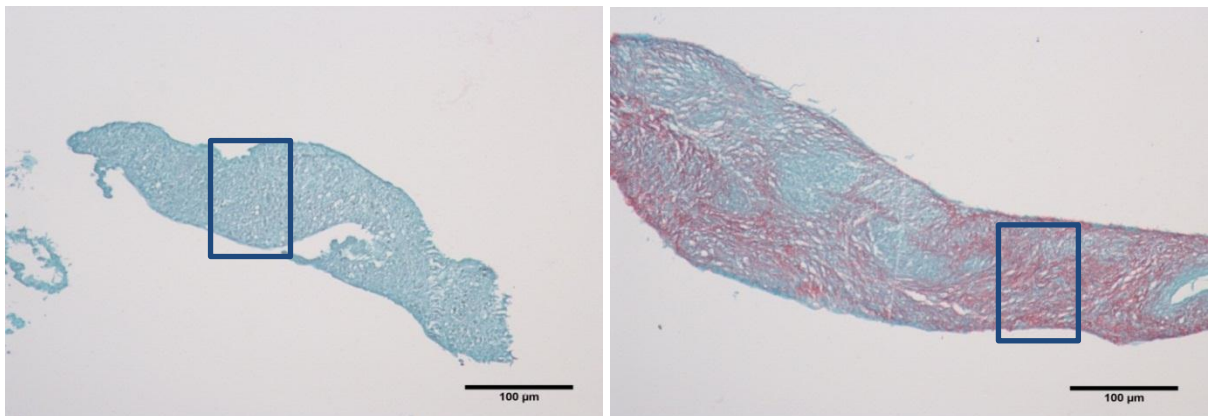


Figure 36: Picrosirius Red/Fast Green Stain of Fibroblast Sheets. (A) Untreated, (B) 50µg/mL Ascorbic Acid

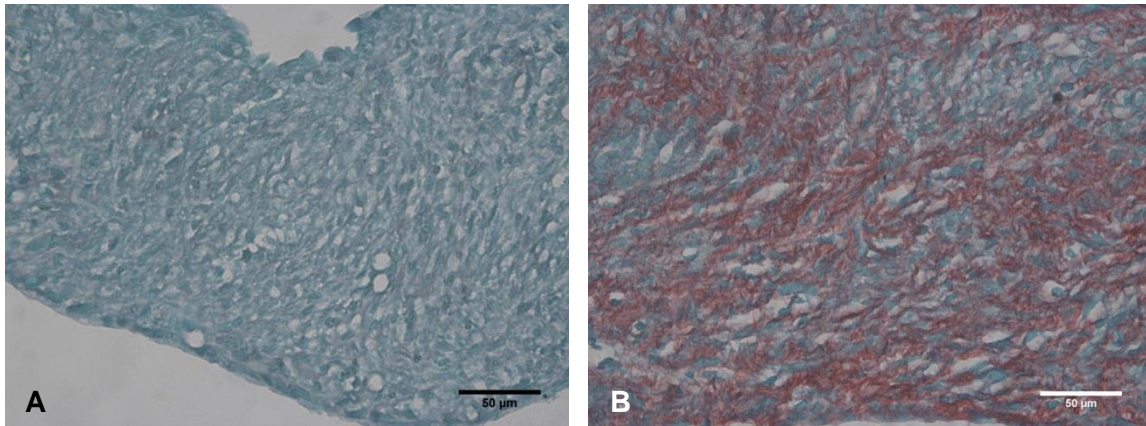


Figure 37: Picrosirius Red/Fast Green Stain of Fibroblast Sheets. (A) Untreated, (B) 50µg/mL Ascorbic Acid

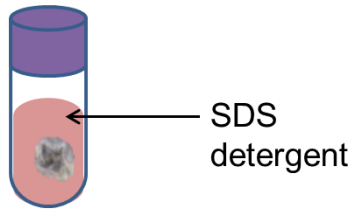
5.3 Decellularization

The team evaluated three different decellularization methods—SDS, freeze-thaw, and hypotonic and hypertonic solutions. As previously discussed, decellularizing tissues isolates the ECM and its beneficial elements while removing any components that might elicit an immune response in the patient (e.g., cells and cellular material).

5.3.1 Experiment 5: SDS Decellularization

The sodium dodecyl sulfate (SDS) decellularization (see Figure 38) was conducted according to a modified protocol by Elder et al. (Elder et al., 2009). Both the fabricated CDSs and foreskins were used for decellularization testing. Neonatal foreskins (received from UMass Memorial University Hospital with IRB approval) were used as a model tissue when CDSs were unavailable (see Appendix I: Decellularization Protocols). Per the original protocol, sodium dodecyl sulfate is dissolved into 1X phosphate buffered saline (PBS) to produce a 2% working solution. Samples are then placed in the solution in a 37°C shaking water bath for 1 hour. The team modified this step by spinning the samples on a Glas-Col tube rotator (Glas-Col) at 33rpm due to unavailability of a shaking water bath. The samples are then washed in 1X PBS five times at room temperature for 10 minutes each on a Labquake tube shaker (Thermo Fisher

Scientific, Inc.) to conclude the protocol. The team also incorporated a DNase treatment after the final wash. Samples were treated with 0.5mL of DNase I (Worthington, 1mg/mL, 10mM MgCl₂) for 15 minutes while rotating at room temperature on the Labquake, followed by three 5 minute washes in PBS while rotating at room temperature on the Labquake. Both the original protocol and modified protocol are available in Appendix I: Decellularization Protocols.



1 hour incubation

Figure 38: SDS Decellularization Approach

5.3.1.1 Experiment 5A: SDS Decellularization of Foreskins

Foreskin samples were prepared by cutting the tissue in 1cmx1cm sized samples. The fatty tissue beneath the dermis was briefly scraped off. Samples were then treated according to the SDS protocol (see Appendix I: Decellularization Protocols) with rotation on the Glas-Col tube rotator (Glas-Col) at 33rpm. After completing the protocol, the samples were fixed in formalin for 1 hour and processed (see Appendix G). The samples were then embedded, sectioned, and stained with Hematoxylin and Eosin (H&E), Hoechst, and Picrosirius Red/Fast Green. Figure 39B illustrates the presence of nuclei throughout the dermis after treatment with SDS, as confirmed by the Hoechst image in Figure 40B. However, Figure 40C shows less defined nuclei at the dermal region farthest from the epidermis, suggesting that the SDS was unable to penetrate through the entire tissue.

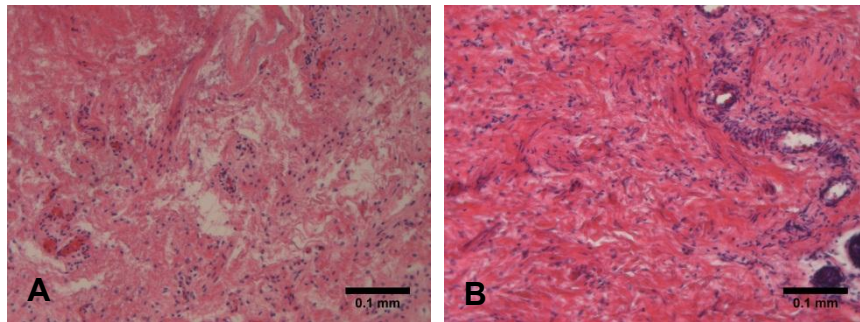


Figure 39: H&E Staining of SDS Decellularized Foreskin. Figure A is a control foreskin and Figure B is of SDS decellularized foreskin.

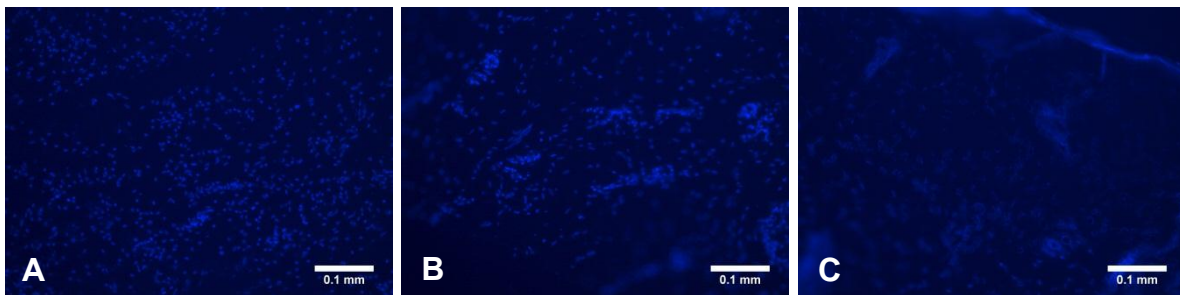


Figure 40: Hoechst Staining of SDS Decellularized Foreskins. Figure A is a control Foreskin; Figure B is the external side of SDS decellularized foreskin; and Figure C is the internal side of SDS decellularized foreskin.

5.3.1.2 Experiment 5B: SDS Decellularization of Foreskins with DNase I

The team repeated the SDS treatment following the modified protocol that includes spinning on the Glas-Col and DNase treatment following the wash steps due to the high levels of DNA observed in Experiment 5A. Following decellularization for 1 hour at 37degrees Celsius, each sample was rotated on the Labquake for 1 hour at room temperature in a solution of PBS and 0.2mg/mL of DNase plus 10mM MgCl₂ (Grauss, Hazekamp, van Vliet, Gittengerger-de Groot, & DeRuiter, 2003).

Following decellularization and DNase treatment, three samples were set aside for mechanical testing and two samples were fixed overnight in formalin, processed, embedded, and stained with H&E, Hoechst, and Picrosirius Red Fast Green (see Figure 41). Figure 41A shows persistent cellularization on the external side of the sample and Figure 41C shows no noticeable disruption of DNA in the epidermis. In Figure B, however, we observed that the dermal region that interfaces with the subcutaneous layer lacks nuclei. Hoechst staining in

Figure 41D confirmed the extent of decellularization observed in H&E. While sections of the tissue are still cellularized, it is clear that the genetic material in other sections of the tissue have been highly disrupted as no distinct nuclei can be seen. In Figure 41E-F, we noted that collagen was retained after decellularization, as indicated by the dark red stain.

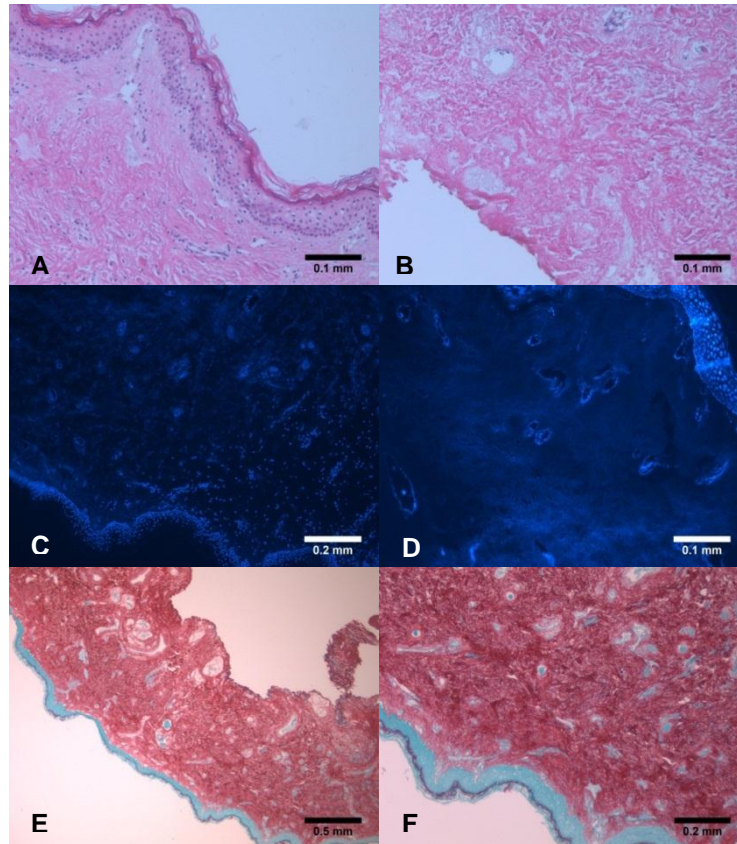


Figure 41: Histology of SDS with DNase Decellularized Foreskins Green. Figures A and B are stained with H&E; Figures C and D with Hoechst; and Figures E and F with Picrosirius Red/Fast Green

5.3.1.3 Experiment 5C: SDS Decellularization of CDSs

Following Experiment 3, in which CDSs were cultured at various densities with and without ascorbic acid, two CDSs were treated with SDS using the Glas-Col at 33rpm for the first rotation step. The tissues were harvested and immediately placed in a 1.5 Eppendorf tube with 1 mL 2% SDS. Due to the fragility of the tissues, the team did not apply the DNase treatment in order to prevent complete disintegration of the tissue.

Following the protocol, the tissues were processed, embedded, and stained with Hoechst. Figure 42A is the control tissue and is representative of all non-decellularized samples, regardless of the seeding density or addition of ascorbic acid; Figure 42B, however, is of the only surviving SDS sample after processing. At the conclusion of decellularization protocol, the other SDS sample had been disintegrated into pieces and was too fragile for processing. The remaining sample (Figure 42B) does not exhibit distinct nuclei, but rather fluorescence from the breakdown of the genetic material, demonstrating decellularization of the sheet.

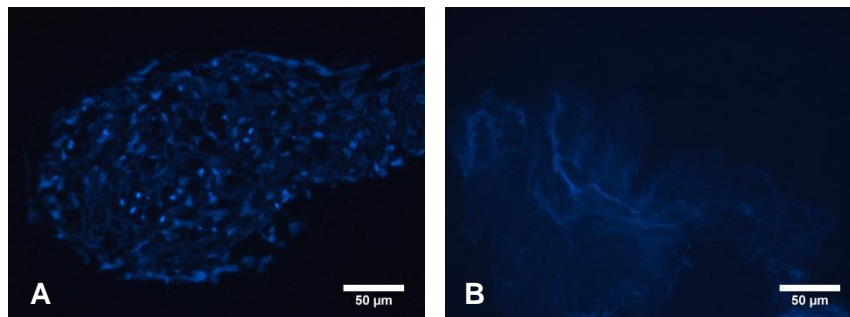


Figure 42: Hoechst Stains of Decellularized CDSs. (A) Control, (B) SDS-decellularized

5.3.1.4 Experiment 5D: Final Validation of Decellularizing Foreskins using SDS

Due to availability of the cell-derived sheets, the team continued testing on neonatal foreskins as proof-of-concept of the final SDS decellularization protocol. Six samples were treated according to the final, modified version of the protocol using the Glas-Col rotator and revised DNase concentration (see Appendix I: Decellularization Protocols). Samples were prepared by scraping off fatty tissue and cutting the tissue to the size of 0.5cm x 0.25cm and immediately placed in a 1.5mL conical tube with 1mL SDS and rotated at 37 degrees Celsius on the Glas-Col at 33rpm. In order to determine more exact specifications of the protocol, time points and the addition of DNase were considered. For each time point (1 hour, 5 hours, 24 hours), one sample was treated with DNase and one sample without DNase. Treated samples received 0.5mL of DNase I (Worthington, 1mg/mL, 10mM MgCl₂) and were rotated on the

Labquake for 15 minutes at room temperature, followed by three 5 minutes PBS washes per the protocol in Appendix I: Decellularization Protocols. Tissues with and without DNase treatment were taken from the same foreskin in order to control structural and cellular variability.

Following decellularization, samples were fixed, embedded, processed, and stained with H&E (Figure 43B,D,H,L,F,J,N) and Hoechst (Figure 43A,C,G,K,E,I,M). Control images are shown in Figure 43A-B, 1 hour SDS in Figure 43C-F, 5 hour SDS in Figure 43G-J, 24 hour SDS in Figure 43K-N, without DNase treatment in Figure 43C,D,G,H,K,L and with DNase treatment in Figure 43E,F,I,J,M,N. Figure 43C shows incomplete breakdown of genetic material throughout the tissue, as confirmed by nuclei remaining in the H&E (Figure 43D). In Figure 43E, however, the epidermis has been separated from the dermis, with Hoechst indicating degeneration of DNA throughout the dermis and H&E confirming decellularization of the dermis. Figure 43G shows partial decellularization of the dermis, but no removal of genetic material in the epidermis, as confirmed by nuclei present in Figure 43H. With the DNase treatment (Figure 43I), there is more complete decellularization in the dermis, as observed by no defined nuclei, unlike the epidermis which still has defined nuclei. The Hoechst images for both 24 hour samples show decellularization of the dermis (Figure 43K,M), as confirmed by no visible nuclei in the H&E (Figure 43L,N). Figure 43N shows extensive damage to the dermal region, which is noticeably thinner than other samples, due to the extensive SDS wash and subsequent DNase treatment. This aggressive protocol may also explain the lack of genetic material in Figure 43K, which was not treated with DNase.

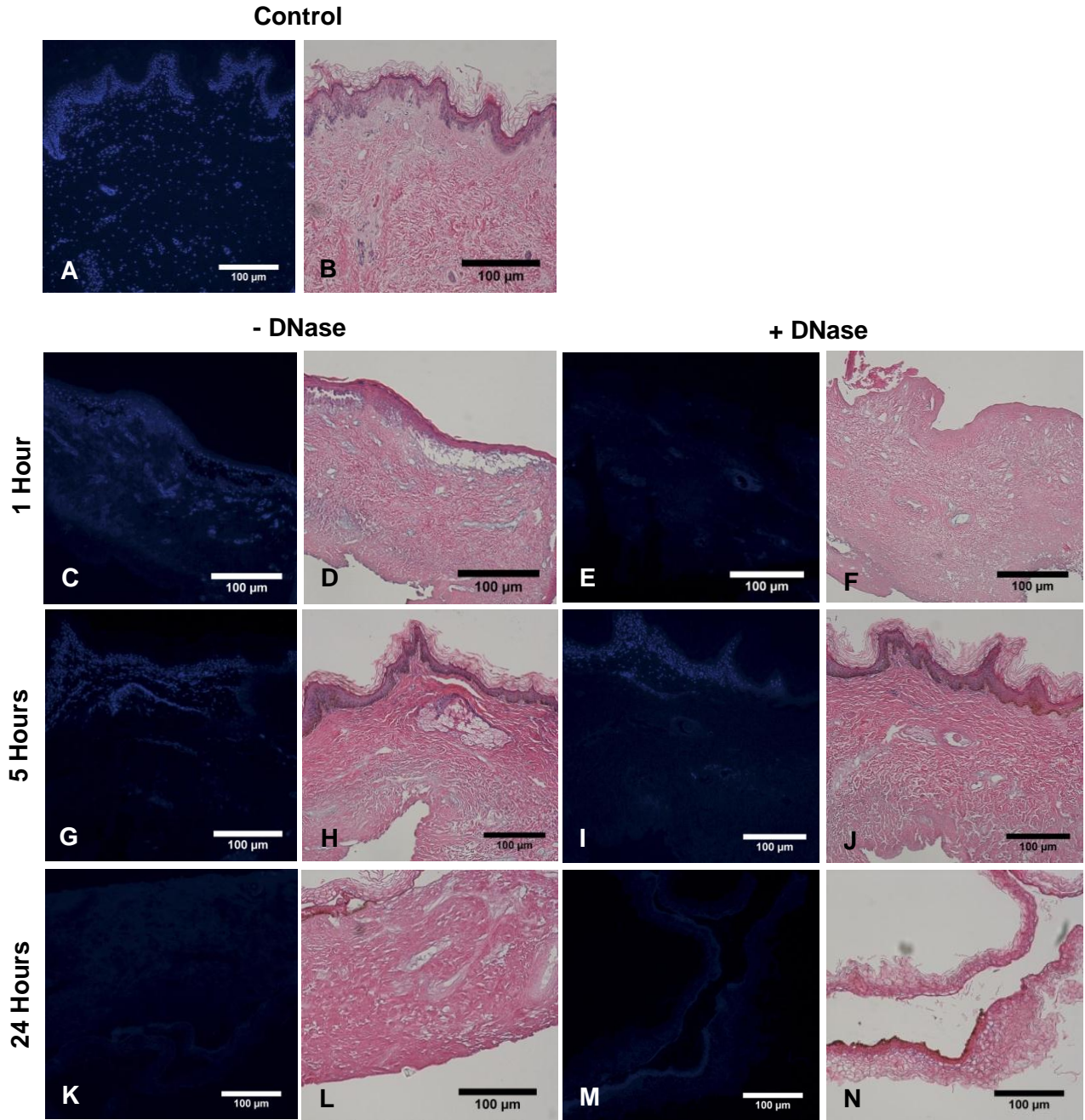


Figure 43: Hoechst and H&E Stains of SDS-decellularized Foreskins

5.3.2 Experiment 6: Freeze-Thaw Decellularization

The team modified the protocol published by Ngangan and McDevitt (Ngangan & McDevitt, 2009). Samples are placed in a 1.5mL Eppendorf tube and immersed in liquid

nitrogen for 2 minutes. 1mL of 1X PBS is then added to each tube and the samples are rotated for 5 minutes at room temperature on the Labquake tube rotator. The PBS is then aspirated and the process repeated for a total of three cycles. Each sample was then treated with 0.5mL of DNase I (Worthington, 1mg/mL, 10mM MgCl₂) while rotating at room temperature on the Labquake. Samples are then washed three times for 5 minutes each in 1X PBS and left on the benchtop to sit for 8 hours. The team adapted this protocol from the original version which included centrifugation and did not include a DNase step. Both the original and modified protocols are reported in Appendix I: Decellularization Protocols.

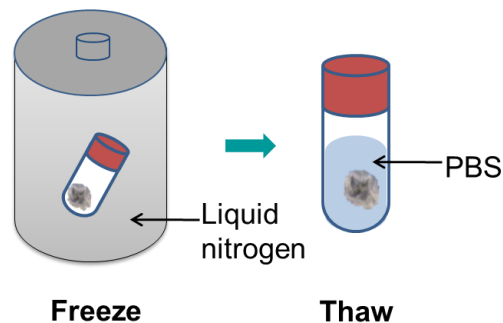


Figure 44: Freeze-Thaw Decellularization Approach

5.3.2.1 Experiment 6A: Freeze-thaw Decellularization of Foreskins

Five samples were decellularized according to the reported protocol without the DNase treatment. Samples were prepared by scraping off fatty tissue and cutting the tissue to the size of 1.0cmx1.0cm and immediately placed in a custom-made aluminum foil “boat” for better thermal conductivity. The boat was floated on the liquid nitrogen for 30 seconds. The samples were then rotated in 1 mL of 1X phosphate buffered saline (PBS) for five minutes at room temperature. Because the centrifuging step was specifically created to pellet the embryoid bodies in the reported experiment (Ngangan & McDevitt, 2009), this step was bypassed by the team. The whole freeze-thaw cycle was completed three times. Each sample was then rotated on the Labquake for 1 hour at room temperature in a solution of PBS and 0.2mg/mL of DNase plus 10mM MgCl₂ (Grauss et al., 2003).

Following freeze-thaw treatment, three samples were set aside for mechanical testing and two samples were fixed overnight in formalin, processed, embedded, and stained with H&E, Hoechst, and Picrosirius Red/Fast Green (see Figure 45). The H&E staining in Figure 45A-B indicates very little decellularization in all regions of the tissue sample. This is confirmed by Hoechst staining in Figure 45C. Figure 45D shows that collagen has been retained after decellularization.

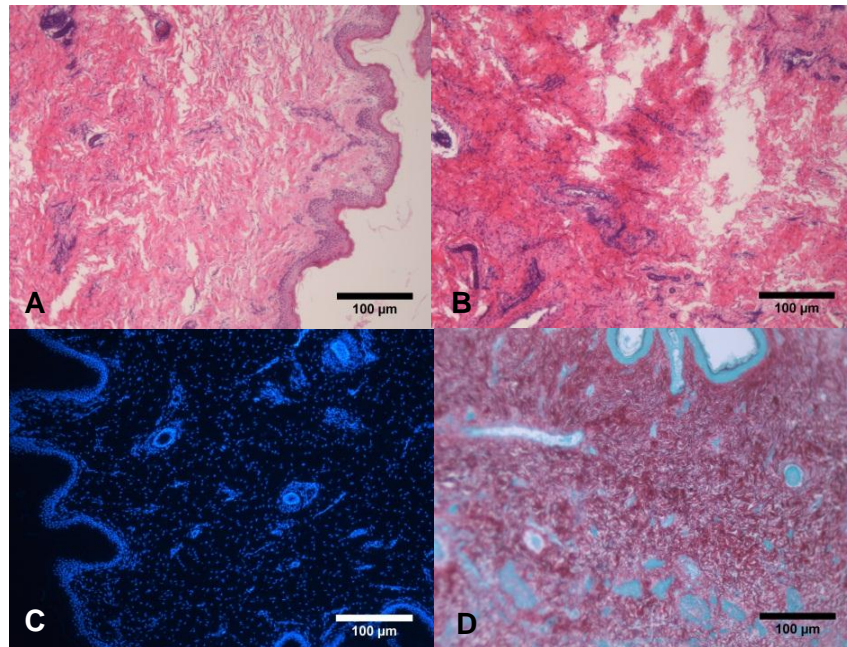


Figure 45: Histology of Freeze-Thaw with DNase Decellularized Foreskins. Figures A and B are stained with H&E; Figure C with Hoechst; and Figure D with Picrosirius Red/Fast Green.

5.3.2.2 Experiment 6B: Freeze-thaw Decellularization of CDSs

Upon availability of CDSs, freeze-thaw was performed on freshly-harvested sheets. Two samples from Experiment 3, in which CDSs were cultured at various densities with and without ascorbic acid, were frozen in liquid nitrogen for about 2 minutes using the aluminum foil boat method (see Figure 46). Each sample was then placed in a 1.5mL Eppendorf tube. Each tube received 1 mL PBS and was rotated on the Labquake for 5 minutes at room temperature. The cycle was repeated for a total of 3 cycles. The samples were not treated with DNase due to

concern that the treatment and subsequent washes would completely disintegrate the cell sheet.

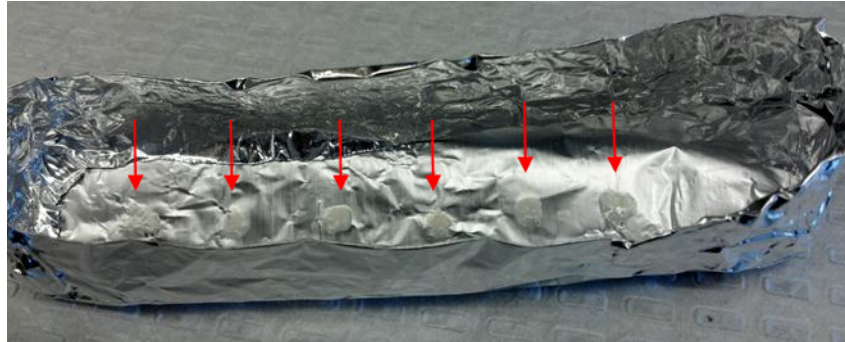


Figure 46: "Boat" for Freeze-Thaw. Red arrow indicates CDS.

After the treatment, two tissues were processed, embedded, and stained with Hoechst. Figure 47B positively compares to the control Figure 47A, expressing distinct nuclei throughout the entire sheet and demonstrating no decellularization.

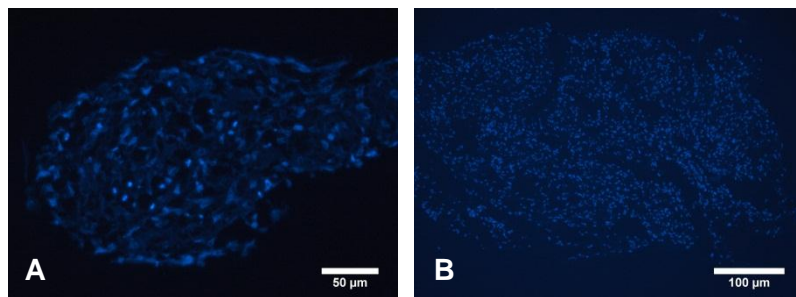


Figure 47: Hoechst Stains of Freeze-thawed CDSs. (A) Control, (B) Freeze-thaw-decellularized

5.3.2.3 Experiment 6C: Final Validation of Decellularizing Foreskins using Freeze-Thaw

Foreskins were again decellularized as proof-of-concept to finalize a freeze-thaw protocol. Five samples were prepared by scraping off fatty tissue and cutting the tissue to the size of 0.5cm x 0.25cm. In order to determine optimal conditions, 2 samples were left to sit for 8 hours in PBS at room temperature before fixation and 2 samples were fixed immediately following the conclusion of the protocol. One sample from each condition received the DNase treatment (0.5mL of 1mg/mL DNase plus 10mM MgCl₂) (Ngangan & McDevitt, 2009)

immediately following the freeze-thaw cycles. A final sample was first left to sit for 8 hours, then treated with DNase, and then finally fixed. Tissues with and without DNase treatment were taken from the same foreskin in order to control structural and cellular variability.

At the conclusion of the protocol, samples were fixed, embedded, processed, and stained with H&E (Figure 48B,D,F,H,J,L) and Hoechst (Figure 48A,C,E,G,I,K). Control images are shown in Figure 48A-B, without DNase treatment in Figure 48C,D,G,H, with DNase treatment in Figure 48E,F,I,J,K,L, fixed immediately in Figure 48C-F, fixed after 8 hours in Figure 48G-J, and treated with DNase after waiting 8 hours in Figure 48K-L. Samples without DNase treatment retained intact nuclei (Figure 48C,G); however, the sample that was fixed after 8 hours had visually less nuclei. The more complete decellularization of the dermis in the sample that was fixed after 8 hours is verified by confirming Figure 48D,H. In the samples with DNase treatment, the Hoechst images again show further decellularization in tissue fixed after 8 hours Figure 48I. While there are still distinct nuclei in the epidermis of the sample fixed after 8 hours, the dermis has been visually completely decellularized, as confirmed by the H&E Figure 48J. The sample treated with DNase after the 8 hour waiting period shows only partial decellularization of the dermis and no noticeable decellularization of the epidermis (see Figure 48K,L).

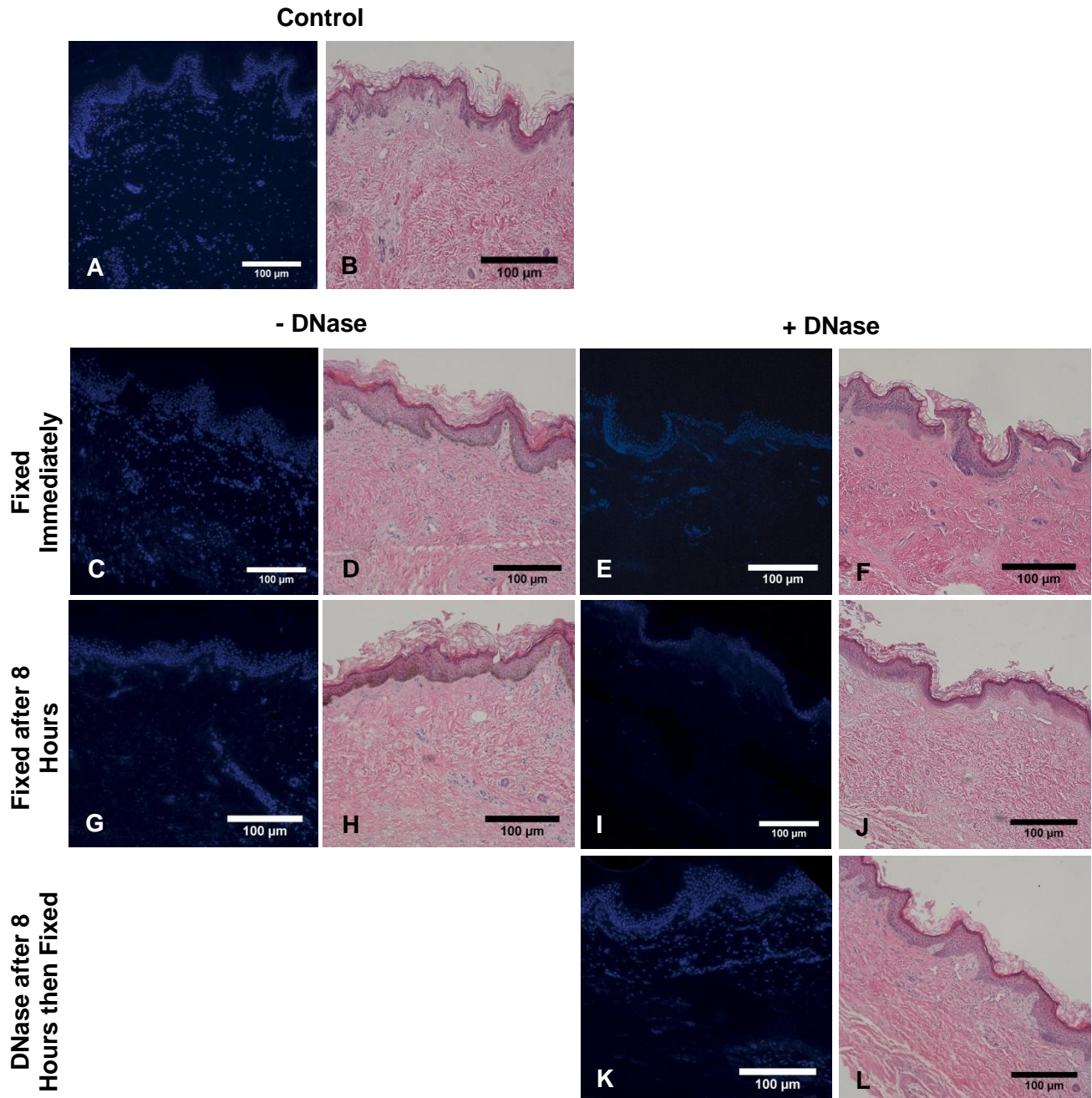


Figure 48: Hoechst and H&E Stains of Freeze-thawed Foreskins

5.3.3 Experiment 7: Hypotonic and Hypertonic Solutions Decellularization

Meyer et al.'s protocol (Meyer et al., 2006) was used for the hypotonic and hypertonic solution decellularization (see Appendix I: Decellularization Protocols). All buffers were prepared

by the team before decellularization by dissolving the components in deionized water and all rotations were completed on a Labquake tube rotator. Due to availability, PMSF, a serine protease inhibitor, was substituted with Complete, Mini, EDTA-free Protease Inhibitor Cocktail Tablets (Roche Applied Science). Also, based on other protocols in literature (Ngangan & McDevitt, 2009; Schaner et al., 2004), the team only included the DNase I in the solution and did not include the RNase A as per the original protocol. Both the original protocol and the team's modified protocol are reported in Appendix I: Decellularization Protocols

5.3.3.1 Experiment 7A: Hypotonic and Hypertonic Solutions Decellularization of Foreskins

Five samples were first submerged in a hypotonic tris HCl buffer (10mM, pH 8.0) solution with EDTA (5mM) and Complete, Mini, EDTA-free protease inhibitor cocktail tablets (Roche Applied Science) and allowed to rotate at 4 degrees Celsius. One cocktail tablet was used per 10 mL of buffer. After rotating in this solution for 48 hours, the samples were transferred to a hypertonic tris HCl buffer solution (50mM, pH 8.0) with EDTA (5mM), KCl (1.5M), Triton X-100 (0.5%), and the cocktail tablets instead of PMSF. Again, the samples rotated for 48 hours at 4 degrees Celsius. The tissues were then rinsed in a Sorensen's buffer solution (pH 7.3) with DNase I (Worthington, 25mcg/mL) and MgCl₂ (10mM) to activate the DNase. The samples were rotated in this solution for 5 hours in 37 degrees Celsius, after which point they were transferred to a tris base buffer (50mM, pH 9.0) with Triton X-100 (0.5%) and allowed to rotate for 48 hours at 4 degrees Celsius. The samples were then rotated at 4 degrees in 1X PBS for 72 hours, changing the wash every 24 hours.

At the conclusion of the final wash, three samples were set aside for mechanical testing and two samples were fixed overnight in formalin, processed, embedded, and stained with H&E, Hoechst, and Picrosirius Red/Fast Green (see Figure 49). Similar to SDS, H&E and Hoechst show cellularization in the epidermis and regions of the dermis (Figure 49A,C). In Figure 49D,

however, various regions of indistinct nuclei suggest partial decellularization of the dermis. Again, we observed collagen retention in the Picosirius Red/Fast Green staining (Figure 49D).

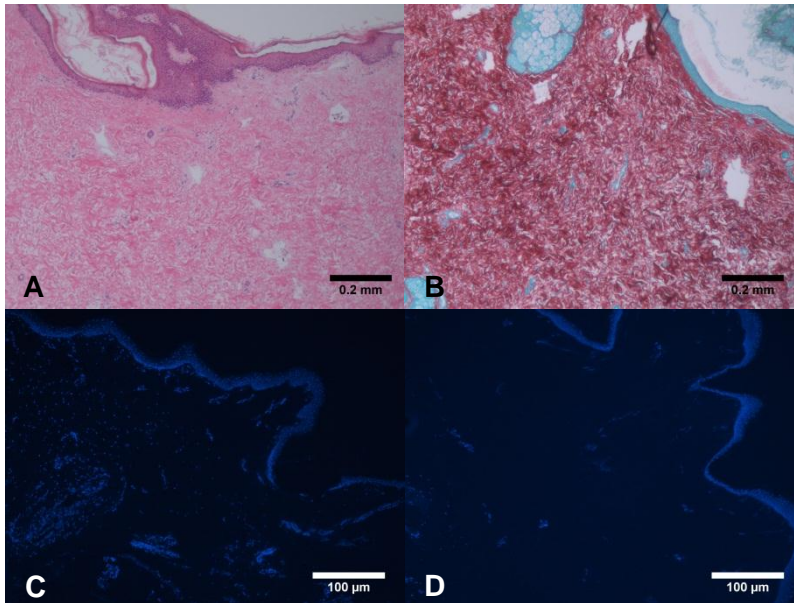


Figure 49: Histology Staining of Hypotonic and Hypertonic Solutions Decellularized Foreskins. Figure A is stained with H&E; Figure B with Picosirius Red; and Figure D with Hoechst.

5.3.3.2 Experiment 7B: Hypotonic and Hypertonic Solutions Decellularization of CDSs

After the culture of CDSs in Experiment 3, in which tissues were cultured at varying densities with and without ascorbic acid, two samples were decellularized using hypotonic and hypertonic solutions. Each sheet was placed in a 1.5mL Eppendorf tube and underwent the exact protocol that is listed Appendix I: Decellularization Protocols and was used in the previous experiment on foreskins.

At the conclusion of the treatment, two tissues were processed, embedded, and stained with Hoechst. The decellularized sample (Figure 50B) resembles the control tissue (Figure 50A), displaying distinct nuclei throughout the tissue and no visible signs of decellularization.

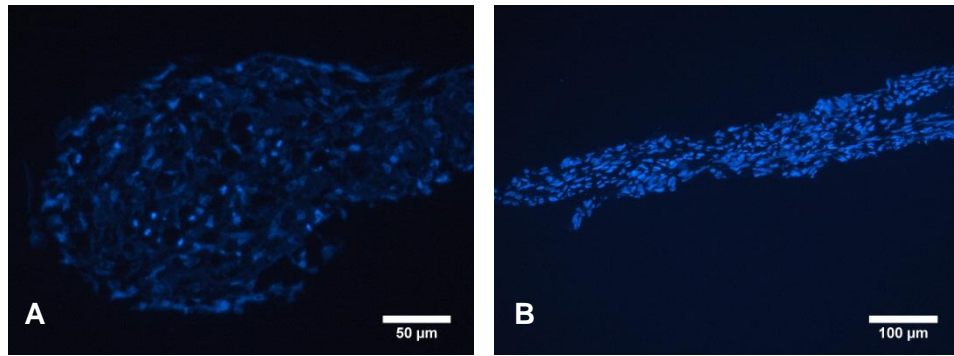


Figure 50: Hoechst Stains of Hypotonic/Hypertonic-Solutions Decellularized CDSs. (A) Control, (B) Hypotonic/Hypertonic-decellularized

5.4 Mechanical Testing of Tissues

The mechanical integrity of CDSs, as well as decellularized foreskins, was determined through tensile testing to failure on an Instron ELECTROPULS E1000, using a strain rate of 10mm/min. Tissues were hydrated in 1X PBS until testing. Appropriate grips and load cells were determined through experimentation.

5.4.1 Uniaxial Tensile Testing of Decellularized Foreskins

A total of 12 foreskin samples were set aside for testing—three samples from each decellularization method and three non-decellularized control tissues. Testing dimensions (tissue width, tissue thickness, distance between grips) were measured with an electronic digital caliper (VWR). The control samples were received less than a week prior to testing and were held in foreskin media at 4 degrees Celsius until testing. Various sized grips were tested to determine the most appropriate grips (see Figure 51). The team first experimented with small clamps and a 50N load cell. The small clamps were unable to fully grip the tissue during the test. The team then tried using larger grips with a 2kN load cell, but the tissue continued to slip through the grips as the tissue was pulled. Sandpaper meshes (Figure 51C) were then implemented to hold the tissue while in the clamps (see Figure 52), which helped the tissue remain in the grips for an extended period of time, but the tissue still slipped before fracture. The team's final approach added gauze in between the mesh to keep the ends of the tissue dry.

However, no method was able to retain the tissue during the testing procedure until failure. The team was unable to collect any data.



Figure 51: Mechanical Testing Setup Accessories. Figure A is the small grips that were first used; Figure B is the large grips; and Figure C is the sandpaper meshes.

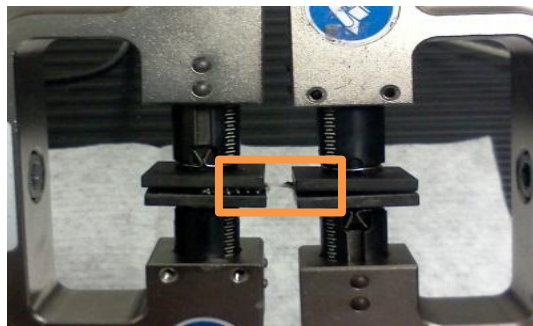


Figure 52: Decellularized Foreskin in Grips during Mechanical Testing

5.4.2 Uniaxial Tensile Testing of CDSs

Tensile testing was used to determine the contribution of ascorbic acid to the mechanical strength of the fibroblast-derived sheets. Freshly harvested fibroblast sheets from Experiments 3 and 4 were used to develop a final protocol for uniaxial tensile testing and analysis of the mechanical data. The raw data was filtered using a MATLAB code developed by Jason Hu.

5.4.2.1 Uniaxial Tensile Testing of CDS from Experiment 3

Fibroblast cell sheets with and without ascorbic acid at densities of 100,000 cells/cm², 50,000 cells/cm², 25,000 cells/cm², and 12,500 cells/cm² were tensile tested immediately after harvesting. A 50N load cell was used with small, custom grips. Gauze was placed so that it held each end of the cell sheet inside of each grip (Figure 53). The samples were pulled to failure on an Instron ELECTROPULS E1000 at a rate of 10mm/min. Preparation of the samples for

mechanical testing included measuring the width, thickness, and distance between the clamps using a manual electronic caliper (VWR) when the cell sheets were loaded in the Instron. Table 24 shows the measurements and results from this experiment. Most of the samples without ascorbic acid broke during preparation for mechanical testing.

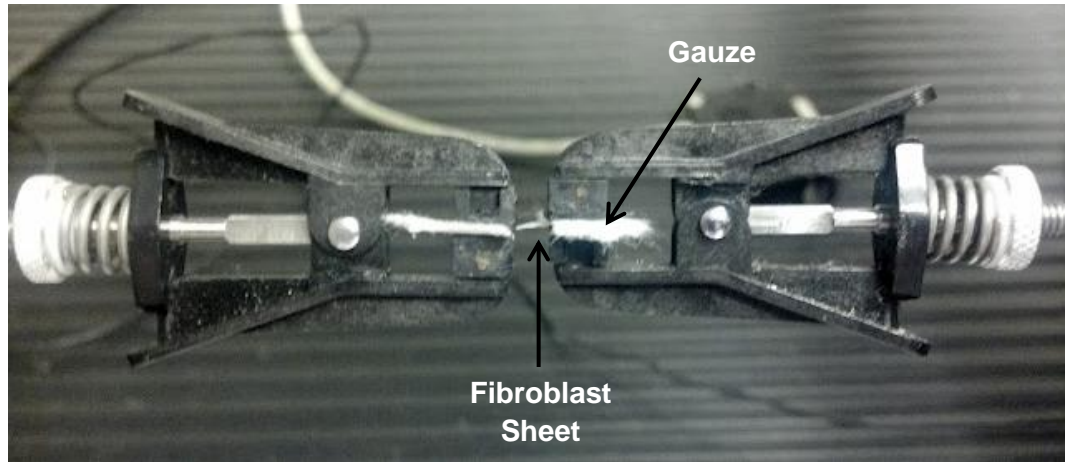


Figure 53: Tensile Testing of Cell-Derived Fibroblast Sheets

Table 24: Measurements and Observations of Mechanical Testing

Sample and Condition		Measurements			Area (mm ²)	Maximum Stress (kPa)	Observations
Cell Density (cells/cm ²)	Ascorbic Acid Treatment	Thickness (mm)	Width (mm)	Grip distance (mm)			
12,500	Yes	0.55	1.62	2.79	0.89	6.96	Passed mechanical testing (failure achieved)
12,500	No	---	---	---	---	---	Broke during prep
25,000	Yes	0.37	2.06	4.77	0.76	7.11	Slipped, then ripped during testing
25,000	No	---	---	---	---	---	Broke during prep
50,000	Yes	0.51	1.67	3.79	0.85	10.40	Passed mechanical testing (failure achieved)
50,000	No	0.47	1.62	3.76	0.76	11.67	Passed mechanical testing (failure achieved)
100,000	Yes	0.35	2.09	3.98	0.74	5.32	Passed mechanical testing (failure achieved)
100,000	No	---	---	---	---	---	Broke during prep

Most of the cell sheets cultured without ascorbic acid broke during handling and measurement preparation, suggesting that these sheets were less durable than the sheets cultured with ascorbic acid. There were not enough samples to determine any significant difference between the sheets cultured with and without ascorbic or between the sheets cultured at different densities. However, two cell sheets of 50,000 cells/cm² cultured with ascorbic acid reached an average tensile stress of 11.03 ±0.9 kPa.

5.4.2.2 Uniaxial Tensile Testing of CDS from Experiment 4

After harvesting fibroblast sheets cultured from an initial cell density of 100,000 cells/cm² from Experiment 4, sheets with and without ascorbic acid were immediately loaded on to an Instron ELECTROPULS E1000 (Figure 54). Sample thickness was measured using a Mitutoyo absolute digital caliper in conjunction with an Olympus CK2 confocal microscope. Width and grip distances were measured using a manual electronic caliper (VWR) once the tissue was placed inside the custom alligator clips. The tissues were hydrated in PBS until testing. The samples were tensile tested to failure using a strain rate of 10mm/min and a 1N load cell.

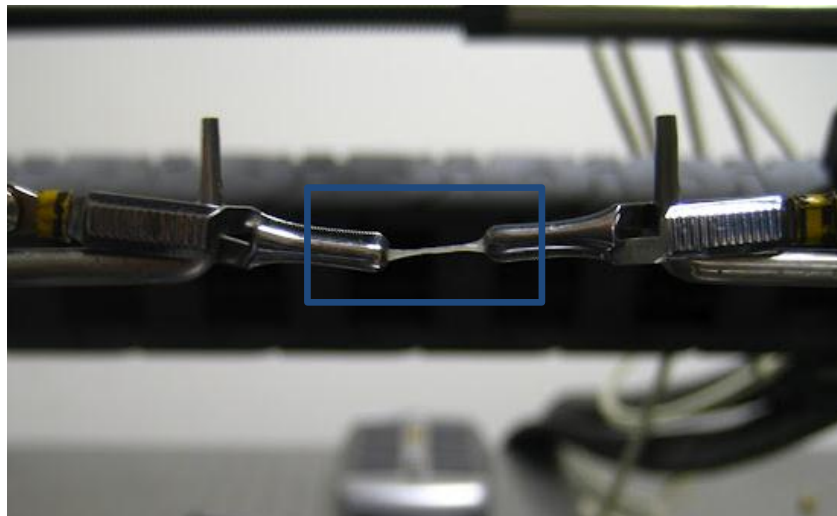


Figure 54: CDS Loaded on Instron

The thickness, width, and area of the cell sheets were recorded in Table 25. Stress was determined by dividing the load output from the raw data by the cross-sectional area. Samples S18, S5, and S6 were not cultured in ascorbic acid, and samples S7 and S8 were cultured in

ascorbic acid. Figure 55 shows the stress strain curve from the tensile test. It appears that tissues grown with ascorbic acid have more of a viscoelastic behavior of natural tissues. The bar graph in Figure 56 shows the that the maximum stress for cell sheets without ascorbic acid range from 1 to 3 kPa, while maximum stress for tissues grown with ascorbic acid range from 2 to 6 kPa. The data from this experiment is not statistically significant according to the t-test ($p=0.172 > p=0.05$); however, power analysis indicates that there is less likely to be a significant difference between the two groups if one exists due to the small sample size.

Table 25: Measurements and Results for Tensile Testing of Fibroblast Sheets

Sample	Thickness (mm)	Width (mm)	Area (mm ²)	Grip Distance (mm)	Max Stress (kPa)
S5 (-aa)	0.337	2.19	0.74	3.15	1.44
S6 (-aa)	0.25	2.28	0.57	3.5	3.29
S18 (-aa)	0.296	2.54	0.75	4.71	1.09
S7 (+aa)	0.283	3	0.85	8.76	5.83
S8 (+aa)	0.447	2.72	1.22	3.16	2.98

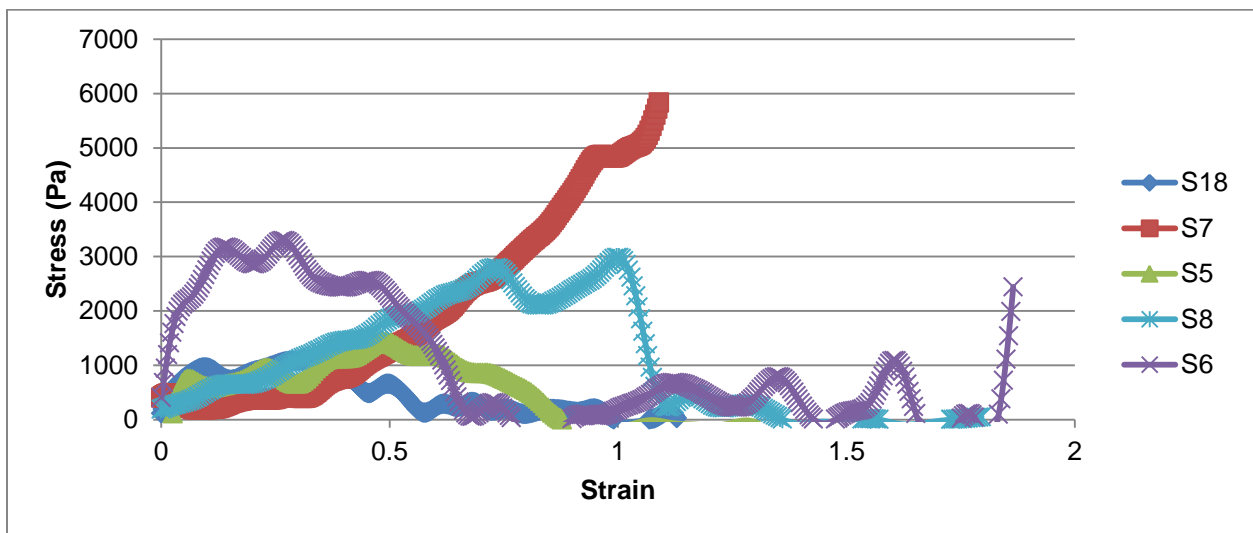


Figure 55: Stress vs. Strain for Cell Sheets with and without Ascorbic Acid

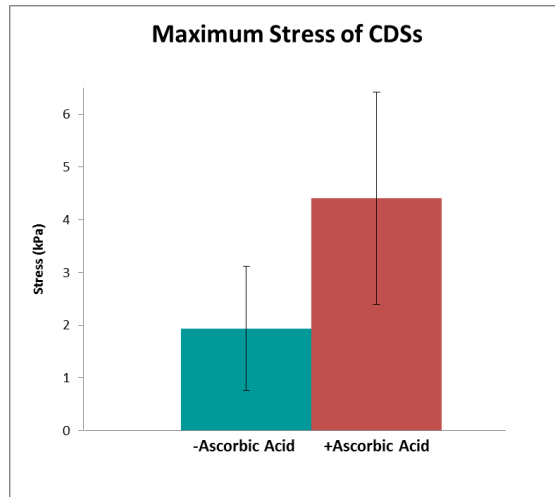


Figure 56: Maximum Stress of Fibroblast Sheets with and without Ascorbic Acid

6 Discussion

The goal of this project was to design and fabricate a cell-derived matrix scaffold with tailored mechanical properties and antimicrobial and angiogenic activity. The highest objectives for this scaffold were that it mimics the mechanical and structural properties of native dermis as well as be bioactive. Due to time and resources constraints, only the mechanical and antimicrobial objectives were considered in the design.

To produce a scaffold with mechanical and structural properties of native dermis, the design fabricated cell sheets and optimized decellularization methods to isolate the ECM from these sheets. The team produced cell sheets using human neonatal dermal fibroblasts and used ascorbic acid as a means to increase the mechanical strength of the scaffold. The team was able to form cohesive fibroblast sheets that could be harvested from poly-NIPAAAM surfaces. Additionally, the team confirmed that ascorbic acid stimulated the fibroblast to increase collagen production. Mechanical testing showed a trend of fibroblast sheets cultured with ascorbic acid tending towards a higher maximum stress; however the sample size was too low to see any significant difference between the groups. The addition of ascorbic acid and the tissue fabrication protocol was not significant enough for the cell sheets to reach strengths reported for current products or of native dermis, which has a tensile strength of 5-30MPa (Lacroix & Planell, 2009). Alloderm, a decellularized cadaveric split thickness skin graft produced by Life Cell, reaches an initial uniaxial tensile strength of 0.125 MPa (LifeCell, 2012). Additionally, DermaSpan, an acellularized dermis produced by Biomet, has been shown to reach a uniaxial tensile strength of 19.2 MPa (Biomet, 2012). Additional means, such as mechanical or additionally chemical stimulation, must be investigated for increasing the mechanical strength of our fibroblast sheets, which only achieved an average failure stress of 4 kPa.

Hypotonic and hypertonic solutions were insufficient at decellularizing the foreskin tissue and fibroblast sheets. This finding is comparable to literature, which states that this method can effectively lyse the cells but does not remove all of the cellular debris (Gilbert et al., 2006). SDS was found to successfully decellularize the foreskin tissue. However, SDS is reported to denature proteins, which could be counterproductive to the bioactivity of the scaffold if it disrupted the cathelicidin (Gilbert et al., 2006). Therefore, freeze-thaw was determined to be the most appropriate decellularization method due to its complete removal of nuclear debris from the dermis of foreskin tissue. It has also been reported that freeze thaw retains maximal matrix components (McDevitt, 2009). Additionally, we were able to optimize the freeze-thaw protocol by including an 8-hour waiting period, which improved the decellularization effects of the method.

To produce a scaffold with innate antimicrobial activity, the team designed and fabricated a gene construct of a chimeric antimicrobial peptide, Cathelicidin, to include one of two collagen binding domains (CBDs). Cathelicidin was chosen as the protein of interest due to its natural expression in the epidermal layer of skin as well as its wide range of bactericidal activity. The two CBDs were derived from fibronectin and collagenase, which were chosen based on their confirmed specificity for collagen I and successful incorporation into various other chimeric constructs by other researchers (Sistiabudi & Ivanisevic, 2008; Zhang et al., 2009). The fabricated cathelicidin-CBD constructs were verified against the original design by sequence analysis, which showed 100% consensus. The protein design was further validated by the successful expression of both recombinant forms of cathelicidin in H1299 lung carcinoma cells.

6.1 Analysis and Limitations of Experiments

The following sections present a detailed analysis of the methods and results, with the limitations addressed for each experiment. Global limitations included becoming proficient in the

required skills and knowledge for laboratory techniques, including mechanical testing, decellularization, cell culture, processing, and histology.

6.1.1 Fabrication of Cell-derived Sheets

Fibroblasts seeded at sub-confluent densities performed best during cell sheet culture. In one experiment, 100,000 cells/cm² was confirmed to be the highest cell density at which the cells would remain adhered to the plate for the 14 day culture period. However, in a proceeding experiment, five out of twenty-four cell sheets seeded at 100,000 cells/cm² detached midway through the culture period. It is possible that these cells detached because they were nutrient deficient, meaning that the feeding interval should be increased from every other day.

Images of fibroblast sheets after 14 days of culture show a difference in cellular alignment in the sheets grown with and without ascorbic acid. Sheets grown without ascorbic acid had a basket weave appearance while sheets grown in the presence of ascorbic acid adopted a linear alignment. It is possible that the fibroblasts sheets grown without ascorbic acid continued to proliferate, contributing to the random, interwoven pattern observed. Additionally, it is likely that the ascorbic acid reduced the proliferative phase of the fibroblasts by stimulating them to produce more collagen, which attributed to the cells linear alignment.

Although cells treated with ascorbic acid may have been less proliferative, our data shows that these sheets were significantly thicker than the untreated cell sheets. The thickness of the cell sheets grown with ascorbic acid reached a mean of 0.388 mm, with the thickest tissue being 0.457 mm. These dimensions are less than that of natural dermis, which is 1-4mm thick. However, our tissue sheets are in the thickness range of the thinnest version of Life Cell's Alloderm. Alloderm ranges from thin (0.23-0.51 mm), medium (0.53-1.02mm), thick (1.04-2.28mm), and extra thick (2.30-3.30mm) (LifeCell, 2012).

Picrosirius Red/Fast Green staining of the cell sheets confirmed that ascorbic acid stimulated the fibroblasts to produce more collagen. The histology showed that fibroblast sheets

grown without ascorbic acid had no visible red fibers, meaning that no collagen was present. Fibroblast sheets grown in the presence of ascorbic acid had red collagen patches throughout the cell sheets. These results were representative for all samples; however, a larger sample size would provide more evidence.

Tensile testing of the cell sheets suggested a trend that sheets grown with ascorbic acid were tending towards a higher maximum stress. The data was not statistically significant; however, the power analysis suggests that there is less likely to be a significant difference if one exists due to the low sample size tested. The mechanical testing was limited by a variety of factors. The time constraint and limitation of fibroblast supply restricted the design team from culturing multiple cell sheets for increased sample numbers. Additionally, the design team did not have the resources to culture larger tissues, which could be cut into rectangles to provide for more accurate tensile testing dimensions. Because the tissue sheets contract when removed from liquid, there was no way to consistently load the cell sheets in to the Instron machine with consistent fiber alignment.

6.1.2 ECM Isolation

Three difference decellularization protocols were tested on both the cultured sheets and foreskins to determine the most appropriate method to isolate the ECM from the tissue. Once the team became familiar with the protocols, the experiments were feasible and easy to perform. Due to the limitation of fibroblast supply, the design team had to optimize the decellularization protocols on foreskins as model tissues. The results are not completely translatable to fibroblast sheets, but can be predicted to work with the same efficacy since foreskin tissue is more robust.

SDS was able to penetrate through both the epidermis and dermis, while freeze-thaw was only able to decellularize the dermis. However, because this project is focused on a dermal regeneration scaffold and the cell-derived sheets do not produce an epidermal-like layer, the

team considered both of these protocols successful. Hypotonic and hypertonic solutions only partially decellularized the tissues, with the majority of decellularization near in the interior/connective tissue region.

The use of DNase was critical to decellularize the tissues. With the exception of the 24 hour SDS treatment, samples required DNase treatment to break down the DNA in the nuclei. The team experimented with DNase concentrations from literature and determined 0.5mL of 1mg/mL DNase to be an effective concentration. Furthermore, the team also observed that freeze-thawed tissues required a waiting period in which samples sat on the benchtop for 8 hours before fixation in order for decellularization to occur. Although literature does not discuss this requirement, the team determined that this “waiting period” was necessary in order for the genetic material to diffuse out of the cell.

6.1.3 Antimicrobial Peptide

As confirmed by the Western blot (Figure 22B) the recombinant cathelicidin constructs were successfully expressed in H1299 human lung carcinoma cells as a model cell type. The absence of bands in the lower molecular weight range of the membrane, suggests that the expressed product is not being cleaved. This is a limitation of using lung carcinoma cells, as opposed to a cell type with the confirmed expression of neutrophil proteinase 3 and elastase, which cleave cathelicidin to its active peptide, LL-37 (Sorensen et al., 2001). This is important to consider for future experiments, in terms of expressing cathelicidin in fibroblasts and whether its cleavage is dependent on the presence of neutrophils.

6.2 Impact Analysis

In addition to its clinical need, the design team analyzed the global impact of this product. The team considered how the scaffold would perform in terms of economics, political ramifications, environmental impact, manufacturability, sustainability, societal influence, ethical concerns, and health and safety issues.

6.2.1 Economics

In the United States alone, \$25 billion is spent annually on the treatment of chronic wounds. This economic burden is growing with the increase in health care costs, aging population, and number of people diagnosed with diabetes, obesity, and other illnesses associated with the development of chronic wounds (Sen et al., 2009). The economic and social impact of wound care in our society supports the need for new regenerative therapies, rather than treatments.

6.2.2 Environmental Impact

The majority of this product's impact on the environment stems from the manufacture of laboratory plasticware required to produce the scaffold. Furthermore, any waste produced during fabrication will be considered biohazard and will have to be properly disposed. In addition, adequate bovine sources will be required to isolate the FBS to supplement the fibroblast media. If the need becomes great enough, land and resources will be affected to maintain the bovine population. Finally, power for running the manufacturing facilities requires natural resources for operation.

6.2.3 Societal Influence

The desired healing capabilities of our novel extracellular matrix scaffold will have a tremendous impact on society. Currently, no artificial skin therapy exists that can completely mimic natural skin, lacking nerve endings, hair follicles, and sweat glands. Additionally, no scaffold exists that can regenerate skin so that its total functionality returns. Having the ability to overcome these limitations will greatly increase the quality of life of patients with burns, ulcers, and other full-thickness wounds. Especially in the case of burn victims, the psychological trauma of their disfiguration will endure long after the wound has been clinically healed; their physical appearance will never return to normal (Smith, Smith, & Rainey, 2006). Our hope is that this

scaffold can also be a cosmetic treatment for the patient so that skin will regenerate back to its initial appearance.

6.2.4 Political Ramifications

The United States, Europe and Japan account for 80% of world's wound care products. The global wound care market is projected to reach \$20.3 billion by 2015 (Global Wound Care, 2010). As a leader in this market, the United States can only strengthen its position by offering governmental funding towards regenerative wound therapy. Additionally, such research funding can be used towards specifically healing soldiers who have been significantly wounded. The economic, ethical, and societal burdens created by chronic wounds, are directly related to healthcare, and must be heavily considered by political figures.

6.2.5 Ethical Concerns

In order to be validated as a successful, therapeutic product, our scaffold will have to undergo multiple animal trials before it can be testing in clinical trials. Scientific testing on animals has brought forth many ethical concerns; proper animal care and scientific protocol must be followed according to the Institutional Animal Care and Use Committees standards. The animals must have living conditions that are appropriate for their species, and procedures should minimize discomfort and pain, using methods of euthanasia only when appropriate.

Additionally, potential users may disagree with the genetic engineering method that is used to fabricate the scaffold. Whether personally or due to religious beliefs, some people may feel that reprogramming a cell to perform a function that it was not created to perform is an ethical breach. However, some people believe that exogenous or synthetic materials should not be placed inside the body. Therefore, our scaffold eliminates this concern due to its potential to be fabricated from autologous cells.

6.2.6 Health and Safety Issues

Our scaffold addresses the limitation of infections that plagues many surgical procedures. Hospitals have struggled with procedure-induced infections, and the loss of barrier function makes skin wounds the most susceptible. The addition of a defense mechanism against infection built into this scaffold will further protect the patient's health and allow for better healing. The safety of this scaffold will be determined through multiple animal and clinical trials according to FDA regulations. It is important that our scaffold is completely decellularized to eliminate the risk of disease transmission from the cell source.

6.2.7 Manufacturability

Although our product has the potential to improve the health of patients with hard-to-heal wounds, it is limited by its manufacturability. The scaffold will require more extensive maintenance and resources for production. Materials, equipment, and labor will be required for cell culture, tissue culture, decellularization, and transfection. Fabricating these scaffolds is at this stage a manual process, making it difficult to produce the product on a large-scale basis.

6.2.8 Sustainability

Because our product is completely cell-derived, the only materials required for production are those required for cell culture. However, because the supplies used to support cell and tissue growth are single-use only, the process is not very sustainable. Also, the production of tissue culture polystyrene, pipettes, and other required plastic/glass tools do not currently operate on renewable energy. However, once the scaffold is produced, only minimal energy is required to store the product until usage. If operations for the disposable resources were to use renewable energy, the process would become much more sustainable and would not have a major negative impact on the biological/ecological environment.

7 Final Design and Validation

The final design was developed through iterations of the design process. Using the allotted time and material resources, three components of the design were finalized, including fibroblast sheet fabrication, ECM isolation using decellularization, and construction of a unique cathelicidin construct. Our final approach (Figure 57) brings these three components together: genetically modified fibroblasts are cultured into a cell sheet, which is then decellularized to isolate the final ECM scaffold with tailored mechanical strength and antimicrobial activity. The following sections detail the final design components.

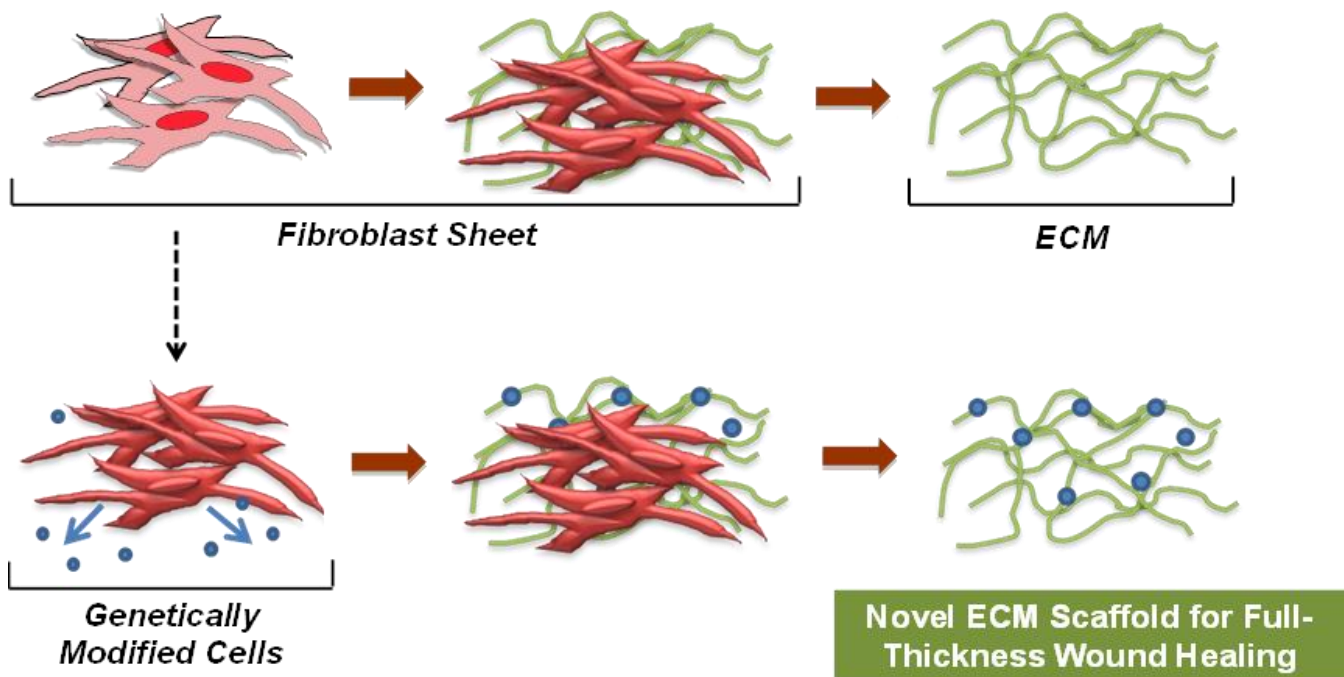


Figure 57: Final Design Approach

7.1 Part 1: Fabricating Fibroblast Sheets

Human neonatal fibroblasts were grown at 5% CO₂ in IMDM containing 10% FBS, penicillin/streptomycin, L-glutamine, and 25 mM HEPES. Fibroblasts were seeded at 100,000

cells/cm² on NIPAAAM (poly(N-isopropylacrylamide)-coated UpCell™ 24-well plates (Thermo Fisher Scientific, Inc.) and cultured for 14 days. Tissues received 1mL of IMDM containing 5% FBS with 50µg/mL of L-ascorbic acid to increase collagen production, which was changed every 2 days. To harvest the tissues, the UpCell™ was incubated at 25°C for 60 minutes.

7.2 Part 2: Isolating the ECM via Decellurization

Samples were placed in a 1.5mL Eppendorf tube and immersed in liquid nitrogen for 2 minutes. PBS (1mL) was added to each tube and the samples were rotated for 5 minutes on a Labquake tube rotator. The PBS was then aspirated. This process was repeated for a total of three cycles. Each sample was then treated with 0.5mL of DNase (Worthington, 1mg/mL, 10mM MgCl₂) while rotating on the Labquake. Samples were washed three times for 5 minutes each in PBS while rotating and left on the bench top to sit for 8 hours.

7.3 Part 3: Incorporating Antimicrobial Protein into the ECM

A construct for human cathelicidin was designed to include a collagen binding domain to assure retention of the protein in the extracellular matrix scaffold. The construct was also designed with FLAG epitopes for verification of cell expression of the constructs using Western blot.

8 Conclusions and Recommendations

The following discussion presents recommendations for overcoming our project limitations as well as future methods for realizing the successful production of our novel cell-derived ECM scaffold for dermal wound healing.

8.1 Future Work

Future direction includes optimizing the structure and mechanics of the scaffold. The fibroblast sheets will be decellularized using the freeze-thaw protocol as stated in the final design. The effects of freeze-thaw on the scaffold will be assessed, including mechanical integrity, retention of matrix components, and retention of cellular debris. The mechanical integrity of the scaffold will be determined by mechanically testing the fibroblast sheets before and after decellularization. The retention of matrix components will be assessed after freeze-thaw using histology and quantification techniques. Components include collagen, GAG, fibronectin, and cathelicidin. Additionally, gel electrophoresis will be used to determine DNA fragment length of any remaining DNA in the scaffold. The fragment length of the DNA cannot be greater than 200 base pairs (Crapo et al., 2011). Quant-iT™ PicoGreen dsDNA Assay Kit (Invitrogen) will be used to verify that the DNA concentration is below the accepted limit for decellularized tissues. The scaffold cannot contain more than 50 ng of double stranded DNA per mg of ECM dry weight (Crapo et al., 2011).

In order for the novel recombinant cathelicidin to be incorporated into a matrix scaffold, the next steps would include validating its activity. It is expected that the signal peptide which cathelicidin naturally possesses will allow for the secretion of the protein from the cell. Because the p3xFLAG vector fused three FLAG epitopes directly to the signal peptide on the N-terminal domain of the cathelicidin protein, it would need to be verified that the signal peptide is still fully functional. The localization of the protein would have to be tested by immunocytochemistry and cell fractionation experiments. Additionally, the collagen affinity and retention rate of the two

constructs would need to be analyzed to select the best recombinant form compatible with the tissue decellularization process of fabricating a matrix scaffold.

Natural cathelicidin is known to have a broad range of activity against both Gram positive and Gram negative bacteria (Sorensen et al., 2001). It is expected that the addition of either of the collagen binding domains, with the FLAG linker, will not have significantly altered the activity of the peptide. The recombinant cathelicidin will need to be tested for its potency against common strains of microbes found in chronic wounds: *Staphylococcus aureus*, *Enterococcus faecalis*, and *Pseudomonas aeruginosa*.

The recombinant cathelicidin would ultimately need to be expressed in primary dermal fibroblasts, which would synthesize both the extracellular matrix and the antimicrobial peptide. It would need to be verified that these cells could produce the peptide in sufficient concentrations, and secrete it into their extracellular matrices to allow for its cleavage by proteinases and adhesion to the collagen within the matrix. The scaffold should destroy at least 99.9% of bacteria to be comparable to current antimicrobial therapies (Dowling, 2012).

8.2 Recommendations

Through the various experiments, the team was able to determine which methods work best for our design and modifications we would make to improve the project. The following are recommendations that we advise in order to better the design and validation testing.

8.2.1 Fibroblast Sheet Fabrication

For future fibroblast cell sheet fabrication, we recommend changing the media every day, as opposed to every other day, to provide more nutrients. This may resolve the problem of the cell sheets dislodging from the plate before 14 days of culture. Additionally, sheet fabrication should be further explored on transwell inserts. This will allow for better media access to both sides of the tissue, which may enhance collagen production. We recommend using Thermo Scientific UpCell™ Surface Technology to increase the thickness of the fibroblast sheets. Six

well multidish UpCell™ plates with 9.6 cm² culture surface area include membranes that can be used for 3D tissue culture. The membranes are applied to the sheet before detachment, which are both then placed directly on top of a new sheet. Since multiple layers can be added to increase thickness, this allows for flexibility in the desired cell sheet thickness.

8.2.2 Histological Analysis

For future analysis of the cell sheets, we recommend using Picrosirius Red stains to quantify collagen using Image J (NIH) or MATLAB image analysis. This will provide for a quantitative analysis of the increase in collagen production contributed by the ascorbic acid.

8.2.3 Mechanical Testing

The mechanical testing procedure can be improved through the following considerations. Thickness measurements should be obtained using an Apotome microscope. This will allow for more accurate measurements by focusing on the top and bottom Z-planes of the tissue. For additional tensile testing, the dimensions of the scaffold should be optimized. We recommend growing larger samples in six well plates so that they can be cut into rectangles that are at least 5 times longer than they are wide. Alternatively, dog bone molds can be used to grow the tissues so that they are harvested with ASTM dimensions for uniaxial tensile testing. Additionally, a method should be determined for controlling fiber orientation and direction so that they are the same for every tissue loaded onto the Instron. The cell sheets should also undergo cyclic pre-loading to better prepare the sheets for testing. However, we also recommend that testing on cell sheets be switched to biaxial mechanical testing using an inflation device. This is because we predict that the fiber alignment in the fibroblast sheets is anisotropic; therefore, uniaxial testing does not properly reflect the strength of the sheet.

8.2.4 Mechanical Strength of the Cell Sheets

Mechanical strength of the fibroblast sheets can be enhanced chemically or mechanically. Other components, in addition to ascorbic acid, can be explored for their enhancement of mechanical strength, including epidermal growth factor, insulin, and cytokines (Throm, Liu, Lock, & Billiar, 2010). Cyclic mechanical stimulation has been shown to induce tenascin-C in fibroblasts, which enhances mechanical strength (Chiquet, Gelman, Lutz, & Maier, 2009). We recommend that the fibroblast sheets be mechanically stimulated using the FlexCell equibiaxial stretching device. The vacuum pressure used to provide a uniform stretch of the tissue was shown to increase the mechanical strength of fibroblast sheets by 100 kPa (Balestrini & Billiar, 2006).

References

- Agache, P., Monneur, C., Leveque, J., & De Rigal, J. (1980). Mechanical Properties and Young's Modulus of Human Skin in Vivo. *Archives of Dermatological Research*, 269, 221-232.
- Ahlfors, J., & Billiar, K. (2007). Biomechanical and biochemical characteristics of a human fibroblast-produced and remodeled matrix. *Biomaterials*, 28, 2183-2191.
- Alexander, H., & Cook, T. (1977). Accounting for the Natural Tension in the Mechanical Testing of Human Skin. *The Journal of Investigative Dermatology*, 69, 310-314.
- Badylak, S. (2002). The extracellular matrix as a scaffold for tissue reconstruction. *Seminars in Cell & Developmental Biology*, 13, 377-383.
- Badylak, S. (2007). The extracellular matrix as a biologic scaffold material. *Biomaterials*, 28, 3587-3593.
- Balestrini, J., & Billiar, K. (2006). Equibiaxial Cyclic Stretch Stimulates Fibroblasts to Rapidly Remodel Fibrin. *Journal of Biomechanics*, 39, 2983-2990.
- Billiar, K. L., Throm, A. M., & Frey, M. T. (2005). Biaxial failure properties of planar living tissue equivalents. *J Biomed Mater Res A*, 73(2), 182-191. doi: 10.1002/jbm.a.30282
- Biomet. (2012). DermaSpan Acellular Dermal Matrix Retrieved April 20, 2012
- Bucki, R., Leszczynska, K., & Namiot, A. S., Wojciech. (2010). Cathelicidin LL-37: A Multitask Antimicrobial Peptide. *Archivum Immunologiae et Therapiae Experimentalis*, 58, 15-25.
- Bush, K. (2009). *Designing Bioengineered Skin Substrates Containing Microfabricated Basal Lamina Analogs to Enhance Skin Regeneration*. (Doctorate in Philosophy), Worcester Polytechnic Institute.
- Carretero, M., Escamez, M. J., Garcia, M., Duarte, B., Holguin, A., Retamosa, L., . . . Larcher, F. (2007). In vitro and In vivo Wound Healing-Promoting Activities of Human Cathelicidin LL-37. *J Invest Dermatol*, 128(1), 223-236. doi: 10.1038/sj.jid.5701043
- Chiquet, M., Gelman, L., Lutz, R., & Maier, S. (2009). From Mechanotransduction to Extracellular Matrix Gene Expression in Fibroblasts. *Biochimica et Biophysica Acta*, 1793(5), 911-920.
- Church, D., Elsayed, S., Reid, O., Winston, B., & Lindsay, R. (2006). Burn wound infections. *Clin Microbiol Rev*, 19(2), 403-434.
- Clark, R., Ghosh, K., & Tonnesen, M. (2007). Tissue Engineering for Cutaneous Wounds. *Journal of Investigative Dermatology*, 127(5), 1018-1029.
- Crapo, P., Gilbert, T., & Badylak, S. (2011). Review: An overview of tissue and whole organ decellularization processes. *Biomaterials*, 32(12), 3233-3243.
- Cukierman, E., Pankov, R., Stevens, D., & Yamada, K. (2001). Take cell-matrix adhesions to the third-dimension. *Science*, 294(5547), 1708-1712.
- De Smet, K., & Contreras, R. (2005). Human antimicrobial peptides: defensins, cathelicidins and histatins. *Biotechnol Lett*, 27(18), 1337-1347. doi: 10.1007/s10529-005-0936-5
- Dowling, P. (2012). *The PK/PD Approach to Antimicrobial Therapy*. Paper presented at the 84th Annual Western Veterinary Conference, Canada.
http://www.wvc.org/downloads/conference_notes/2012/2012_SA237.pdf
- Edwards, C., & Marks, R. (1995). Evaluation of Biomechanical Properties of Human Skin. *Clinics in Dermatology*, 13, 375-380.
- Elder, B., Eleswarapu, S., & Athanasiou, K. (2009). Extraction techniques for the decellularization of tissue engineered articular cartilage constructs. *Biomaterials*, 30(22), 3749-3756.
- Fathke, C., Wilson, L., Hutter, J., Kapoor, V., Smith, A., Hocking, A., & Isik, F. (2004). Contribution of bone marrow-derived cells to skin: collagen deposition and wound repair. *Stem Cells*, 22(5), 812-822. doi: 10.1634/stemcells.22-5-812

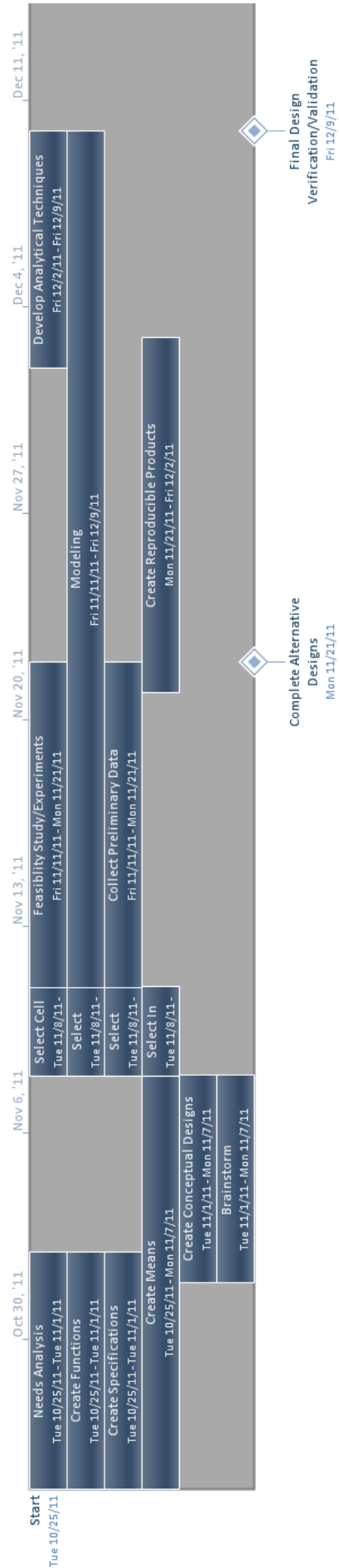
- Flynn, L., & Woodhouse, K. (2009). Burn Dressing Biomaterials and Tissue Engineering. In R. Narayan (Ed.), *Biomedical Materials* (pp. 371-414). New York: Springer Science + Business Media.
- Freinkel, R., & Woodley, D. (2001). *The Biology of Skin*. New York: Parthenon Pub. Group.
- Gilbert, T., Sellaro, T., & Badylak, S. (2006). Decellularization of tissues and organs. *Biomaterials*, 27, 3675-3683.
- Gjodsbol, K., Christensen, J. J., Karlsmark, T., Jorgensen, B., Klein, B. M., & Kroghfelt, K. A. (2006). Multiple bacterial species reside in chronic wounds: a longitudinal study. *Int Wound J*, 3(3), 225-231. doi: 10.1111/j.1742-481X.2006.00159.x
- Goldsmith, L. (1983). *Biochemistry and physiology of the skin* (Vol. 1). New York: Oxford University Press.
- Grauss, R., Hazekamp, M., van Vliet, S., Gittengerger-de Groot, A., & DeRuiter, M. (2003). Decellularization of rat aortic valve allografts reduces leaflet destruction and extracellular matrix remodeling. *Journal of Thoracic and Cardiovascular Surgery*, 126(6), 2003-2010.
- Gurtner, G., Werner, S., Barrandon, Y., & Longaker, M. (2008). Wound repair and regeneration. *Nature*, 453(15), 314-321.
- Hancock, R. E. W., & Sahl, H.-G. (2006). Antimicrobial and host-defense peptides as new anti-infective therapeutic strategies. [10.1038/nbt1267]. *Nat Biotech*, 24(12), 1551-1557. doi: 10.1038/nbt1267
- Heilborn, J. D., Nilsson, M. F., Kratz, G., Weber, G., Sorensen, O., Borregaard, N., & Stahle-Backdahl, M. (2003). The cathelicidin anti-microbial peptide LL-37 is involved in re-epithelialization of human skin wounds and is lacking in chronic ulcer epithelium. *J Invest Dermatol*, 120(3), 379-389. doi: 10.1046/j.1523-1747.2003.12069.x
- Heilman, D. W., Teodoro, J. G., & Green, M. R. (2006). Apoptin nucleocytoplasmic shuttling is required for cell type-specific localization, apoptosis, and recruitment of the anaphase-promoting complex/cyclosome to PML bodies. *J Virol*, 80(15), 7535-7545.
- Hendriks, F. (2005). *Mechanical Behaviour of Human Epidermal and Dermal Layers in vivo*. Technische Universiteit Eindhoven, Eindhoven.
- Hess, C. (2005). *Wound Care*. Philadelphia: Lippincott Williams & Wilkins.
- Holt, B., Tripathi, A., & Morgan, J. (2008). Viscoelastic response of human skin to low magnitude physiologically relevant shear. *Journal of Biomechanics*, 41(12), 2689-2695.
- Hu, J. (2010). *Assessment of Ascorbic Acid Effects on the Properties of Cell-Derived Tissue Rings*. (Master of Science), Worcester Polytechnic Institute.
- Izadpanah, A., & Gallo, R. L. (2005). Antimicrobial peptides. *J Am Acad Dermatol*, 52(3 Pt 1), 381-390; quiz 391-382. doi: 10.1016/j.jaad.2004.08.026
- James, S. (2009). Clinical Approaches to Skin Regeneration. In M. Santin (Ed.), *Strategies in Regenerative Medicine: Integrating Biology with Materials Design* (pp. 155-187). New York: Springer.
- Klein, M. (2010). Skin Grafting. In H. Hyakusoku (Ed.), *Color Atlas of Burn Reconstructive Surgery* (pp. 132-138). Heidelberg: Springer.
- Krejci, N., Cuono, C., Langdon, R., & McGuire, J. (1991). In Vitro Reconstitution of Skin: Fibroblasts Facilitate Keratinocyte Growth and Differentiation on Acellular Reticular Dermis. *Journal of Investigative Dermatology*, 97, 843-848.
- Lacroix, D., & Planell, J. (2009). Biomaterials: Processing, Characterization, and Applications. In R. Narayan (Ed.), *Biomedical Materials* (pp. 123-154). New York: Springer Science + Business Media.
- Landis, S. J. (2008). Chronic wound infection and antimicrobial use. *Adv Skin Wound Care*, 21(11), 531-540; quiz 541-532. doi: 10.1097/01.ASW.0000323578.87700.a5
- Lavik, E., & Langer, R. (2004). Tissue Engineering: Current State and Perspectives. *Applied Microbiology and Biotechnology*, 65, 1-8.
- LifeCell. (2012). AlloDerm Retrieved April 20, 2012

- Liu, C., Xia, Z., & Czernuszka, J. (2007). Design and Development of Three-Dimensional Scaffolds for Tissue Engineering. *Chemical Engineering Research and Design*, 85(A7), 1051-1064.
- Lu, H., Hoshiba, T., Kawazoe, N., Song, M., & Chen, G. (2011). Cultured cell-derived extracellular matrix scaffolds for tissue engineering. *Biomaterials*, 32(36), 9658-9666.
- Ma, P. (2004). Scaffolds for Tissue Fabrication. *Materials Today, Review Feature*, 30-40.
- MacNeil, S. (2008). Biomaterials for Tissue Engineering of Skin. *Materials Today*, 11(5), 26-35.
- Macri, L., & Clark, R. (2009). Tissue Engineering for Cutaneous Wounds: Selecting the Proper Time and Space for Growth Factors, Cells and the Extracellular Matrix. *Skin Pharmacology and Physiology*, 22(2), 83-89.
- Mansbridge, J. N., Liu, K., Pinney, R. E., Patch, R., Ratcliffe, A., & Naughton, G. K. (1999). Growth factors secreted by fibroblasts: role in healing diabetic foot ulcers. *Diabetes Obes Metab*, 1(5), 265-279.
- Manschot, J., & Brakkee, A. (1986). The measurement and modelling of the mechanical properties of human skin in vivo-I. The measurement. *Journal of Biomechanics*, 19(7), 511-515.
- Martin, P. (1997). Wound Healing-Aimed for Perfect Skin Regeneration. *Science*, 276, 75-81.
- Menke, N., Ward, K., Witten, T., Bonchev, D., & Diegelmann, R. (2007). Impaired Wound Healing. *Clinics in Dermatology*, 25(1), 19-25.
- Meyer, S., Chiu, B., Churchill, T., Zhu, L., Lakey, J., & Ross, D. (2006). Comparison of aortic valve allograft decellularization techniques in the rat. *Journal of Biomedical Materials Research Part A*, 79(2), 254-262.
- Morgan, J., Sheridan, R., Tompkins, R., Yarmush, M., & Burke, J. (2004). Burn Dressings and Skin Substitutes. In B. D. Ratner, A. S. Hoffman, F. J. Schoen & J. E. Lemons (Eds.), *Biomaterials Science* (pp. 602-614). San Diego: Elsevier.
- Ngangan, A., & McDevitt, T. (2009). Acellularization of embryoid bodies via physical disruption methods. *Biomaterials*, 30(6), 1143-1149.
- O'Brien, F. (2011). Biomaterials & Scaffolds for tissue engineering. *Materials Today*, 14(3), 88-95.
- Place, E., George, J., & Williams, C. (2009). Synthetic Polymer Scaffolds for Tissue Engineering. *Chemical Society Reviews*, 38, 1139-1151.
- Rode, H., Vale, I. D., & Millar, A. J. W. (2008). Burn Wound Infection. *Continuing Medical Education*, 26(9), 440-443.
- Rosso, F., Giordano, A., Barbarisi, M., & Barbarisi, A. (2004). From Cell-ECM Interactions to Tissue Engineering. *Journal of Cellular Physiology*, 199, 174-180.
- Rouabhia, M. (1997). Structural and Functional Complexity of the Skin. In M. Rouabhia (Ed.), *Skin Substitute Production by Tissue Engineering: Clinical and Fundamental Applications* (pp. 3-22). New York, New York: Chapman & Hall.
- Saltzman, W. (2004). The State-of-the-Art in Tissue Exchange *Tissue Engineering: Engineering Principles for the Design of Replacement Organs and Tissues* (pp. 1-15). New York: Oxford University Press.
- Schaner, P., Martin, N., Tulenko, T., Shapiro, I., Tarola, N., Leichter, R., . . . DiMuzio, P. (2004). Decellularized vein as a potential scaffold for vascular tissue engineering. *Journal of Vascular Surgery*, 40(1), 146-153.
- Schoen, F., & Mitchell, R. (2004). Tissue, the extracellular matrix, and cell-biomaterial interactions. In B. D. Ratner, A. S. Hoffman, F. J. Schoen & J. E. Lemons (Eds.), *Biomaterials Science* (2nd ed., pp. 260-281). San Diego: Elsevier.
- Seal, B., Otero, T., & Panitch, A. (2001). Review: Polymeric biomaterials for tissue and organ regeneration. *Materials Science and Engineering: R: Reports*, 34(4-5), 147-230.

- Sen, C., Gordillo, G., Roy, S., Kirsner, R., Lambert, L., Hunt, T., . . . Longaker, M. (2009). Human Skin Wounds: A Major and Snowballing Threat to Public Health and the Economy. *Wound Repair and Regeneration*, 17(6), 763-771.
- Shai, A. (2005). *Wound Healing and Ulcers of the Skin*. New York: Springer-Verlag.
- Shier, D., Butler, J., & Lewis, R. (2009). Integumentary System *Hole's Essentials of Human Anatomy & Physiology* (10th ed., pp. 116-129). New York: McGraw-Hill.
- Shores, J., Gabriel, A., & Gupta, S. (2007). Skin Substitutes and Alternatives. *Advances in Skin & Wound Care*, 20(9), 493-508.
- Siddiqui, A. R., & Bernstein, J. M. (2010). Chronic wound infection: facts and controversies. *Clin Dermatol*, 28(5), 519-526. doi: 10.1016/j.clindermatol.2010.03.009
- Silver, F., Freeman, J., & DeVore, D. (2001). Viscoelastic properties of human skin and processed dermis. *Skin Research and Technology*, 7, 18-23.
- Singer, A., & Clark, R. (1999). Cutaneous Wound Healing. *The New England Journal of Medicine*, 341, 738-746.
- Sistiabudi, R., & Ivanisevic, A. (2008). Collagen-binding peptide interaction with retinal tissue surfaces. *Langmuir*, 24(5), 1591-1594.
- Smith, J., Smith, K., & Rainey, S. (2006). The Psychology of Burn Care. *Journal of Trauma Nursing*, 13(3), 105-106.
- Sorensen, O. E., Follin, P., Johnsen, A. H., Calafat, J., Tjabringa, G. S., Hiemstra, P. S., & Borregaard, N. (2001). Human cathelicidin, hCAP-18, is processed to the antimicrobial peptide LL-37 by extracellular cleavage with proteinase 3. *Blood*, 97(12), 3951-3959.
- Thermo Fisher Scientific, I. (2010). UpCell™ SurfaceTemperature-responsive cell culture surface Retrieved April 20, 2012
- Throm, A., Liu, W., Lock, C., & Billiar, K. (2010). Development of a cell-derived matrix: effects of epidermal growth factor in chemically defined culture. *Journal of Biomedical Research Part A*, 92(2), 533-541.
- Tremblay, P., Hudon, V., Berthod, F., Germain, L., & Auger, F. (2005). Inosculation of tissue-engineered capillaries with the host's vasculature in a reconstructed skin transplanted on mice. *American Journal of Transplantation*, 5(5), 1002-1010.
- Téot, L. (2010). Dermal Substitutes. In H. Hyakusoku (Ed.), *Color Atlas of Burn Reconstructive Surgery* (pp. 90-98). Heidelberg: Springer.
- Van der Veen, V. (2011). New Dermal Substitutes. *Wound Repair and Regeneration*, 19, 59-65.
- Wan Abas, W., & Barbenel, J. (1982). Uniaxial tension test of human skin in vivo. *Journal of Biomedical Engineering*, 4(1), 65-71.
- Yang, D., Biragyn, A., Hoover, D. M., Lubkowski, J., & Oppenheim, J. J. (2004). Multiple roles of antimicrobial defensins, cathelicidins, and eosinophil-derived neurotoxin in host defense. *Annu Rev Immunol*, 22, 181-215. doi: 10.1146/annurev.immunol.22.012703.104603
- Yannas, I., Lee, E., Orgill, D., Skrabut, E., & Murphy, G. (1989). Synthesis and characterization of a model extracellular matrix that induces partial regeneration of adult mammalian skin. *Proc. Natl. Acad. Sci. USA*, 86, 933-937.
- Yoon, D., & Fisher, J. (2009). Natural and Synthetic Polymeric Scaffolds. In R. Narayan (Ed.), *Biomedical Materials* (pp. 415-442). New York: Springer Science + Business Media.
- Zahouani, H., Paillet-Matteri, C., Sohm, B., Vargiolu, R., Cenizo, V., & Debret, R. (2009). Characterization of the mechanical properties of a dermal equivalent compared with human skin in vivo by indentation and static friction tests. *Skin Research and Technology*, 15, 68-76.
- Zhang, J., Ding, L., Zhao, Y., Sun, W., Chen, B., Lin, H., . . . Dai, J. (2009). Collagen-targeting vascular endothelial growth factor improves cardiac performance after myocardial infarction. *Circulation*, 119(13), 1776-1784.
- Zhong, S., Zhang, Y., & Lim, C. (2010). Tissue scaffolds for skin wound healing and dermal reconstruction. *WIREs Nanomedicine and Nanobiotechnology*, 2, 510-525.

Appendices

Appendix A: B-Term Gantt Chart



Appendix B: Metrics

Structurally and mechanically similar to native dermal tissue—5

Objective: Scaffold achieves a tensile strength of similar value to native dermis—5

Specification: Dermis has tensile strength of 5-30 MPa

Units: Rating the strength of the scaffold

- 1) Not within 100 +/- 20% of native dermis
- 2) Within 100 +/- 20% of native dermis

Objective: Scaffold achieves a stiffness of similar value to native dermis—5

Specification: Dermis has a modulus of elasticity of 15-150 MPa

Units: Rating the stiffness of the scaffold

- 1) Not within 100 +/- 20% of native dermis
- 2) Within 100 +/- 20% of native dermis

Objective: Scaffold achieves a shear resistance of similar value to native dermis—4

Specification: Dermis has a shear resistance within 435-6620 Pa

Units: Rating the shear resistance of the scaffold

- 1) Not within 100 +/- 20% of native dermis
- 2) Within 100 +/- 20% of native dermis

Objective: Scaffold is permeable to cells—3

Specification: Scaffold has pores of 20-125 μm

Units: Rating the porosity of the scaffold to determine permeability

- 1) Not within 100 +/- 20% of native dermis
- 2) Within 100 +/- 20% of native dermis

Objective: Biomolecules should be able to diffuse at a natural rate—3

Specification: Scaffold has pores of 20-125 μm

Units: Rating the porosity of the scaffold to determine diffusion rate

- 1) Not within 100 +/- 20% of native dermis
- 2) Within 100 +/- 20% of native dermis

Objective: Scaffold has a thickness similar to native dermis—2

Specification: Scaffold has a thickness of 1-4 mm

Units: Rating the thickness of the scaffold

- 1) Not within 100 +/- 20% of native dermis
- 2) Within 100 +/- 20% of native dermis

Objective: Scaffold has a high suture pullout strength—1

Not used as an objective for alternative design evaluations

Objective: Scaffold firmly adheres to wound bed—1

Not used as an objective for alternative design evaluations

Bioactive—4

Objective: Scaffold actively inhibits microbial infections—3

Specification: Scaffold kills 99.9% of streptococcus aureus, enterococcus faecalis, and pseudomonas aeruginosa (and candida)

Units: Rating the amount of dead microbes using MIC90 and MBC analysis

- 1) Less than 99.9%
- 2) 99.9% or greater

Objective: Scaffold promotes angiogenesis—2

Specification: Scaffold shows signs of blood vessel formation when reseeded with endothelial cells

Units: Rating the ability to form vessels

- 1) Promotes vasculature
- 2) Promotes and produces vasculature

Objective: Improved wound healing—1

Not used as an objective for alternative design evaluations

Ease of Laboratory Processing—3

Objective: Repeatable process to minimize variation in results—5

Specification: Process can be repeatable with a variation in quantitative results of 5% or less

Units: Rating the variation of quantitative results

- 1) Variation is greater than 5%
- 2) Variation is 5% or less

Objective: Minimize production costs—4

Specification: Supplies for scaffold fabrication require minimal charges

Units: Rating the amount of time and money

- 1) Requires extensive time and money
- 2) Requires minimal time and money

Objective: Minimize the production area—3

Specification: Scaffold production requires an area no larger than a standard-sized lab bench, hood, and incubator

Units: Rating the size of the production area

- 1) Production uses more area than specified
- 2) Production uses the amount of area specified or less

Objective: Minimize the equipment and technology required—2

Specification: Scaffold can be produced with standard laboratory equipment

Units: Rating the availability of equipment and technology

- 1) Necessary equipment and technology needs to be purchased
- 2) Necessary equipment and technology needs to be borrowed
- 3) Necessary equipment and technology does not need to be purchased or borrowed (already available)

Objective: Minimize the difficulty of process steps—1

Specification: Scaffold can be produced with minimal expertise

Units: Rating the laboratory experience required for scaffold production

- 1) Much experience is necessary
- 2) Some experience is necessary
- 3) No experience is necessary

Clinical Ease of Use—2

Objective: Scaffold can be easily implanted—minimal preparation from shelf to body—3

Specification: Scaffold can be transported directly from the package to the patient

Units: Rating the time and extent of preparation required before implantation

- 1) Major preparation is necessary (more than 1 hour)
- 2) Minor preparation is necessary (less than 1 hour)
- 3) No preparation is necessary

Objective: Scaffold can be easily implanted—can be handled without tearing—3

Specification: Scaffold does not rip or tear during handling or implantation

Units: Rating the durability of the scaffold

- 1) Major rips or tears occur
- 2) Minor rips or tears occur
- 3) No rips or tears occur

Objective: Scaffold can be easily implanted—simple in-vivo attachment to wound bed—3

Specification: Scaffold attachment to wound bed can be quickly completed with minimal expertise

Units: Rating the attachment method

- 1) Attachment requires major additional training
- 2) Attachment requires minor additional training
- 3) Attachment requires no additional training

Objective: Scaffold can be used to treat various wound sizes and shapes—3

Specification: Scaffold can be formed into multiple shapes

Units: Rating the number of shapes and sizes

- 1) Scaffold comes in 1 size/shape
- 2) Scaffold comes in 2 size/shapes
- 3) Surgeon can form scaffold into any shape

Objective: Treatment with scaffold uses a minimal number of applications—2

Specification: Treatment only requires one scaffold application

Units: Rating the number scaffold applications required

- 1) More than 2 applications are necessary
- 2) More than 1 application is necessary
- 3) Only 1 application is necessary

Objective: Scaffold can be stored for extended periods of time—1

Specification: Scaffold remains functional after 1 year of storage

Units: Rating the amount of time the scaffold can be stored and still usable

- 1) Can be stored less than 6 months
- 2) Can be stored for 6 months-1 year
- 3) Can be stored for 1 year or more

Ease of Production—1

Objective: Scaffold requires minimal costs for production—2

Specification: Scaffold fabrication requires minimal use of materials and time to fabricate scaffold

Units: Rating the amount of time and supplies needed

- 1) Requires extensive use of materials and time

2) Requires minimal use of materials and time

Objective: Scaffold can be manufactured in large quantities—1

Specification: Scaffold fabrication requires minimal use of labor and time to scale-up production

Units: Rating the amount of labor and time needed

3) Requires extensive use of labor and time

4) Requires minimal use of labor and time

Appendix C: Decision Matrices

(1) Function: Withstands mechanical forces similar to native dermis *()=prioritized

Overall Weighting	Attribute	Chemically Crosslink	Normalized Sum	Weighted Sum	Physically Crosslink	Normalized Sum	Weighted Sum	Biologically crosslink	Normalized Sum	Weighted Sum	Proteoglycans to ECM	Normalized Sum	Weighted Sum
C	Budget (\$368 USD)	Y			Y			Y			N		
C	Time (21 weeks)	Y			Y			Y			Y		
C	Cell-derived tissue	Y			Y			Y			Y		
C	Acellular	Y			Y			Y			Y		
C	Biodegradable	Y			Y			Y			Y		
C	Biocompatible	Y			Y			Y			Y		
C	Does not harm scaffold	N			N			Y			Y		
	.333	Structurally and mechanically similar to native dermal tissue							4/5	.266 (.229)			
O	(.208)	Tensile strength						2	1.0	(.208)			
O	(.208)	Stiffness						2	1.0	(.208)			
O	(.167)	Shear resistance						2	1.0	(.167)			
O	(.125)	Permeability/Diffusivity						1	0.5	(.063)			
O	(.083)	Thickness						1	0.5	(.042)			
	.267	Bioactive											
O	(.500)	Inhibits microbial infections											
O	(.333)	Promotes angiogenesis											
	.200	Ease of Laboratory Processing							3/4	0.15 (.127)			
O	(.333)	Repeatable process						1	0.5	(.167)			
O	(.267)	Minimize production costs						1	0.5	(.134)			
O	(.200)	Minimize production area						2	1.0	(.200)			
O	(.133)	Minimize equipment						3	1.0	(.133)			
O	.133	Clinical Ease of Use						2	1/1	.133			
O	.067	Ease of Production						2	1/1	.067			
		TOTAL							9/11	.616 (.556)			

Overall Weighting	Attribute	Grow cells on a substrate	Normalized Sum	Weighted Sum	Bioreactor	Normalized Sum	Weighted Sum	Ascorbic Acid	Normalized Sum	Weighted Sum	Protease inhibitors	Normalized Sum	Weighted Sum
C	Budget (\$368 USD)	Y			Y			Y			Y		
C	Time (21 weeks)	Y			Y			Y			Y		
C	Cell-derived tissue	Y			Y			Y			Y		
C	Acellular	Y			Y			Y			Y		
C	Biodegradable	Y			Y			Y			Y		
C	Biocompatible	Y			Y			Y			Y		
C	Does not harm scaffold	Y			Y			Y			Y		
	.333	Structurally and mechanically similar to native dermal tissue	2.5/4	.208 (.125)		3.5/4	.291 (.208)		4/4	.333 (.222)		2.5/4	.208 (.125)
O	(.208)	Tensile strength	1	0.5 (.104)	2	1.0 (.208)	2	1.0 (.208)	2	1.0 (.208)	1	0.5 (.104)	(.104)
O	(.208)	Stiffness	1	0.5 (.104)	2	1.0 (.208)	2	1.0 (.208)	2	1.0 (.208)	1	0.5 (.104)	(.104)
O	(.167)	Shear resistance	1	0.5 (.084)	2	1.0 (.167)	2	1.0 (.167)	2	1.0 (.167)	1	0.5 (.084)	(.084)
O	(.125)	Permeability/Diffusivity	X		X		X		X		X		
O	(.083)	Thickness	2	1.0 (.083)	1	0.5 (.042)	2	1.0 (.083)	2	1.0 (.083)	2	1.0 (.083)	(.083)
	.267	Bioactive											
O	(.500)	Inhibits microbial infections											
O	(.333)	Promotes angiogenesis											
	.200	Ease of Laboratory Processing	3.17/4	.159 (.145)		3.17/4	.159 (.145)		4/4	.200 (.187)		4/4	.200 (.187)
O	(.333)	Repeatable process	1	0.5 (.167)	1	0.5 (.167)	2	1.0 (.333)	2	1.0 (.333)	2	1.0 (.333)	(.333)
O	(.267)	Minimize production costs	2	1.0 (.267)	2	1.0 (.267)	2	1.0 (.267)	2	1.0 (.267)	2	1.0 (.267)	(.267)
O	(.200)	Minimize production area	2	1.0 (.200)	2	1.0 (.200)	2	1.0 (.200)	2	1.0 (.200)	2	1.0 (.200)	(.200)
O	(.133)	Minimize equipment	2	.667 (.089)	2	.667 (.089)	3	1.0 (.133)	3	1.0 (.133)	3	1.0 (.133)	(.133)
O	.133	Clinical Ease of Use	2	1/1 .133	2	1/1 .133	2	1/1 .133	2	1/1 .133	2	1/1 .133	.133
O	.067	Ease of Production	2	1/1 .067	1	0.5/1 .034	2	1/1 .067	2	1/1 .067	2	1/1 .067	.067
		TOTAL	7.67/10	.567 (.470)		8.17/10	.617 (.520)		10/10	.733 (.609)		8.5/10	.608 (.512)

(2) Function: Actively Inhibits Microbial Infection *()=prioritized

Overall Weighting	Attribute	Gen Mod Cells to Produce AMPs	Normalized Sum	Weighted Sum	Exogenously Add AMPs	Normalized Sum	Weighted Sum	Exogenously Add AMP Inducer (keratinocytes)	Normalized Sum	Weighted Sum
C	Budget (\$368 USD)	Y			Y			N		
C	Time (21 weeks)	Y			Y			Y		
C	Cell-derived tissue	Y			Y			Y		
C	Acellular	Y			Y			Y		
C	Biodegradable	Y			Y			Y		
C	Biocompatible	Y			Y			Y		
C	Does not harm scaffold	Y			Y			Y		
	.333	Structurally and mechanically similar to native dermal tissue								
O	(.208)	Tensile strength								
O	(.208)	Stiffness								
O	(.167)	Shear resistance								
O	(.125)	Permeability/Diffusivity								
O	(.083)	Thickness								
	.267	Bioactive		2/2	.267 (.222)		2/2	.267 (.222)		
O	(.500)	Inhibits microbial infections	2	1.0	(.500)	2	1.0	(.500)		
O	(.333)	Promotes angiogenesis	2	1.0	(.333)	2	1.0	(.333)		
	.200	Ease of Laboratory Processing		3.17/4	.159 (.151)		3/4	.150 (.127)		
O	(.333)	Repeatable process	2	1.0	(.333)	1	0.5	(.167)		
O	(.267)	Minimize production costs	1	0.5	(.134)	1	0.5	(.134)		
O	(.200)	Minimize production area	2	1.0	(.200)	2	1.0	(.200)		
O	(.133)	Minimize equipment	2	.667	(.089)	3	1.0	(.133)		
O	.133	Clinical Ease of Use	2	1/1	.133	2	1/1	.133		
O	.067	Ease of Production	1	0.5/1	.034	1	0.5/1	.034		
		TOTAL		6.67/8	.593 (.540)		7/8	.589 (.516)		

	Overall Weighting	Attribute	Conjugate antibiotic to ECM	Normalized Sum	Weighted Sum	Metallic beads	Normalized Sum	Weighted Sum	Exogenously add terpenes	Normalized Sum	Weighted Sum
C		Budget (\$368 USD)	Y			Y			Y		
C		Time (21 weeks)	Y			Y			Y		
C		Cell-derived tissue	Y			Y			Y		
C		Acellular	Y			Y			Y		
C		Biodegradable	Y			N			Y		
C		Biocompatible	Y			N			Y		
C		Does not harm scaffold	Y			Y			Y		
	.333	Structurally and mechanically similar to native dermal tissue									
O	(.208)	Tensile strength									
O	(.208)	Stiffness									
O	(.167)	Shear resistance									
O	(.125)	Permeability/Diffusivity									
O	(.083)	Thickness									
	.267	Bioactive		1.5/2	.200 (.178)					1.5/2	.200 (.178)
O	(.500)	Inhibits microbial infections	2	1.0	(.500)				2	1.0	(.500)
O	(.333)	Promotes angiogenesis	1	0.5	(.167)				1	0.5	(.167)
	.200	Ease of Laboratory Processing		3.5/4	.175 (.153)					3.5/4	.175 (.153)
O	(.333)	Repeatable process	1	0.5	(.167)				1	0.5	(.167)
O	(.267)	Minimize production costs	2	1.0	(.267)				2	1.0	(.267)
O	(.200)	Minimize production area	2	1.0	(.200)				2	1.0	(.200)
O	(.133)	Minimize equipment	3	1.0	(.133)				3	1.0	(.133)
O	.133	Clinical Ease of Use	2	1/1	.133				2	1/1	.133
O	.067	Ease of Production	1	0.5/1	.034				1	0.5/1	.034
		TOTAL		6.5/8	.542 (.498)					6.5/8	.542 (.498)

	Overall Weighting	Attribute	Induce prevascular network with endothelial	Normalized Sum	Weighted Sum	Induce prevascular network with animal	Normalized Sum	Weighted Sum	Exogenously add angiogenic protein to ECM	Normalized Sum	Weighted Sum
C		Budget (\$368 USD)	Y			N			N		
C		Time (21 weeks)	Y			Y			Y		
C		Cell-derived tissue	Y			Y			Y		
C		Acellular	Y			Y			Y		
C		Biodegradable	Y			Y			Y		
C		Biocompatible	Y			Y			Y		
C		Does not harm scaffold	Y			Y			Y		
	.333	Structurally and mechanically similar to native dermal tissue									
O	(.208)	Tensile strength									
O	(.208)	Stiffness									
O	(.167)	Shear resistance									
O	(.125)	Permeability/Diffusivity									
O	(.083)	Thickness									
	.267	Bioactive		1/1	.267 (.089)						
O	(.500)	Inhibits microbial infections	X			X			X		
O	(.333)	Promotes angiogenesis	2	1.0	(.333)						
	.200	Ease of Laboratory Processing		3/4	.150 (.127)						
O	(.333)	Repeatable process	1	0.5	(.167)						
O	(.267)	Minimize production costs	1	0.5	(.134)						
O	(.200)	Minimize production area	2	1.0	(.200)						
O	(.133)	Minimize equipment	3	1.0	(.133)						
O	.133	Clinical Ease of Use	2	1/1	.133						
O	.067	Ease of Production	1	0.5/1	.034						
		TOTAL		5.5/7	.584 (.383)						



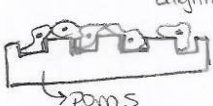




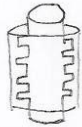
Appendix D: Conceptual Designs

11/4

Bioactive Scaffold - MQP

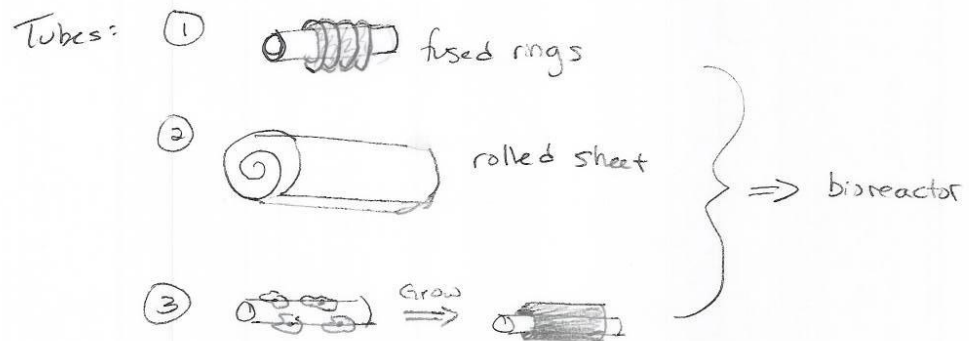
Brainstorming

Number/Name	Description/Components	Picture
1: AMP-Producing Fibroblasts	<ol style="list-style-type: none"> 1. Genetically modified fibroblasts produce AMPs that bind to ECM 2. Decellularization leaves behind matrix with bound AMPs 	<p>gen. mod. HDF → Decell → ECM + AMP</p>
2: Add AMP to CDM	<ol style="list-style-type: none"> 1. CDM made by HDF 2. After decellularization, add and crosslink growth factors or AMPs 3. (2A) HDFs + Chemically defined media 	<p>GF + AMP added to x-linked CDM made by HDF</p>
3: Enhance keratinocyte binding sites	<ol style="list-style-type: none"> 1. Grow genetically modified fibroblasts that produce AMPs 2. Add keratinocytes 3. Decellularize 	<p>① fibroblasts (gen mod) → Decell → AMP binding sites</p>
4: Prevascular network	<ol style="list-style-type: none"> 1. Coculture HDF and endothelial cells 2. Decellularize 	<p>endo + HDF → Decell → prevascular network</p>
5: Porogens	<ol style="list-style-type: none"> 1. Add microparticles to cells 2. Decellularize 3. Remove particles 	<p>porogens - microparticles - salt → Decell → pore</p>
6: Cell Tube	<ol style="list-style-type: none"> 1. Grow cells in sheet bioreactor around silicone solid mandrel 2. Cut sheet to flatten 3. Decellularize 	<p>cell tube in bioreactor → cut → Silicon Solid mandrel</p>
7: Two layer cell tube	<ol style="list-style-type: none"> 1. Culture around tube/bioreactor 2. Reculture as a sheet 3. (7a) Add keratinocytes 	<p>culture → reculture as sheet → (7a) keratinocytes → Devices</p>

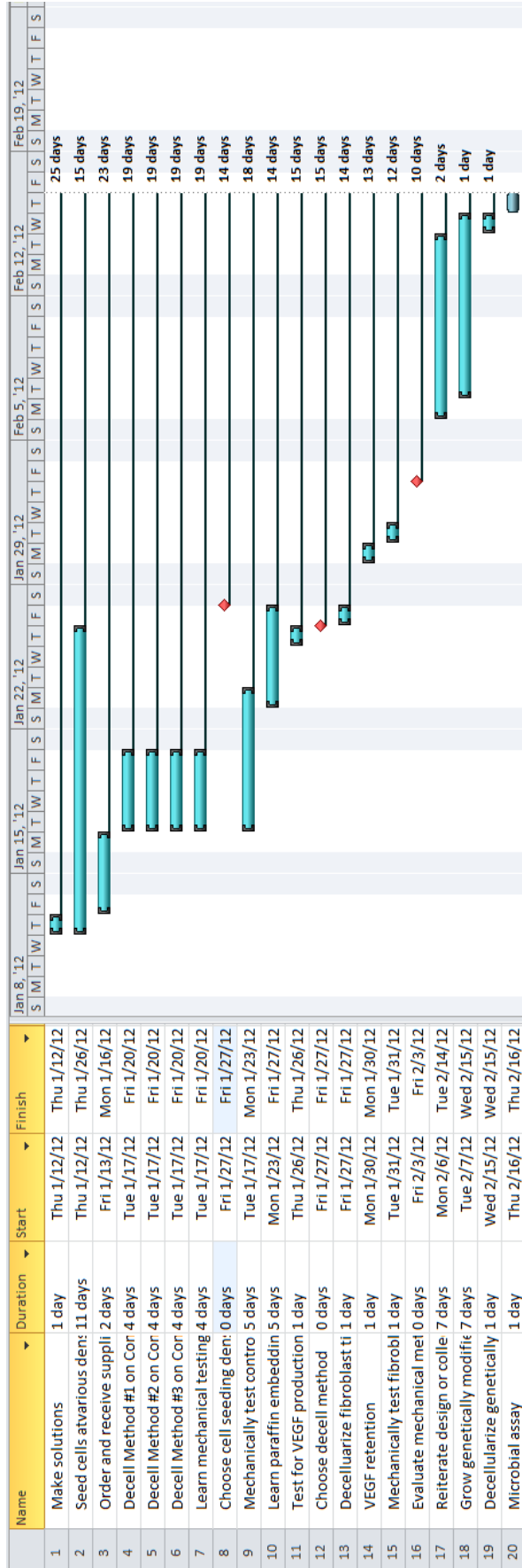
8: Porous mandrel tube culture (static)	<ol style="list-style-type: none"> 1. Culture cells around porous mandrel tube 2. Cut and flatten 3. Decellularize 	 <p>porous mandrel (static)</p>
9: Luminal flow	<ol style="list-style-type: none"> 1. Grow cells around luminal flow tube 2. Cut and flatten 3. Decellularize 	 <p>luminal flow</p>
10: 3D Culture on micro patterned substrate	<ol style="list-style-type: none"> 1. Grow cells on micropatterned PDMS substrate 	 <p>matrix alignment (3D) PDMS</p>
11: 3D Culture in Hydrogel	<ol style="list-style-type: none"> 1. Grow cells in hydrogel 2. Remove hydrogel 3. Decellularize 	 <p>hydrogel for 3D</p>
12: FN (or GF) Soak	<ol style="list-style-type: none"> 1. Decellularize 2. Soak CDM in fibronectin (or growth factors) 	 <p>FN (or GF) + soak after decell</p>
13: Crosslink after decell	<ol style="list-style-type: none"> 1. Decellularize 2. Crosslink CDM 	 <p>① decell ② xlink</p>
14: Crosslink before decell	<ol style="list-style-type: none"> 1. Crosslink CDM 2. Decellularize → Physical method 	 <p>① xlink ② decell w/ physical</p>
15: (6 + 10) Micropatterned tube	<ol style="list-style-type: none"> 1. Grow cells on micropatterned bioreactor (silicone solid mandrel) 2. Cut sheet to flatten Decellularize 	

Notes:

Tubes grown as: fused rings, rolled sheet, grown on bioreactor \Rightarrow into bioreactor



Appendix E: C-Term Gantt Chart



Appendix F: Materials List

1	Materials List			
2		Supplier	Catalogue Number	Cost (\$)/unit
3	Dulbecco's Modified Eagle Medium (1X)	Invitrogen	11960	52.8
4	IMEM	Mediatech, Inc	10-016-CV	92
5	0.5% trypsin-EDTA (10X)	Invitrogen	15400	126
6	Cultureware with Nunc UpCell Surface (24 well dish)	Thermo Fisher Scientific, Inc	174899	
7	EDTA	Sigma-Aldrich	60-00-4	16.6
8	Complete mini, EDTA-free Protease Inhibitor Cocktail	Roche	11 836 170 001	
9	SDS	Sigma-Aldrich	151-21-3	76.7
10	Trizma base	Sigma-Aldrich	77-86-1	15.4
11	L-ascorbic acid phosphate magnesium salt n-hydrate	Wake Pure Chemical Industries	013-19641	55
12	Sodium pyruvate 100mM (100X)	Invitrogen	11360	8.84
13	Penicillin-Streptomycin	Invitrogen	15140	17.94
14	MEM Non-Essential Amino Acids Solution (100X)	Invitrogen	11140	15.71
15	GlutaMAX™ - 1 (100X)	Invitrogen	35050	28.08
16	DNase I	Worthington Biochemical, Corp	LS002006	45
17	Triton X-100	Sigma-Aldrich	9002-93-1	21.4
18	FBS	PAA	A15-201 / A11-201	
19	Total cost of materials per unit*			571.47

*Total cost does not reflect the amount spent by the design team, or account for tissue culture and histology costs

Appendix G: Tissue Processing Protocol

	<u>Foreskins</u>	<u>Fibroblast Sheets</u>
Formalin	Overnight	60 Min
70% Alcohol	15 Min	15 Min or Overnight
80% Alcohol	15 Min	15 Min
90% Alcohol	20 Min	20 Min
95% Alcohol	30 Min	25 Min
100% Alcohol	30 Min	25 Min
100% Alcohol	30 Min	25 Min
100% Alcohol	30 Min	25 Min
Xylene	45 Min	30 Min
Xylene	45 Min	30 Min
Paraffin	45 Min	30 Min
Paraffin	45 Min	30 Min

Appendix H: Staining Protocols for Paraffin Sections

Hematoxylin and Eosin Staining

1. Xylene.....	3 Minutes
2. Xylene.....	3 Minutes
3. Xylene.....	3 Minutes
4. 100% ETOH.....	3 Minutes
5. 100% ETOH.....	3 Minutes
6. 95% ETOH.....	1 Minute
7. 70% ETOH.....	1 Minute
8. Rinse in running H2O.....	Until Clear
9. Harris Hematoxylin.....	5 Minutes
10. Rinse in running H2O.....	Until Clear
11. Differentiate sections in 1% HCL mixed in 70% ETOH (0.25ml HCL to 100 ml of 70% ETOH).....	2-3 quick dips
12. Rinse in running H2O.....	30 seconds
13. Blue sections in ammonia solution.....	1 Minute
14. Rinse in running warm H2O.....	5 Minutes
15. 95% ETOH.....	30 seconds
16. Counterstain in Eosin-Y.....	1 Minute
17. 70% ETOH.....	30 seconds
18. 95% ETOH.....	30 seconds
19. 95% ETOH.....	30 seconds
20. 100% ETOH.....	1 Minute
21. 100% ETOH.....	1 Minute
22. 100% ETOH.....	1 Minute
23. Xylene.....	1 Minute
24. Xylene.....	1 Minute
25. Xylene.....	1 Minute

Results:

Nuclei = blue

Cytoplasm = pink

Blood = red

Picrosirius Red Staining

Reagents:

0.1% Sirius Red Solution

1. Xylene.....	3 Minutes
2. Xylene.....	3 Minutes
3. Xylene.....	3 Minutes
4. 100% ETOH.....	3 Minutes
5. 100% ETOH.....	3 Minutes
6. 95% ETOH.....	1 Minute
7. 95% ETOH.....	3 Minute
8. 70% ETOH.....	3 Minute
9. Rinse in running H2O.....	Until Clear
10. Picrosirius Fast Green.....	30 minutes
11. 17. 80% ETOH.....	1 min
12. 18. 95% ETOH.....	1 min
13. 19. 95% ETOH.....	1 min
14. 100% ETOH.....	5 min
15. 100% ETOH.....	5 min
16. 100% ETOH.....	10 min
17. Xylene.....	3 min
18. Xylene.....	3 min
19. Xylene.....	3 min

Results:

Collagen fibers = red

Other tissue fibers = green

Hoechst Staining

1. Xylene.....3 Minutes
2. Xylene.....3 Minutes
3. Xylene.....3 Minutes
4. 100% ETOH.....3 Minutes
5. 100% ETOH.....3 Minutes
6. 95% ETOH.....1 Minute
7. 70% ETOH.....1 Minute
8. Rinse in running H₂O.....Until Clear
9. 1 mL Hoescht/1 mL diH₂O.....2 Minutes
10. PBS.....5 Minutes
11. PBS.....5 Minutes
12. PBS.....5 Minutes
13. Coverslip with Prolong Gold

Results:

Neon blue = nuclei

Appendix I: Decellularization Protocols

Original SDS Decellularization (Elder et al., 2009)

1. Place the specimens in 2% SDS in a 37°C shaking water bath for 1 hour
2. Wash with agitation 5 times in phosphate-buffered saline (PBS) for periods of 10 minutes each

Modified SDS Decellularization (for small tissues)

1. Dissolve SDS in diH₂O to produce a 2% working solution
2. Place tissue in 15mL conical tube and add 10mL of SDS solution
3. Spin tubes on Glas-Col rotator at 33rpm for 1 hour at 37°C
4. Aspirate SDS
5. Add 10mL 1X PBS to tube and rotate on Labquake on 10 minutes at room temperature. Repeat this step for a total of 5 washes.
6. Aspirate PBS
7. Add 0.5mL of 1mg/mL DNase (plus 10mM MgCl₂) to tube and rotate for 15 minutes on Labquake rotator at room temperature
8. Aspirate DNase solution
9. Add 10mL 1X PBS to tube and rotate on Labquake for 5 minutes at room temperature. Repeat this step for a total of 3 washes.

Original Freeze-Thaw Decellularization (Ngangan & McDevitt, 2009)

1. Immerse tube with tissue into liquid nitrogen and allow liquid nitrogen to boil off
2. Add 1mL PBS to tube while rotating sample for 5 minutes at room temperature
3. Centrifuge for 2 minutes at 18000 rcf at room temperature
4. Repeat 3 times

Modified Freeze-Thaw Decellularization (for small tissues)

1. Place sample in 1.5mL Eppendorf tube
2. Submerge tube in liquid nitrogen and allow to freeze for 2 minutes
3. Remove tube and add 1mL of 1X PBS to tube
4. Rotate tube on Labquake for 5 minutes at room temperature.
5. Aspirate PBS
6. Repeat steps 2-5 for a total of 3 cycles
7. Add 0.5mL of 1mg/mL DNase (plus 10mM MgCl₂) to tube and rotate for 15 minutes on Labquake rotator at room temperature
8. Aspirate DNase solution
9. Add 10mL 1X PBS to tube and rotate on Labquake for 5 minutes at room temperature. Repeat this step for a total of 3 washes.
10. Let sample sit in PBS at room temperature for 8 hours

Original Hypotonic and Hypertonic Solutions Decellularization (Meyer et al., 2006)

1. Rinse in saline solution (PBS)
2. Hypotonic tris buffer (10mM, pH 8.0) with 0.1mM PMSF and 5mM EDTA for 48h for 4 degrees celsius
3. Hypertonic Tris buffer solution (50mM, pH 8.0, PMSF 0.1 mM, EDTA 5mM, KCL 1.5M) with 0.5% Triton X-100 for 48 hr at 4 degrees celsius
4. Rinse in Sorensen's buffer (pH 7.3) containing DNase I (25 mcg/mL), RNase A (10 mcg/mL) and MgCl₂ (10 mM) for 5 hr at 37 degrees Celsius
5. Tris buffer (base)(50mM, pH 9.0, Triton X-100 0.5%) for 48 hr at 4 degrees Celsius
6. PBS wash at 4 degrees Celsius for 72 hr, changing the solution every 24 hr

Modified Hypotonic and Hypertonic Solutions Decellularization (for small tissues)

1. Rinse samples in 1X PBS
2. Dissolve tris HCl (10mM), cOmplete mini cocktail tablet (1 tablet/10mL), and EDTA (5mM) in diH₂O to produce a hypotonic solution (pH 8.0). Rotate samples in 10mL of solution on a Labquake rotator for 48 hours at 4 degrees Celsius
3. Aspirate hypotonic solution.
4. Dissolve tris HCl (50mM), cOmplete mini cocktail tablet (1 tablet/10mL), EDTA (5mM), KCl (1.5M), and Triton X-100 (0.5%) in diH₂O to produce a hypertonic solution (pH 8.0). Rotate samples in 10mL of solution on a Labquake rotator for 48 hours at 4 degrees Celsius.
5. Prepare Sorenson's buffer
6. Add DNase I (25mcg/mL) and MgCl₂ (10mM) to Sorenson's buffer and rotate samples in 10mL of solution on a Labquake rotator for 5 hours at 37 degrees Celsius
7. Aspirate Sorenson's buffer solution
8. Dissolve Trizma base and Triton X-100 (0.5%) in diH₂O to produce the final tris buffer
9. Rotate samples in 10mL of final tris buffer on a Labquake rotator for 48 hours at 4 degrees Celsius.
10. Aspirate buffer.
11. Add 10mL 1X PBS to samples and rotate on Labquake for 72 hours at 4 degrees Celsius, changing the wash every 24 hours.